Supporting Information

Mechanochemistry for the synthesis of non-classical *N*-metalated palladium(II) pincer complexes

Diana V. Aleksanyan,*[a] Svetlana G. Churusova,[a] Valentina V. Brunova,[a] Alexander S. Peregudov,[a] Aleksander M. Shakhov,[b] Ekaterina Yu. Rybalkina,[c] Zinaida S. Klemenkova,[a] Elena G. Kononova,[a] Gleb L. Denisov,[a] and Vladimir A. Kozlov[a]

[a] *Nesmeyanov Institute of Organoelement Compounds, Russian Academy of Sciences, ul. Vavilova 28, Moscow, 119991 Russia*

[b] *N.N. Semenov Federal Research Center for Chemical Physics, Russian Academy of Sciences, ul. Kosygina 4, Moscow, 119991 Russia*

[c] *Blokhin National Medical Research Center of Oncology of the Ministry of Health of the Russian Federation, Kashirskoe shosse 23, Moscow, 115478 Russia*

*corresponding author: aleksanyan.diana@ineos.ac.ru

Table of contents

Experimental section

General remarks

If not mentioned otherwise, all manipulations were carried out without taking precautions to exclude air and moisture. Dichloromethane was distilled from P_2O_5. The functionalized chloroacetamides [1, 2] and ligand **6** [3] were synthesized according to the published or analogous procedures. All other chemicals and solvents were used as purchased.

The NMR spectra were recorded on Bruker Avance 400, Avance 500, and Avance 600 spectrometers, and the chemical shifts (δ) were referenced internally by the residual (^{1}H) or deuterated (^{13}C) solvent signals relative to tetramethylsilane or externally to H_3PO_4 (^{31}P) or $MeNO_2$ (^{15}N). The ^{13}C{^{1}H} NMR spectra were registered using the *J*MODECHO mode; the signals for the *C* nuclei bearing odd and even numbers of protons have opposite polarities. The ^{15}N chemical shifts were extracted from the ^{1}H–^{15}N HMBC spectra. The NMR peak assignments for compounds **1**–**3**, **7**–**12** were based on the analysis of ^{1}H–^{1}H-COSY, HMBC, HMQC (**1**–**3**, **7**, **9**–**11**) or HSQC (**8**, **12**), and NOESY (**3**) spectra. Along with the previously reported data for the related derivatives [3], the results obtained were used to assign the NMR spectra of the other compounds from this study.

The IR spectra were recorded on a Nicolet Magna-IR750 FT spectrometer (resolution 2 cm^{-1}, 128 scans). The assignment of absorption bands in the IR spectra was made according to Ref. 4. Column chromatography was carried out using Macherey-Nagel silica gel 60 (MN Kieselgel 60, 70–230 mesh). Melting points were determined with an MPA 120 EZ-Melt automated melting point apparatus (Stanford Research Systems).

Syntheses

General procedure for the synthesis of ligands 1, 2

A suspension of elemental sulfur (0.29 g) and morpholine (7.84 g, 90.00 mmol) in 5 mL of DMF was stirred at room temperature for 1 h. Then, a solution of the corresponding chloroacetamide (3.00 mmol) in 7 mL of DMF was added. The reaction mixture was stirred at room temperature for 12 h and poured into 50 mL of distilled water. The target product was extracted with chloroform. The organic layer was separated, dried over anhydrous Na_2SO_4, and evaporated to dryness. The resulting precipitate was purified by column chromatography (eluent: CH_2Cl_2–MeOH (75:1)) to give the target compounds as beige (**1**) or light-gray (**2**) crystalline solids.

2-Morpholin-4-yl-*N*-(pyridin-2-ylmethyl)-2-thioxoacetamide, 1

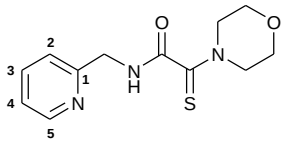

Yield: 0.67 g (84%). Mp: 108–110 °C. ^{1}H NMR (500.13 MHz, $CDCl_3$): δ 3.78–3.79 (m, 2H, CH_2O), 3.84–3.86 (m, 2H, CH_2O), 3.90–3.92 (m, 2H, CH_2N), 4.24–4.26 (m, 2H, CH_2N), 4.66 (d, 2H, CH_2Py, $^{3}J_{HH}$ = 5.4 Hz), 7.22–7.25 (m, 1H, H(C4)), 7.33 (d, 1H, H(C2), $^{3}J_{HH}$ = 7.9 Hz), 7.65 (br s, 1H, NH), 7.69–7.72 (m, 1H, H(C3)), 8.56 (d, 1H, H(C5), $^{3}J_{HH}$ = 4.9 Hz) ppm. ^{13}C{^{1}H} NMR (125.76 MHz, $CDCl_3$): δ 44.67 (s, CH_2Py), 48.82 and 52.57 (both s, CH_2N), 66.23 and 66.87 (both s, CH_2O), 121.85 (s, C2), 122.64 (s, C4), 137.02 (s, C3), 149.16 (s, C5), 155.45 (s, C1), 164.59 (s, C=O), 192.30 (s, C=S) ppm. ^{15}N NMR (60.85 MHz, $CDCl_3$): δ –269.0 (C(O)NH), –226.0 (Morph), –77.4 (Py) ppm. IR (KBr, ν/cm^{-1}): 538(w), 605(vw), 646(vw), 693(br, vw), 756(w), 886(w), 993(w), 1032(w), 1064(w), 1095(w), 1109(m), 1151(vw), 1239(m), 1274(m), 1301(w), 1353(w), 1439(m), 1480(m), 1498(m), 1542(br, m) (C(O)NH), 1570(w), 1591(w), 1648(s) (νC=O), 2861(w), 2921(w), 2976(w), 3065(w), 3268(br, m) (νNH). Anal. Calcd for $C_{12}H_{15}N_3O_2S$: C, 54.32; H, 5.70; N, 15.84. Found: C, 54.38; H, 5.51; N, 15.69%.

2-Morpholin-4-yl-*N*-(2-pyridin-2-ylethyl)-2-thioxoacetamide, 2

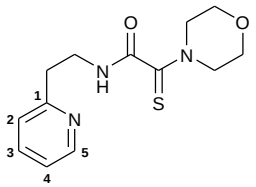

Yield: 0.45 g (54%). Mp: 118–119 °C. ^{1}H NMR (500.13 MHz, $CDCl_3$): δ 3.09 (t, 2H, CH_2Py, $^{3}J_{HH}$ = 6.4 Hz), 3.73–3.83 (m, 8H, $C\underline{H}_2NHC(O)$ + $2CH_2O$ + CH_2N), 4.20–4.22 (m, 2H, CH_2N), 7.20 (dd, 1H, H(C4), $^{3}J_{HH}$ = 7.7 Hz, $^{3}J_{HH}$ = 4.9 Hz), 7.25 (d, 1H, H(C2), $^{3}J_{HH}$ = 7.7 Hz), 7.39 (br s, 1H, NH), 7.67 (dt, 1H, H(C3), $^{3}J_{HH}$ = 7.7 Hz, $^{4}J_{HH}$ = 1.9 Hz), 8.56 (dd, 1H, H(C5), $^{3}J_{HH}$ = 4.9 Hz, $^{4}J_{HH}$ = 1.9 Hz) ppm. ^{13}C{^{1}H} NMR (125.76 MHz, $CDCl_3$): δ 36.41 (s, CH_2Py), 39.08 (s, $\underline{C}H_2NHC(O)$), 48.75 and 52.44 (both s, CH_2N), 66.21 and 66.84 (both s, CH_2O), 121.86 (s, C4), 123.71 (s, C2), 136.99 (s, C3), 149.09 (s, C5), 158.88 (s, C1), 164.53 (s, C=O), 192.83 (s, C=S) ppm. ^{15}N NMR (60.85 MHz, $CDCl_3$): δ –264.0 (C(O)NH), –225.1 (Morph), –77.1 (Py) ppm. IR (KBr, ν/cm^{-1}): 413(w), 512(vw), 533(w), 584(w), 626(w), 722(br, m), 792(m), 843(w), 870(vw), 920(w), 1003(w), 1023(m), 1041(m), 1065(m), 1112(s), 1148(w), 1192(w), 1221(w), 1244(m), 1278(m), 1303(m), 1352(w), 1387(w), 1437(m), 1479(m), 1497(s), 1568(br, m) (C(O)NH), 1589(m), 1625(br, s) and 1652(m) (both νC=O) 2870(m), 2921(m), 2968(w), 3068(w), 3209(br, m) (νNH). Anal. Calcd for $C_{13}H_{17}N_3O_2S$: C, 55.89; H, 6.13; N, 15.04. Found: C, 55.38; H, 6.33; N, 14.90%.

General procedure for the synthesis of ligands 3–5

A suspension of elemental sulfur (0.29 g) and morpholine (7.84 g, 90.00 mmol) in 5 mL of DMF was stirred at room temperature for 1.5 h. Then, a solution of the corresponding chloroacetamide (3.00 mmol) in 7 mL of DMF was added. The reaction mixture was stirred at room temperature for 12 h and poured into 75 mL of distilled water. The resulting precipitate was filtered off, rinsed with an additional portion of water, and dried under vacuum. To remove residual sulfur, the solid obtained was dissolved in acetone and filtered. The solvent was removed under reduced pressure. In the case of compounds **3**, **4**, the resulting residue was recrystallized from ethanol to give the target ligand as yellow (**3**) or light-yellow (**4**) crystalline solids. In the case of compound **5**, the resulting brown viscous oil was left to solidify in air to give the target ligand as a light-brown solid.

2-Morpholin-4-yl-*N*-quinolin-8-yl-2-thioxoacetamide, 3

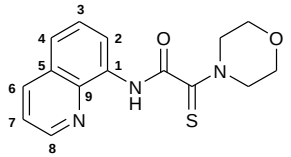

Yield: 0.59 g (65%). Mp: 165–167 °C. ^{1}H NMR (500.13 MHz, $(CD_3)_2SO$): δ 3.72–3.74 (m, 2H, CH_2O), 3.80–3.82 (m, 2H, CH_2O), 3.83–3.85 (m, 2H, CH_2N), 4.16–4.18 (m, 2H, CH_2N), 7.62–7.65 (m, 1H, H(C3)), 7.67 (dd, 1H, H(C7), $^{3}J_{HH}$ = 8.4 Hz, $^{3}J_{HH}$ = 4.3 Hz), 7.78 (dd, 1H, H(C4), $^{3}J_{HH}$ = 8.3 Hz, $^{4}J_{HH}$ = 1.4 Hz), 8.46 (dd, 1H, H(C6), $^{3}J_{HH}$ = 8.4 Hz, $^{4}J_{HH}$ = 1.7 Hz), 8.58 (dd, 1H, H(C2), $^{3}J_{HH}$ = 7.8 Hz, $^{4}J_{HH}$ = 1.3 Hz), 8.95 (dd, 1H, H(C8), $^{3}J_{HH}$ = 4.3 Hz, $^{4}J_{HH}$ = 1.7 Hz), 10.71 (br s, 1H, NH) ppm. $^{13}C\{^{1}H\}$ NMR (125.76 MHz, $(CD_3)_2SO$): δ 48.12 and 52.78 (both s, CH_2N), 65.81 and 66.35 (both s, CH_2O), 117.77 (s, C2), 122.88 (s, C7), 123.68 (s, C4), 127.37 (s, C3), 128.41 (s, C5), 134.05 (s, C1), 137.19 (s, C6), 138.74 (s, C9), 149.79 (s, C8), 163.23 (s, C=O), 190.84 (s, C=S) ppm. ^{15}N NMR (60.85 MHz, $CDCl_3$): δ –257.8 (C(O)NH), –221.2 (Morph), –88.7 (Qui) ppm. IR (KBr, ν/cm^{-1}): 423(vw), 472(w), 493(w), 529(w), 577(w), 632(w), 645(w), 670(m), 753(m), 793(m), 826(m), 859(w), 923(m), 958(w), 1021(m), 1040(m), 1062(w), 1110(m), 1175(w), 1209(m), 1227(m), 1239(m), 1258(m), 1272(m), 1299(w), 1326(m), 1390(m), 1430(m), 1464(m), 1487(s), 1504(s), 1529(br, s) (C(O)NH), 1578(w), 1595(w), 1663(s) (νC=O), 2858(w), 2923(w), 2970(w), 3052(vw), 3331(br, m) (νNH). Anal. Calcd for $C_{15}H_{15}N_3O_2S$: C, 59.78; H, 5.02; N, 13.94. Found: C, 59.67; H, 5.09; N, 14.01%.

***N*-[2-(1,3-Benzothiazol-2-yl)phenyl]-2-morpholin-4-yl-2-thioxoacetamide, 4**

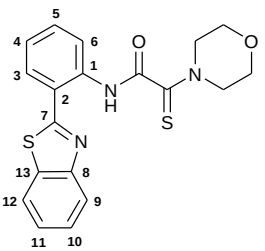

Yield: 0.78 g (66%). Mp: 192–194 °C. ^{1}H NMR (400.13 MHz, $CDCl_3$): δ 3.81–3.83 (m, 2H, CH_2), 3.92–3.94 (m, 2H, CH_2), 3.97–4.00 (m, 2H, CH_2), 4.35–4.38 (m, 2H, CH_2), 7.25 (dt, 1H, H_{Ar}, $^{3}J_{HH}$ = 7.7 Hz, $^{4}J_{HH}$ = 1.1. Hz), 7.45 (dt, 1H, H_{Ar}, $^{3}J_{HH}$ = 7.6 Hz, $^{4}J_{HH}$ = 1.2 Hz), 7.50–7.56 (m, 2H, H_{Ar}), 7.90–7.95 (m, 2H, H_{Ar}), 8.05 (d, 1H, H_{Ar}, $^{3}J_{HH}$ = 8.0 Hz), 8.80 (dd, 1H, H_{Ar}, $^{3}J_{HH}$ = 8.4 Hz, $^{4}J_{HH}$ = 1.2 Hz), 13.56 (br s, 1H, NH) ppm. ^{13}C{^{1}H} NMR (100.61 MHz, $CDCl_3$): δ 48.85 and 52.54 (both s, CH_2N), 66.26 and 66.81 (both s, CH_2O), 119.86 (s, C2), 120.69 (s, C6), 121.26 and 123.00 (both s, C9 and C12), 124.08 (s, C4), 125.85 and 126.61 (both s, C10 and C11), 129.80 and 131.73 (both s, C3 and C5), 133.24 (s, C13), 137.00 (s, C1), 152.65 (s, C8), 162.74 (s, C7), 167.76 (s, C=O), 192.43 (s, C=S) ppm. IR (KBr, ν/cm^{-1}): 456(vw), 518(w), 557(vw), 645(vw), 695(w), 724(m), 742(m), 753(s), 781(w), 858(w), 923(w), 967(m), 1027(m), 1064(m), 1110(s), 1217(m), 1245(m), 1262(m), 1276(m), 1302(m), 1313(m), 1436(m), 1444(m), 1454(s), 1496(s), 1533(br, m) (C(O)NH), 1591(s), 1615(m), 1665(s) (νC=O), 2864(w), 2962(w), 3061(vw). Anal. Calcd for $C_{19}H_{17}N_3O_2S_2 \cdot 0.5H_2O$: C, 58.14; H, 4.62; N, 10.71. Found: C, 57.86; H, 4.26; N, 10.52%.

_N_-[2-(Methylthio)phenyl]-2-morpholin-4-yl-2-thioxoacetamide, 5

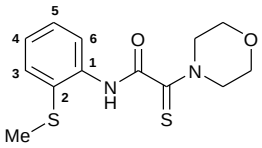

Yield: 0.60 g (67%). Mp: 107–109 °C. ^{1}H NMR (400.13 MHz, $CDCl_3$): δ 2.44 (s, 3H, SMe), 3.80–3.83 (m, 2H, CH_2), 3.86–3.90 (m, 2H, CH_2), 4.00–4.03 (m, 2H, CH_2), 4.27–4.30 (m, 2H, CH_2), 7.11–7.16 (m, 1H, H_{Ar}), 7.30–7.35 (m, 1H, H_{Ar}), 7.52–7.55 (m, 1H, H_{Ar}), 8.26–8.29 (m, 1H, H_{Ar}), 9.50 (br s, 1H, NH) ppm. ^{13}C{^{1}H} NMR (100.61 MHz, $CDCl_3$): δ 18.98 (s, SMe), 49.25 and 52.56 (both s, CH_2N), 66.06 and 66.70 (both s, CH_2O), 120.29 (s, C6), 125.16 (s, C4), 126.58 (s, C2), 128.65 (s, C3), 133.00 (s, C5), 137.33 (s, C1), 161.17 (s, C=O), 191.29 (s, C=S) ppm. IR (KBr, ν/cm^{-1}): 518(w), 632(w), 744(m), 760(w), 841(vw), 923(w), 1028(m), 1063(w), 1110(m), 1211(w), 1228(w), 1242(m), 1265(m), 1274(m), 1301(w), 1312(w), 1386(vw), 1434(m), 1448(m), 1466(w), 1497(s), 1509(s), 1539(br, s) (C(O)NH), 1573(m), 1590(w), 1638(s) and 1664(m) (both νC=O), 2858(w), 2922(w), 2969(w), 3057(w), 3221(br, w) (νNH). Anal. Calcd for $C_{13}H_{16}N_2O_2S_2$: C, 52.68; H, 5.44; N, 9.45. Found: C, 52.71; H, 5.44; N, 9.58%.

2-(Dimethylamino)-_N_-quinolin-8-yl-2-thioxoacetamide, 7

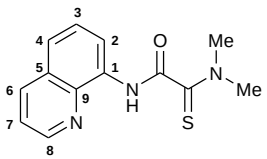

A suspension of elemental sulfur (0.05 g, 1.56 mmol) and 2-chloro-_N_-quinolin-8-ylacetamide (0.34 g, 1.54 mmol) in 10 mL of DMF was refluxed for 5 h. After cooling to room

temperature, the reaction mixture was poured into 50 mL of distilled water. The target product was extracted with chloroform. The organic layer was separated, dried over anhydrous Na_2SO_4, and evaporated to dryness. The resulting residue was purified by column chromatography on silica gel (CH_2Cl_2–MeOH (100:1)) to give the target product as a beige crystalline solid. Yield: 0.04 g (10%). Mp: 172–175 °C. ^{1}H NMR (500.13 MHz, $CDCl_3$): δ 3.53 and 3.55 (both s, 3H + 3H, NMe_2), 7.50 (dd, 1H, H(C7), $^3J_{HH}$ = 8.3 Hz, $^3J_{HH}$ = 4.3 Hz), 7.56–7.61 (m, 2H, H(C3) + H(C4)), 8.20 (dd, 1H, H(C6), $^3J_{HH}$ = 8.3 Hz, $^4J_{HH}$ = 1.7 Hz), 8.77 (dd, 1H, H(C2), $^3J_{HH}$ = 6.3 Hz, $^4J_{HH}$ = 2.7 Hz), 8.87 (dd, 1H, H(C8), $^3J_{HH}$ = 4.3 Hz, $^4J_{HH}$ = 1.7 Hz), 10.74 (br s, 1H, NH) ppm. ^{13}C{^{1}H} NMR (125.76 MHz, $CDCl_3$): δ 42.65 and 43.56 (both s, NMe_2), 116.93 (s, C2), 121.86 (s, C7), 122.64 (s, C4), 127.19 (s, C3), 128.04 (s, C5), 133.87 (s, C1), 136.46 (s, C6), 138.55 (s, C9), 148.65 (s, C8), 162.48 (s, C=O), 192.45 (s, C=S) ppm. ^{15}N NMR (60.85 MHz, $CDCl_3$): δ –257.1 (C(O)NH), –236.0 (NMe_2), –92.4 (Qui) ppm. IR (KBr, ν/cm^{-1}): 444(w), 592(w), 683(w), 754(w), 788(m), 822(m), 852(w), 926(w), 1100(w), 1154(m), 1221(w), 1261(w), 1330(m), 1390(m), 1411(w), 1427(m), 1487(m), 1526(br, s) (C(O)NH), 1578(w), 1597(w), 1670(s) (νC=O), 2852(w), 2922(m), 3047(vw), 3317(br, m) (νNH). Anal. Calcd for $C_{13}H_{13}N_3OS$: C, 60.21; H, 5.05; N, 16.20. Found: C, 60.00; H, 5.57; N, 16.71%.

General procedure for the synthesis of Pd(II) complexes 8–14

A solution of $PdCl_2(NCPh)_2$ (77 mg, 0.200 mmol) in 3 mL of CH_2Cl_2 was slowly added dropwise to a solution of the corresponding ligand (0.200 mmol) and Et_3N (28 μL, 0.200 mmol) in 3 mL of CH_2Cl_2. The reaction mixture was stirred at room temperature for 30 min and left under ambient conditions for 12 h. Evaporation of the mixture to dryness afforded the residue which was purified by column chromatography on silica gel (eluent: CH_2Cl_2–MeOH (50:1)) to give the target complexes as yellow (**8**, **9**) or orange (**10–14**) crystalline solids.

Complex [κ^3-*S,N,N*-(L)Pd(II)Cl], 8

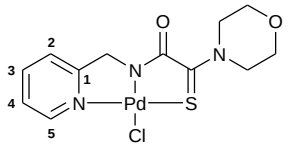

Yield: 53 mg (65%). Mp: >225 °C (dec.). ^{1}H NMR (500.13 MHz, $CDCl_3$): δ 3.84–3.86 (m, 2H, CH_2O), 3.96–3.98 (m, 2H, CH_2O), 4.26–4.28 (m, 2H, CH_2N), 4.94 (s, 2H, CH_2Py), 5.05–5.07 (m, 2H, CH_2N), 7.36–7.39 (m, 1H, H(C4)), 7.42 (d, 1H, H(C2), $^3J_{HH}$ = 7.8 Hz), 7.89 (dt, 1H, H(C3), $^3J_{HH}$ = 7.8 Hz, $^4J_{HH}$ = 1.7 Hz), 8.97 (d, 1H, H(C5), $^3J_{HH}$ = 5.6 Hz) ppm. ^{13}C{^{1}H} NMR (125.76 MHz, $CDCl_3$): δ 49.73 and 53.57 (both s, CH_2N), 57.20 (s, CH_2Py), 66.37 and 67.59 (both s, CH_2O), 121.37 (s, C2), 123.18 (s, C4), 138.99 (s, C3), 148.67 (s, C5), 164.78 (s, C1), 165.99 (s, C=O), 190.75 (s, C=S) ppm. ^{15}N NMR (50.67 MHz, $CDCl_3$): δ –242.8 (C(O)N), –206.5 (Morph), –143.4 (Py) ppm. IR (KBr, ν/cm^{-1}): 496(w), 639(vw), 708(vw), 762(m),

858(w), 934(w), 1027(m), 1052(w), 1091(w), 1105(m), 1159(w), 1177(w), 1214(w), 1252(m), 1269(m), 1301(w), 1372(m), 1438(m), 1484(w), 1528(s), 1567(w), 1612(sh, m) and 1626(s) (*ν*C=O), 2858(w), 2925(w), 3039(w). Anal. Calcd for $C_{12}H_{14}ClN_3O_2PdS$: C, 35.48; H, 3.47; N, 10.34. Found: C, 34.84; H, 3.55; N, 10.04%.

Complex [κ^3-*S,N,N*-(L)Pd(II)Cl], 9

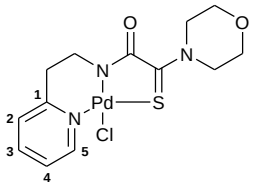

Yield: 71 mg (84%). Mp: > 250 °C. ^{1}H NMR (600.22 MHz, $CDCl_3$): δ 3.17–3.19 (m, 2H, CH_2Py), 3.34 (br s, 2H, C$\underline{H}_2$NC(O)), 3.81–3.83 (m, 2H, CH_2O), 3.94–3.96 (m, 2H, CH_2O), 4.23–4.24 (m, 2H, CH_2N), 5.01–5.03 (m, 2H, CH_2N), 7.33–7.36 (m, 2H, H(C2) + H(C4)), 7.84 (dt, 1H, H(C3), $^3J_{HH}$ = 7.7 Hz, $^4J_{HH}$ = 1.1 Hz), 9.26 (d, 1H, H(C5), $^3J_{HH}$ = 5.7 Hz) ppm. ^{13}C{^{1}H} NMR (150.93 MHz, $CDCl_3$): δ 40.03 (s, CH_2Py), 41.60 (s, $\underline{C}H_2$NC(O)), 50.44 and 53.98 (both s, CH_2N), 66.40 and 67.57 (both s, CH_2O), 123.09 (s, C4), 124.65 (s, C2), 139.38 (s, C3), 152.66 (s, C5), 159.15 (s, C1), 168.22 (s, C=O), 190.19 (s, C=S) ppm. ^{15}N NMR (60.85 MHz, $CDCl_3$): δ –240.0 (C(O)N), –211.1 (Morph), –147.6 (Py) ppm. IR (KBr, *ν*/cm^{-1}): 432(vw), 529(w), 584(vw), 642(w), 758(w), 769(m), 778(w), 850(w), 913(w), 1030(m), 1062(w), 1111(m), 1148(w), 1232(m), 1250(m), 1270(m), 1305(m), 1356(w), 1442(m), 1482(m), 1530(s), 1608(s) (*ν*C=O), 2842(w), 2923(w), 3037(w). Far IR (nujol, *ν*/cm^{-1}): 205(m), 244(m), 281(m), 319(s), 353(w), 392(w), 416(w), 432(w), 454(w), 528(m), 584(m). Anal. Calcd for $C_{13}H_{16}ClN_3O_2PdS$: C, 37.16; H, 3.84; N, 10.00. Found: C, 37.29; H, 3.81; N, 10.06%.

Complex [κ^3-*S,N,N*-(L)Pd(II)Cl], 10

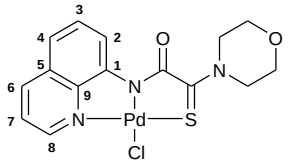

Yield: 77 mg (87%). Mp: >250 °C. ^{1}H NMR (500.13 MHz, $(CD_3)_2SO$): δ 3.84–3.86 (m, 2H, CH_2O), 3.91–3.93 (m, 2H, CH_2O), 4.26–4.28 (m, 2H, CH_2N), 4.90–4.92 (m, 2H, CH_2N), 7.63 (t, 1H, H(C3), $^3J_{HH}$ = 8.0 Hz), 7.75 (dd, 1H, H(C4), $^3J_{HH}$ = 8.0 Hz, $^4J_{HH}$ = 1.1 Hz), 7.78 (dd, 1H, H(C7), $^3J_{HH}$ = 8.3 Hz, $^3J_{HH}$ = 5.0 Hz), 8.69 (dd, 1H, H(C6), $^3J_{HH}$ = 8.3 Hz, $^4J_{HH}$ = 1.6 Hz), 8.88–8.90 (m, 2H, H(C2) + H(C8)) ppm. ^{13}C{^{1}H} NMR (125.76 MHz, $(CD_3)_2SO$): δ 51.45 and 54.07 (both s, CH_2N), 66.14 and 66.98 (both s, CH_2O), 123.02 and 123.10 (both s, C2 and C4), 123.45 (s, C7), 129.51 (s, C3), 130.63 (s, C5), 140.13 (s, C6), 146.24 (s, C1), 146.60 (s, C9), 148.41 (s, C8), 164.52 (s, C=O), 188.33 (s, C=S) ppm. ^{15}N NMR (60.85 MHz, $CDCl_3$): δ –199.9 (Morph), –152.9 (Qui) ppm. IR (KBr, *ν*/cm^{-1}): 532(w), 651(vw), 753(m), 779(w), 826(m),

872(w), 921(w), 955(w), 1034(m), 1060(m), 1111(m), 1168(w), 1255(m), 1271(m), 1332(m), 1382(s), 1438(m), 1462(s), 1503(s), 1527(m), 1571(w), 1622(s) (*ν*C=O), 2854(w), 2924(m), 3049(w). Anal. Calcd for $C_{15}H_{14}ClN_3O_2PdS$: C, 40.74; H, 3.19; N, 9.50. Found: C, 40.62; H, 3.14; N, 9.34%.

Complex [κ^3-*S,N,N*-(L)Pd(II)Cl], 11

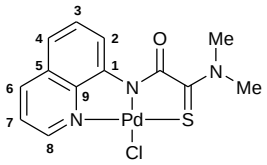

Yield: 66 mg (82%). Mp: >250 °C (dec.). ^{1}H NMR (600.22 MHz, $CDCl_3$): δ 3.63 and 4.04 (both s, 3H + 3H, NMe_2), 7.50–7.53 (m, 3H, H(C3) + H(C4) + H(C7)), 8.31 (dd, 1H, H(C6), $^3J_{HH}$ = 8.3 Hz, $^4J_{HH}$ = 1.6 Hz), 8.94–8.97 (m, 1H, H(C2)), 9.07 (dd, 1H, H(C8), $^3J_{HH}$ = 5.0 Hz, $^4J_{HH}$ = 1.6 Hz) ppm. ^{13}C{^{1}H} NMR (150.93 MHz, $CDCl_3$): δ 43.61 and 47.03 (both s, NMe_2), 121.60 (s, C7), 122.32 (s, C4), 123.12 (s, C2), 129.08 (s, C3), 130.22 (s, C5), 138.61 (s, C6), 146.60 (s, C1), 147.25 (s, C9), 147.92 (s, C8), 164.68 (s, C=O), 191.11 (s, C=S) ppm. ^{15}N NMR (50.67 MHz, $CDCl_3$): δ –218.3 (NMe_2), –148.4 (Qui) ppm. IR (KBr, *ν*/cm^{-1}): 472(w), 583(w), 634(w), 755(m), 783(m), 825(m), 948(w), 1043(w), 1095(w), 1163(w), 1210(w), 1233(w), 1254(w), 1333(m), 1381(m), 1406(m), 1462(m), 1502(m), 1551(m), 1571(m), 1636(s) (*ν*C=O), 2851(vw), 2921(w), 3014(w), 3063(w). Anal. Calcd for $C_{13}H_{12}ClN_3OPdS$: C, 39.02; H, 3.02; N, 10.50. Found: C, 39.04; H, 2.97; N, 10.51%.

Complex [κ^3-*S,N,N*-(L)Pd(II)Cl], 12

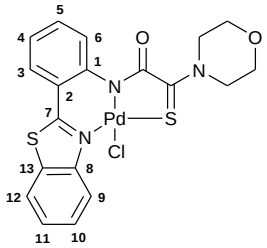

Yield: 74 mg (70%). Mp: >240 °C (dec.). ^{1}H NMR (500.13 MHz, $CDCl_3$): δ 3.89–3.91 (m, 2H, CH_2O), 4.02–4.04 (m, 2H, CH_2O), 4.30–4.31 (m, 2H, CH_2N), 4.56–4.58 (m, 2H, CH_2N), 7.20 (ddd, 1H, H(C4), $^3J_{HH}$ = 7.9 Hz, $^3J_{HH}$ = 7.3 Hz, $^4J_{HH}$ = 1.2 Hz), 7.46–7.50 (m, 2H, H(C5) + H(C10)), 7.59 (ddd, 1H, H(C11), $^3J_{HH}$ = 8.6 Hz, $^3J_{HH}$ = 7.3 Hz, $^4J_{HH}$ = 1.3 Hz), 7.75 (dd, 1H, H(C3), $^3J_{HH}$ = 7.9 Hz, $^4J_{HH}$ = 1.6 Hz), 7.85 (dd, 1H, H(C9), $^3J_{HH}$ = 8.1 Hz, $^4J_{HH}$ = 1.3 Hz), 8.29 (dd, 1H, H(C6), $^3J_{HH}$ = 8.5 Hz, $^4J_{HH}$ = 1.2 Hz), 9.36 (dd, 1H, H(C12), $^3J_{HH}$ = 8.6 Hz, $^4J_{HH}$ = 1.2 Hz) ppm. ^{13}C{^{1}H} NMR (125.76 MHz, $CDCl_3$): δ 51.93 and 53.47 (both s, CH_2N), 66.42 and 67.02 (both s, CH_2O), 121.34 (s, C9), 124.71 and 124.74 (both s, C4 and C6), 125.56 (s, C12), 126.17 (s, C2), 126.60 (s, C10), 127.31 (s, C11), 131.04 (s, C3), 132.69 (s, C5), 133.22 (s, C13), 141.45 (s, C1), 151.04 (s, C8), 166.22 (s, C=O), 166.67 (s, C7), 193.20 (s, C=S) ppm. IR (KBr,

ν/cm^{-1}): 508(w), 644(w), 668(vw), 728(w), 755(s), 892(w), 949(w), 987(w), 1029(m), 1053(m), 1105(m), 1118(m), 1168(w), 1231(m), 1251(m), 1270(s), 1305(m), 1323(m), 1387(w), 1440(m), 1458(m), 1478(s), 1496(m), 1542(s), 1560(w), 1592(m), 1627(s) (νC=O), 2853(w), 2923(w), 3074(w), 3095(w). Anal. Calcd for $C_{19}H_{16}ClN_3O_2PdS_2$: C, 43.52; H, 3.08; N, 8.01. Found: C, 43.59; H, 3.04; N, 7.97%.

Complex [κ^3-*S,N,S*-(L)Pd(II)Cl], 13

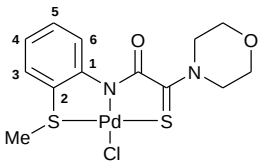

Yield: 82 mg (93%). Mp: >240 °C (dec.). ^{1}H NMR (400.13 MHz, $CDCl_3$): δ 2.91 (s, 3H, SMe), 3.89–3.92 (m, 2H, CH_2), 3.98–4.00 (m, 2H, CH_2), 4.26–4.29 (m, 2H, CH_2), 4.80–4.90 (m, 2H, CH_2), 7.11–7.15 (m, 1H, H_{Ar}), 7.29–7.33 (m, 1H, H_{Ar}), 7.39 (dd, 1H, H_{Ar}, $^3J_{HH}$ = 7.8 Hz, $^4J_{HH}$ = 1.5 Hz), 8.80 (dd, 1H, H_{Ar}, $^3J_{HH}$ = 8.6 Hz, $^4J_{HH}$ = 1.2 Hz) ppm. ^{13}C{^{1}H} NMR (100.61 MHz, $CDCl_3$): δ 27.67 (s, SMe), 51.81 and 53.23 (both s, CH_2N), 66.12 and 67.23 (both s, CH_2O), 124.66 (s, C4 or C6), 125.22 (s, C2), 125.43 (s, C6 or C4), 130.59 and 132.44 (both s, C3 and C5), 152.13 (s, C1), 165.37 (s, C=O), 191.08 (s, C=S) ppm. IR (KBr, ν/cm^{-1}): 419(w), 528(w), 650(w), 762(s), 890(m), 946(m), 1035(m), 1060(w), 1119(s), 1178(m), 1208(w), 1249(s), 1267(s), 1302(m), 1321(m), 1419(m), 1437(m), 1466(s), 1498(s), 1579(w), 1611(s) (νC=O), 2867(w), 2927(w), 3063(w). Anal. Calcd for $C_{13}H_{15}ClN_2O_2PdS_2$: C, 35.71; H, 3.46; N, 6.41. Found: C, 35.57; H, 3.44; N, 6.29%.

Complex [κ^3-*S,N,S*-(L)Pd(II)Cl], 14

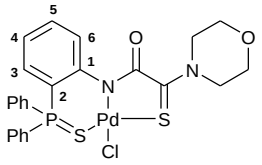

Yield: 100 mg (82%). Mp: >250 °C. ^{31}P{^{1}H} NMR (161.98 MHz, $CDCl_3$): δ 38.65 ppm. ^{1}H NMR (400.13 MHz, $CDCl_3$): δ 3.61–3.63 (m, 2H, CH_2O), 3.86–3.88 (m, 2H, CH_2O), 4.08–4.13 (m, 4H, CH_2N), 6.81 (dd, 1H, H(C3), $^3J_{HP}$ = 14.8 Hz, $^3J_{HH}$ = 7.8 Hz), 7.05–7.09 (m, 1H, H_{Ar}), 7.56–7.61 (m, 6H, H_{Ar}), 7.64–7.68 (m, 2H, H_{Ar}), 7.77–7.82 (dd, 4H, *o*-H in P(S)Ph_2, $^3J_{HP}$ = 13.6 Hz, $^3J_{HH}$ = 7.7 Hz) ppm. ^{13}C{^{1}H} NMR (100.61 MHz, $CDCl_3$): δ 51.37 and 52.86 (both s, CH_2N), 65.97 and 66.62 (both s, CH_2O), 123.20 (d, C2, $^1J_{CP}$ = 86.5 Hz), 124.23 (d, C4, $^3J_{CP}$ = 13.1 Hz), 128.84 (d, *m*-C in P(S)Ph_2, $^3J_{CP}$ = 13.1 Hz), 128.9 (d, C6, $^3J_{CP}$ = 8.0 Hz), 130.75 (d, C3, $^2J_{CP}$ = 9.1 Hz), 132.57 (d, *o*-C in P(S)Ph_2, $^2J_{CP}$ = 11.1 Hz), 132.59 (d, *p*-C in P(S)Ph_2, $^4J_{CP}$ = 2.2 Hz), 133.09 (d, C5, $^4J_{CP}$ = 2.0 Hz), 148.27 (d, C1, $^2J_{CP}$ = 3.0 Hz), 167.07 (s, C=O), 192.98 (s, C=S) ppm (the signals of *ipso*-C carbon nuclei in P(S)Ph_2 were not observed). IR (KBr, ν/cm^{-1}):

467(w), 515(m), 523(m), 600(m) (*ν*P=S), 620(w), 691(m), 713(m), 755(m), 789(s), 848(w), 895(w), 938(w), 951(w), 998(w), 1033(w), 1069(w), 1107(m), 1184(w), 1208(w), 1271(m), 1307(w), 1341(m), 1437(s), 1464(m), 1480(w), 1561(m), 1579(m), 1624(s) (*ν*C=O), 2864(w), 2928(w), 2960(w), 3047(w). Anal. Calcd for $C_{24}H_{22}ClN_2O_2PPdS_2$: C, 47.46; H, 3.65; N, 4.61. Found: C, 47.61; H, 3.74; N, 4.35%.

General procedure for the reactions of ligands 1–4 with $PdCl_2(NCPh)_2$ in dichloromethane in the absence of a base

A solution of $PdCl_2(NCPh)_2$ (33 mg, 0.086 mmol) in 3.5 mL of CH_2Cl_2 was slowly added dropwise to a solution of the corresponding ligand (0.086 mmol) in 2 mL of CH_2Cl_2. The reaction mixture was left under ambient conditions for 1 day. The resulting mixture was filtered; the filtrate was purified by column chromatography on silica gel (eluent: neat CH_2Cl_2, then CH_2Cl_2–EtOH (100:1 (**1**, **2**) or 200:1 (**3**, **4**)) followed by recrystallization from CH_2Cl_2/Et_2O/hexane (1:2:2) to give the corresponding pincer-type complexes in 59% (**8**), 47% (**9**), 94% (**10**), and 85% (**12**) yields. In the case of ligand **9**, the dark-red crystals and beige powder precipitated from the reaction mixture were collected by filtration, rinsed with CH_2Cl_2 and Et_2O, and dried under vacuum to give 17 mg of complex **15**, which was characterized by IR spectroscopy, elemental and single-crystal X-ray diffraction analyses.

Complex $[\kappa^1\text{-}S\text{-(LH)}]^+[PdCl_3]^-$, 15

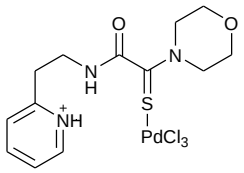

Yield: 40%. IR (KBr, ν/cm^{-1}): 529(w), 569(w), 627(w), 734(w), 756(m), 863(vw), 892(vw), 913(vw), 1027(m), 1061(w), 1109(m), 1182(vw), 1243(m), 1270(m), 1295(w), 1384(w), 1445(m), 1468(w), 1535(br, s) (C(O)NH), 1618(m), 1627(m), 1682(s) (*ν*C=O), 2858(w), 2903(w), 2956(w), 3055(w), 3091(vw), 3157(vw), 3245(w) and 3293(br, w) (both *ν*NH). Anal. Calcd for $C_{13}H_{18}Cl_3N_3O_2PdS$: C, 31.66; H, 3.68; N, 8.52. Found: C, 31.45; H, 3.77; N, 8.22%.

Solid-phase cyclopalladation promoted or accomplished by grinding in a mortar

$PdCl_2(NCPh)_2$ (33 mg, 0.086 mmol) and the corresponding ligand (0.086 mmol) were manually ground in a mortar for several minutes. In the case of ligands **1**, **2**, **4**, and **6**, the resulting slightly oily powders were collected in glass test tubes and left under ambient conditions for 2 days. During this period, the reaction mixtures converted to semi-solids (amorphous masses), which then slowly solidified and lightened to give free-flowing powders. The latter were analyzed by IR spectroscopy without any workup (Figs. S38, S41, S44, and S48

in the Supporting Information). In the case of ligands **1** and **2**, the resulting residues were purified by column chromatography on silica gel (eluent: CH_2Cl_2/EtOH (100:1), 150–170 mL) to give complexes **8** and **9** in 80% and 46% yields, respectively. The IR spectroscopic analysis of the residues obtained with ligands **4** and **6** revealed the quantitative formation of the target pincer products which required no further purification (in the case of complex **14**) or simple rinsing with hexane to remove residual benzonitrile (in the case of complex **12**; for the ^{1}H NMR spectrum of the pure product, see Fig. S45 in the Supporting Information). Analyses found for complex **12** after rinsing with hexane and drying under vacuum: C, 43.67; H, 3.21; N, 8.07% (*cf.* with the calculated values: C, 43.52; H, 3.08; N, 8.01). Analyses found for complex **14** without any workup: C, 47.70; H, 3.72; N, 4.56% (the calculated values: C, 47.46; H, 3.65; N, 4.61%). In the case of ligands **3** and **5**, already manual grinding using a pestle afforded target pincer complexes which were recovered in quantitative yields after simple rinsing with hexane (for the IR spectra registered before workup, see Figs. S51, S54, and S55 in the Supporting Information; for the ^{1}H NMR spectrum of complex **13** after rinsing with hexane, see Fig. S56 in the Supporting Information). Analyses found for complex **10** after rinsing with hexane and drying under vacuum: C, 40.41; H, 3.29; N, 9.41% (the calculated values: C, 40.74; H, 3.19; N, 9.50%). Analyses found for complex **13** after rinsing with hexane and drying under vacuum: C, 35.75; H, 3.58; N, 6.51% (the calculated values: C, 35.71; H, 3.46; N, 6.41%).

Solid-phase reactions in a vibration ball mill

The reactions were carried out by shaking $PdCl_2(NCPh)_2$ (33 mg, 0.086 μmol) and the corresponding ligand (0.086 μmol) in a Narva DDR GM 9458 electrically powered vibration ball mill equipped with a custom-built agate insert and two agate milling balls. The grinding for 1.5 (for ligand **5**), 3 (for **3**) or 7 (for **1**, **2**, **4**) min afforded dark yellow (in the case of ligands **1** and **2**) or orange (in the case of ligands **3** and **4**) powders, or an orange paste (in the case of ligand **5**), which were analyzed by IR spectroscopy prior to any workup (Figs. S57–S59, S65, S67–S69 in the Supporting Information). In the case of ligands **1**, **2**, and **3**, the crude product was collected by washing the insert and milling balls with CH_2Cl_2 (100–170 mL). The resulting mixture was purified by column chromatography on silica gel (eluent: CH_2Cl_2/EtOH = 100:1, 130–200 mL) to give the target pincer complexes as yellow or orange solids. Yields: 91% (**8**), 66% (**9**), 93% (**10**). Note that, in the case of ligand **2**, passing the resulting CH_2Cl_2 mixture through a filter before purification by column chromatography afforded several crystals of complex **15** (for the IR spectrum of the product, see Fig. S62 in the Supporting Information). In the case of ligand **4**, the mixture obtained after grinding was left under ambient conditions for 3 days. According to the IR spectroscopic analysis (Fig. S66 in the Supporting Information), the cyclopalladation was completed over this period of time and thus afforded neat complex **12** in a quantitative yield.

Anal. Calcd for $C_{19}H_{16}ClN_3O_2PdS_2$: C, 43.52; H, 3.08; N, 8.01. Found: C, 43.54; H, 3.11; N, 7.97%. In the case of ligand **5**, the target pincer product was isolated in a quantitative yield after treatment of the insert and milling balls with hexane followed by filtration and drying under vacuum (for the corresponding IR and NMR spectra, see Fig. S70–S72 in the Supporting Information). Anal. Calcd for $C_{13}H_{15}ClN_2O_2PdS_2$: C, 35.71; H, 3.46; N, 6.41. Found: C, 35.80; H, 3.70; N, 6.29%.

Cytotoxicity studies

The cytotoxicities of the functionalized monothiooxamides and their Pd(II) complexes were studied against human colon (HCT116), breast (MCF7), and prostate (PC3) cancer cell lines as well as non-cancer human embryonic kidney cells (HEK293). All the cell lines were obtained from American Type Culture Collection (ATCC). RPMI-1640 and DMEM media were obtained from Gibco. Fetal bovine serum (FBS) was purchased from HyClone. Cells were cultured in RPMI-1640 (in the case of PC3) or DMEM (in the other cases) media supplemented with 10% FBS and 50 μg/mL gentamicin in a humidified incubator with 5% CO_2 atmosphere. The effect of the compounds on cell viability was estimated using the standard MTT assay (ICN Biomedicals, Germany). Cells were seeded in triplicate at a cell density of 5×10^3/well in 96-well plates in 100 μL complete medium and preincubated for 24 h. The tested compounds were initially dissolved in DMSO. Then the compounds at various concentrations were added to the media. The well plates were incubated for 48 h followed by addition of MTT solution (Sigma) (20 μL, 5 mg/mL). The cells were incubated at 37 °C for further 3 h; then the culture medium was removed, and formazan crystals were dissolved in DMSO (70 μL). The absorbance of the resulting solutions was measured on a multi-well plate reader (Multiskan FC, Thermo scientific) at 540 nm to determine the percentage of surviving cells. The reported values of IC_{50} are the averages of three independent experiments (Table S1 in the Supporting Information). Cisplatin from a commercial source (in the initial form of an infusion concentrate in natural saline solution) was used as a reference.

X-ray diffraction

Single crystals of the compounds explored were obtained by slow crystallization from CH_2Cl_2–EtOAc–Et_2O (**12**), CH_2Cl_2–Et_2O (**14**), and CH_2Cl_2 reaction mixture (**15**). The X-ray diffraction data for **12** and **14** were collected using graphite monochromated Mo-Kα radiation (λ = 0.71073 Å, ω-scans) with a Bruker APEX2 DUO CCD diffractometer at 120 K; those for **15**— with a Bruker D8 Quest diffractometer at 296 K. Using Olex2 [5], the structures were solved with the ShelXT [6] structure solution program *via* Intrinsic Phasing and refined with the XL

refinement package [7] using Least-Squares minimization. The hydrogen atom of the NH group was found in the difference Fourier synthesis, the positions of the other hydrogen atoms were calculated, and they all were refined in the isotropic approximation in a riding model. Crystal data and structure refinement parameters are given in the following table. CCDC 1999306, 1999307, and 2091974 contain the supplementary crystallographic data for **12**, **14**, and **15**, respectively.

Crystal data and structure refinement parameters for **12**, **14**, and **15**.

	12	**14**	**15**
Empirical formula	$C_{20}H_{18}Cl_3N_3O_2PdS_2$	$C_{24}H_{22}ClN_2O_2PPdS_2$	$C_{13}H_{18}Cl_3N_3O_2PdS$
Formula weight	609.24	607.37	493.11
Temperature, K	120	120	296
Crystal system	Monoclinic	Triclinic	Monoclinic
Space group	$P2_1/c$	P-1	$P2_1/c$
Z	4	2	4
a, Å	14.1861(11)	9.1078(10)	14.3859(7)
b, Å	12.4176(10)	9.9172(11)	9.6988(4)
c, Å	13.8527(11)	14.3625(16)	14.1556(6)
α, °	90	109.013(2)	90
β, °	116.8300(10)	98.691(2)	112.584(2)
γ, °	90	95.893(2)	90
V, Å^3	2177.6(3)	1196.3(2)	1823.62(14)
D_{calc} (g cm^{-1})	1.858	1.686	1.796
Linear absorption, μ (cm^{-1})	14.37	11.55	15.82
F(000)	1216	612	984
$2\theta_{max}$, °	56	56	54
Reflections measured	23702	13879	28576
Independent reflections	5265	5752	3983
Observed reflections [$I > 2\sigma(I)$]	4078	5099	3204
Parameters	280	298	208
R1	0.0321	0.0284	0.0410
wR2	0.0660	0.0687	0.1092
GOF	1.025	1.031	1.062
$\Delta\rho_{max}$/ $\Delta\rho_{min}$ (e Å^{-3})	0.652/–0.673	0.607/–0.403	1.061/–0.581

SEM and EDS analysis

The samples of complex **13** obtained by grinding in a mortar or vibration ball mill (dry powders) were placed onto electro-conductive carbon tape adhered to SEM sample holder and then installed in a vacuum chamber of a Prisma E (Thermo Fisher) scanning electron microscope. SEM imaging of the samples was performed at low voltage settings (~1kV) in order to provide surface geometry at a number of magnifications. Energy-dispersive X-ray spectroscopy (EDS) was applied to the samples in color SEM imaging mode to resolve elemental anisotropy of the samples. EDS imaging voltage was set at 30kV to yield elemental composition through whole sample depth at 100x magnification.

References

1. V. Yu. Aleksenko, E. V. Sharova, O. I. Artyushin, D. V. Aleksanyan, Z. S. Klemenkova, Yu. V. Nelyubina, P. V. Petrovskii, V. A. Kozlov, I. L. Odinets. Coordination of P(X)-Modified (X= O, S) N-Aryl-carbamoylmethylphosphine Oxides and Sulfides with Pd(II) and Re(I) Ions: Facile Formation of 6,6-Membered Pincer Complexes Featuring Atropisomerism. *Polyhedron*, **2013**, *51*, 168–179. DOI: 10.1016/j.poly.2012.12.025.
2. (a) A. Shockravi, M. Chaloosi, E. Rostami, D. Heidaryan, A. Shirzadmehr, H. Fattahi, H. Khoshsafar. Modified BINOL Podands: Synthesis of Dinaphthosulfide Podands and Their Application in Spectrophotometric Determination of Toxic Metals. *Phosphorus, Sulfur Silicon Relat. Elem.*, **2007**, *182*, 2115–2123, DOI: 10.1080/10426500701372272.

   (b) Y. Zhang, Z. Li, X. Cao, J. Zhao. Methyltrioxorhenium-Catalyzed Epoxidation of Olefins with Hydrogen Peroxide as an Oxidant and Pyridine N-Oxide Ionic Liquids as Additivies. *J. Mol. Catal. A: Chem.*, **2013**, *366*, 149–155, DOI: 10.1016/j.molcata.2012.09.017.

   (c) L. Tang, X. Dai, K. Zhong, X. Wen, D. Wu. A Phenylbenzothiazole Derived Fluorescent Sensor for Zn(II) Recognition in Aqueous Solution Through "Turn-On" Excited-State Intramolecular Proton Transfer Emission. *J. Fluoresc.*, **2014**, *24*, 1487–1493, DOI: 10.1007/s10895-014-1434-8.

   (d) E. A. Ishmaeva, A. Z. Alimova, Ya. A. Vereshchagina, D. V. Chachkov, O. I. Artyushin, E. V. Sharova. Synthesis, Polarity, and Structure of 2-Chloro-*N*-[2-(methylsulfanyl)phenyl]- and 2-(Diphenylthiophosphoryl)-*N*-[2-(methylsulfanyl)phenyl]acetamides. *Russ. J. Org. Chem.*, **2015**, *51*, 943–946, DOI: 10.1134/S107042801507009X.
3. D. V. Aleksanyan, S. G. Churusova, V. V. Brunova, E. Yu. Rybalkina, O. Yu. Susova, A. S. Peregudov, Z. S. Klemenkova, G. L. Denisov, V. A. Kozlov. Synthesis, Characterization, and Cytotoxic Activity of *N*-Metallated Rhenium(I) Pincer Complexes

with (Thio)phosphoryl Pendant Arms. *J. Organomet. Chem*., **2020**, *926*, 121498, DOI: 10.1016/j.jorganchem.2020.121498.

4. L. J. Bellamy, *The Infrared Spectra of Complex Molecules*, Wiley, New York, **1975**.
5. O. V. Dolomanov, L. J. Bourhis, R. J. Gildea, J. A. K. Howard, H. Puschmann. OLEX2: A Complete Structure Solution, Refinement and Analysis Program. *J. Appl. Crystallogr.*, **2009**, *42*, 339–341, DOI: 10.1107/S0021889808042726.
6. G. M. Sheldrick. SHELXT – Integrated Space-Group and Crystal-Structure Determination. *Acta Crystallogr. A: Found. Adv*., **2015**, *71*, 3–8, DOI: 10.1107/S2053273314026370.
7. G. M. Sheldrick. A Short History of SHELX. *Acta Crystallogr., Sect. A: Found. Crystallogr*., **2008**, *64*, 112−122, DOI: 10.1107/S0108767307043930.

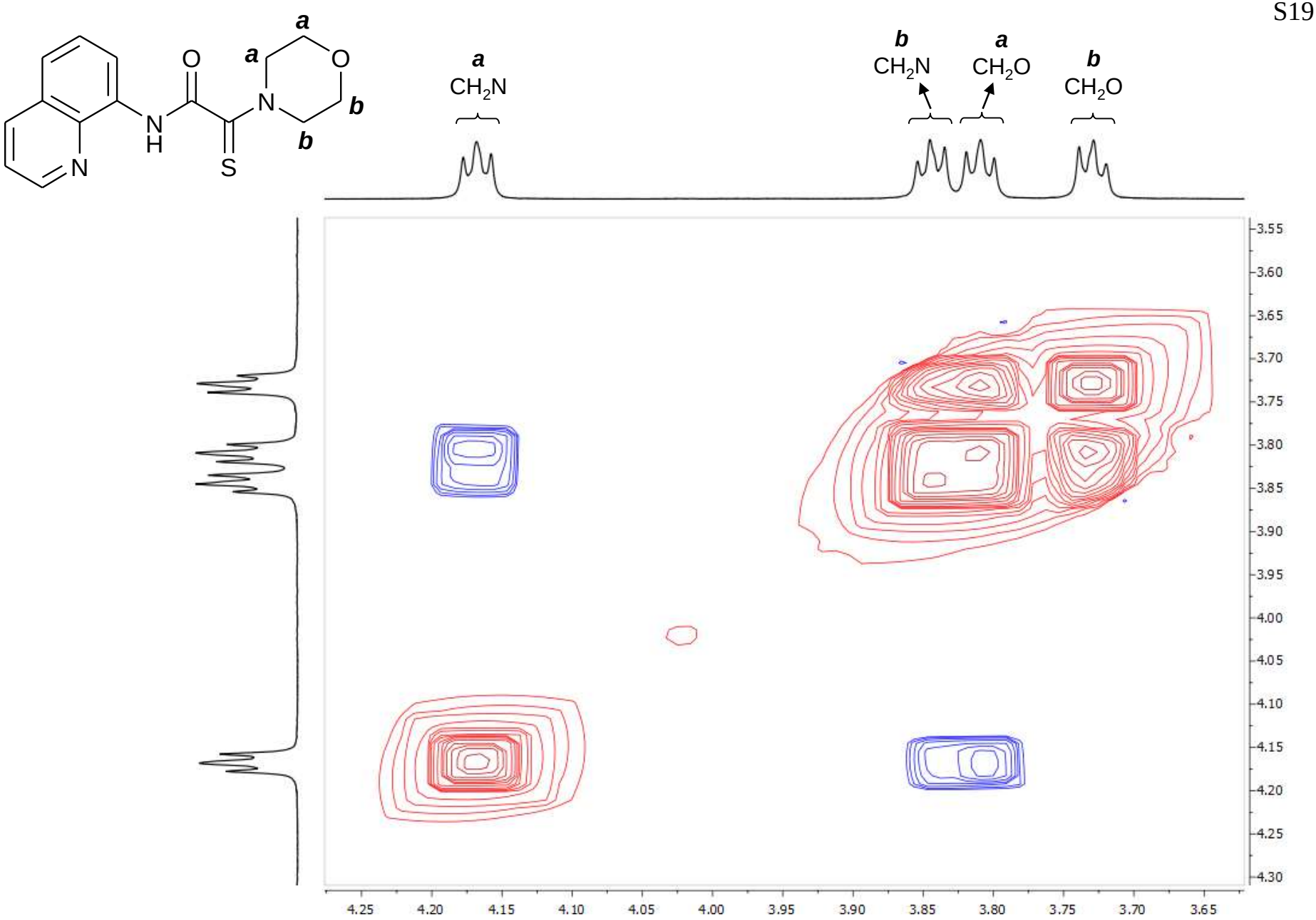

Fig. S1. Extended fragment of the NOESY spectrum of ligand **3** (aliphatic proton region; 500.13 MHz, $CDCl_3$)

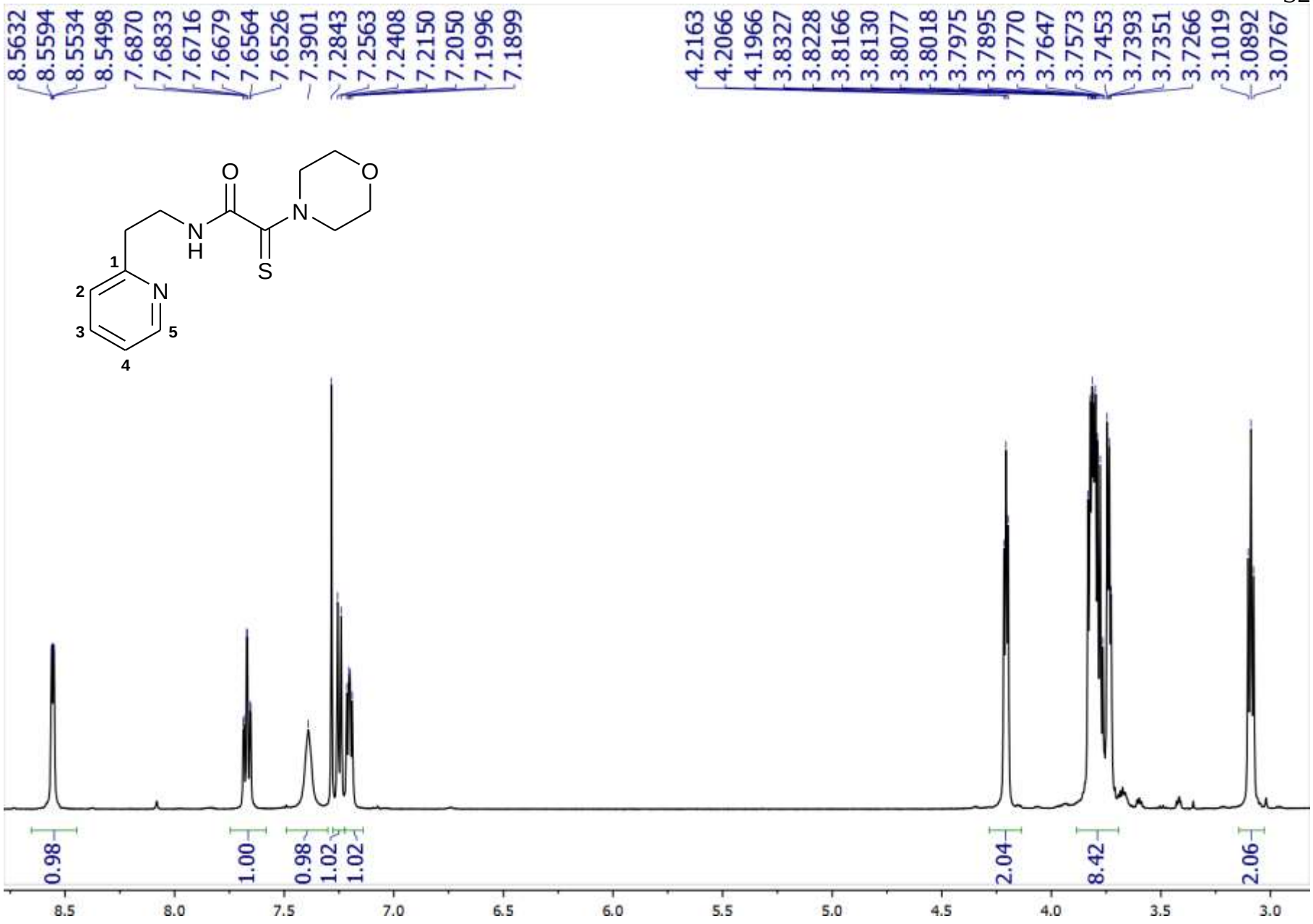

Fig. S2. ^{1}H NMR spectrum of ligand **2** (500.13 MHz, $CDCl_3$)

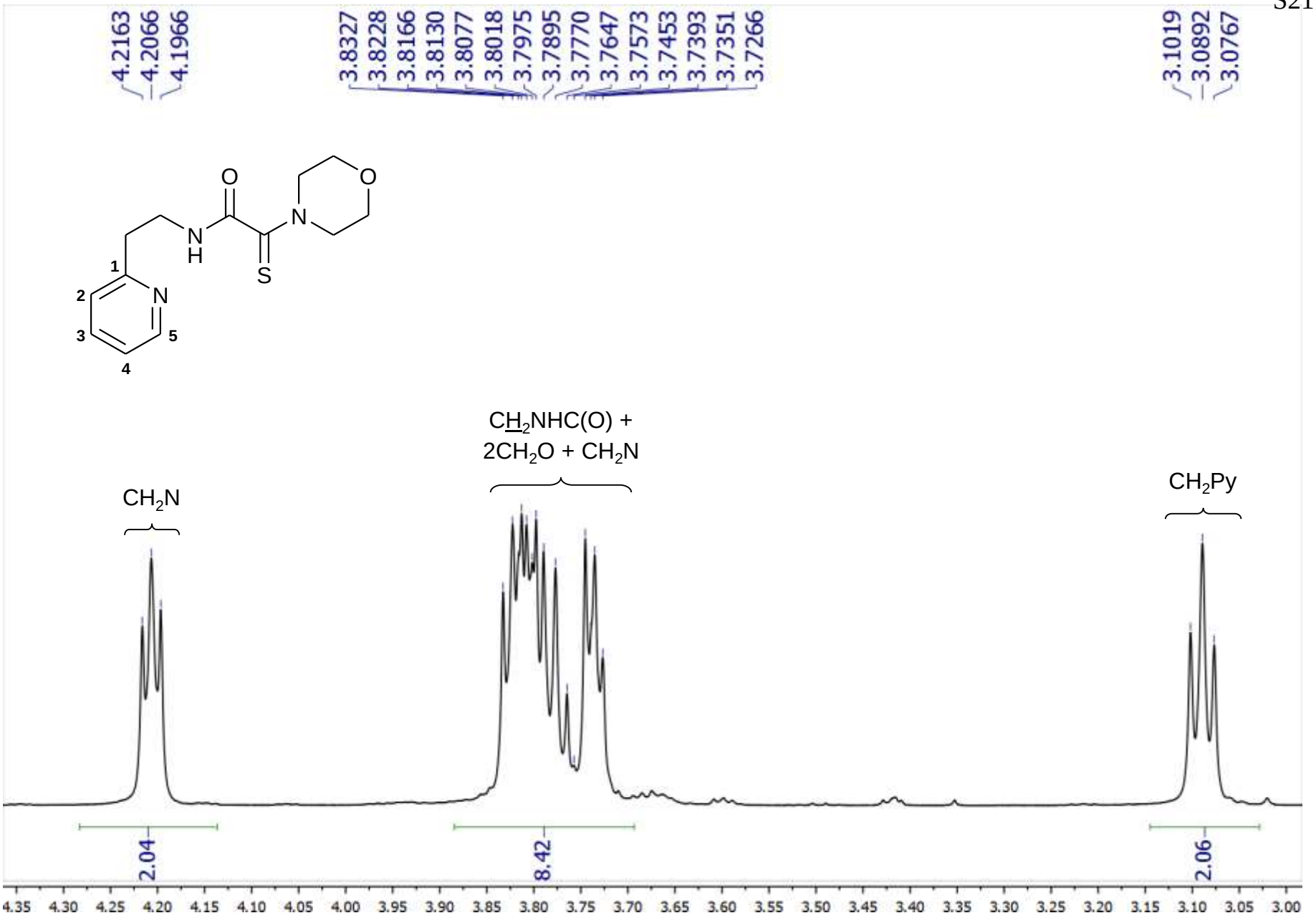

Fig. S3. Extended fragment of the ^{1}H NMR spectrum of ligand **2** (aliphatic proton region; 500.13 MHz, $CDCl_3$)

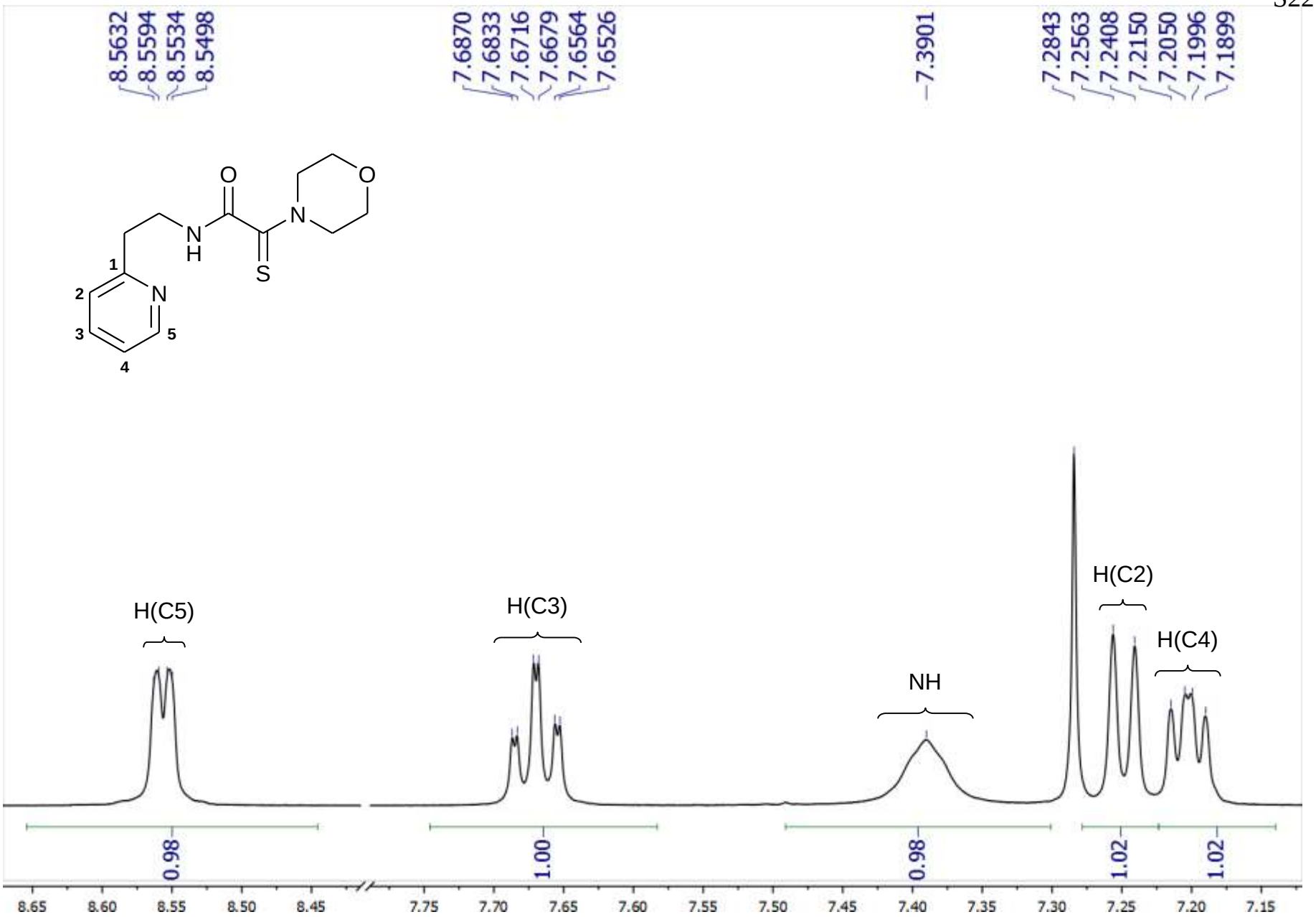

Fig. S4. Extended fragments of the ^{1}H NMR spectrum of ligand **2** (aromatic and NH proton regions; 500.13 MHz, $CDCl_3$)

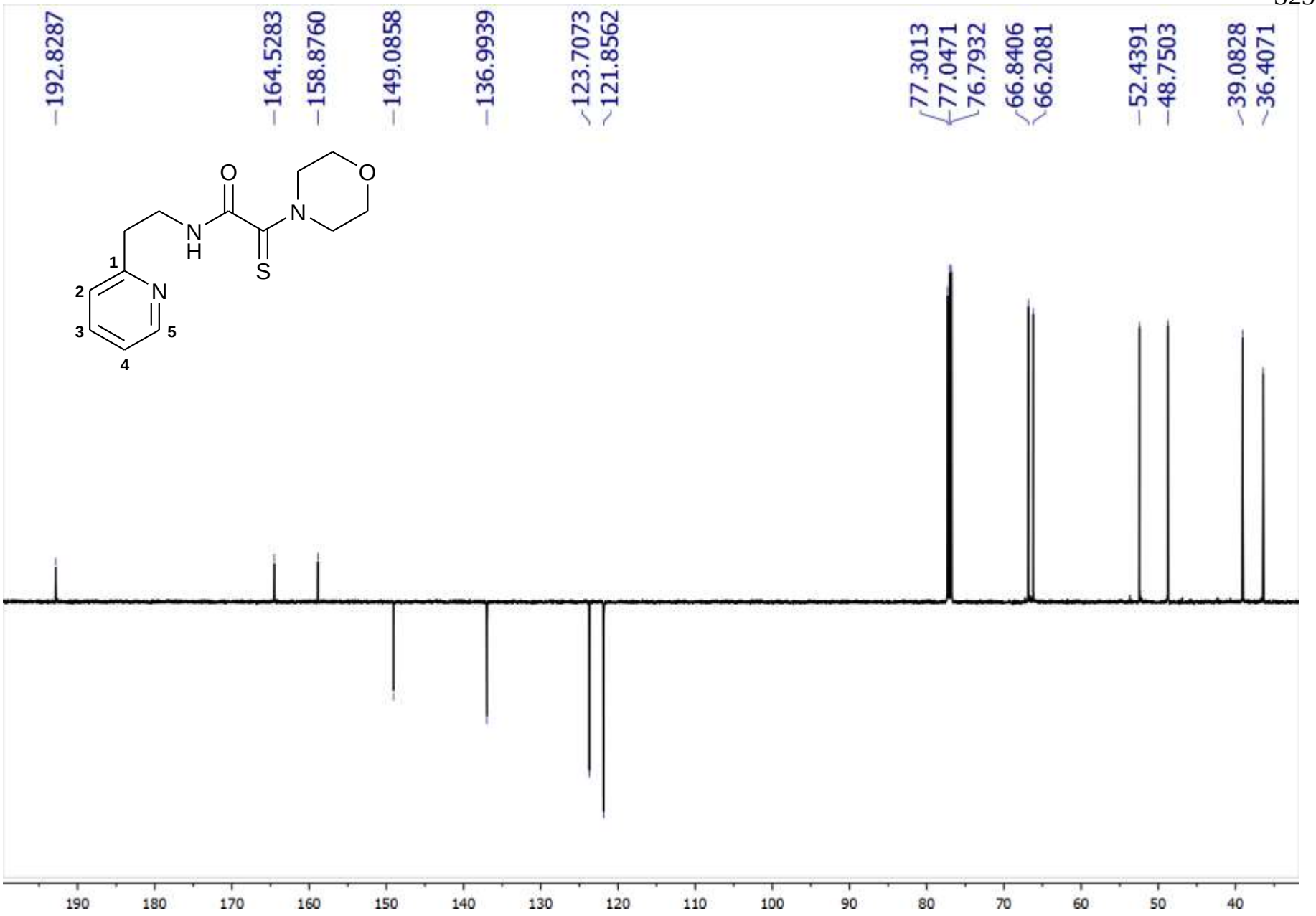

Fig. S5. $^{13}C\{^{1}H\}$ NMR spectrum of ligand **2** (125.76 MHz, $CDCl_3$)

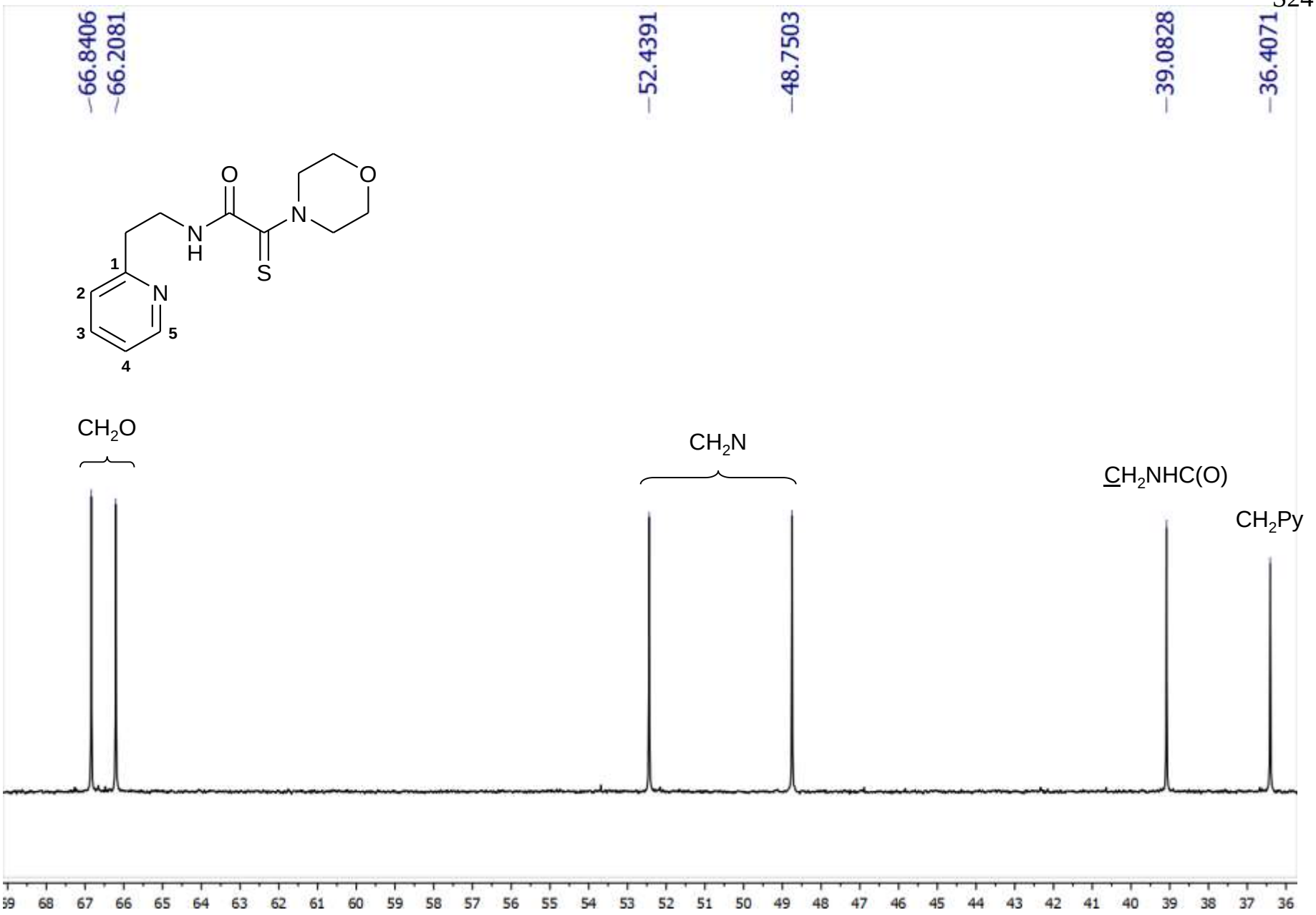

Fig. S6. Extended fragment of the $^{13}C\{^{1}H\}$ NMR spectrum of ligand **2** (aliphatic carbon nuclei; 125.76 MHz, $CDCl_3$)

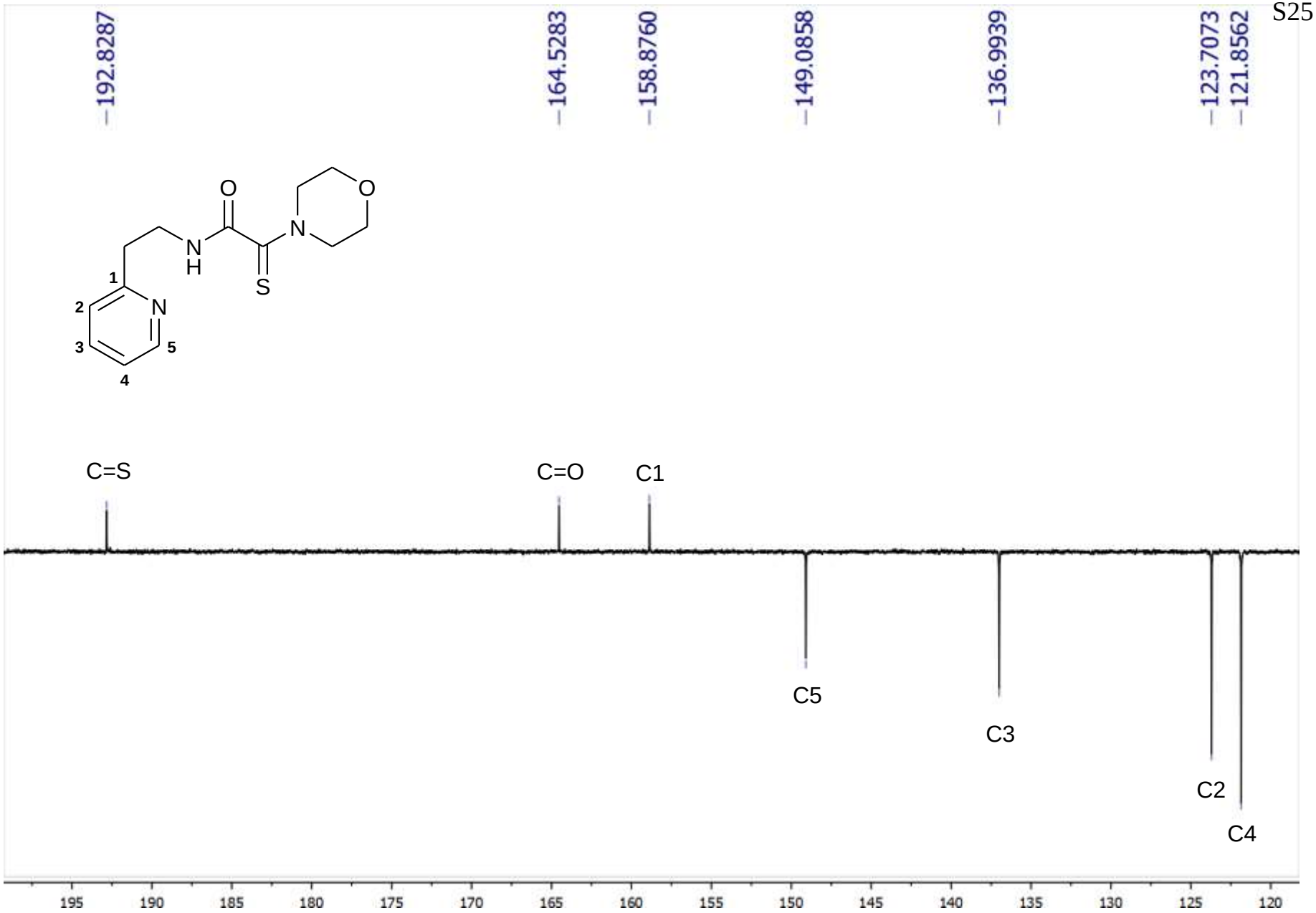

Fig. S7. Extended fragment of the $^{13}C\{^{1}H\}$ NMR spectrum of ligand **2** (aromatic and (thio)carbonyl carbon nuclei; 125.76 MHz, $CDCl_3$)

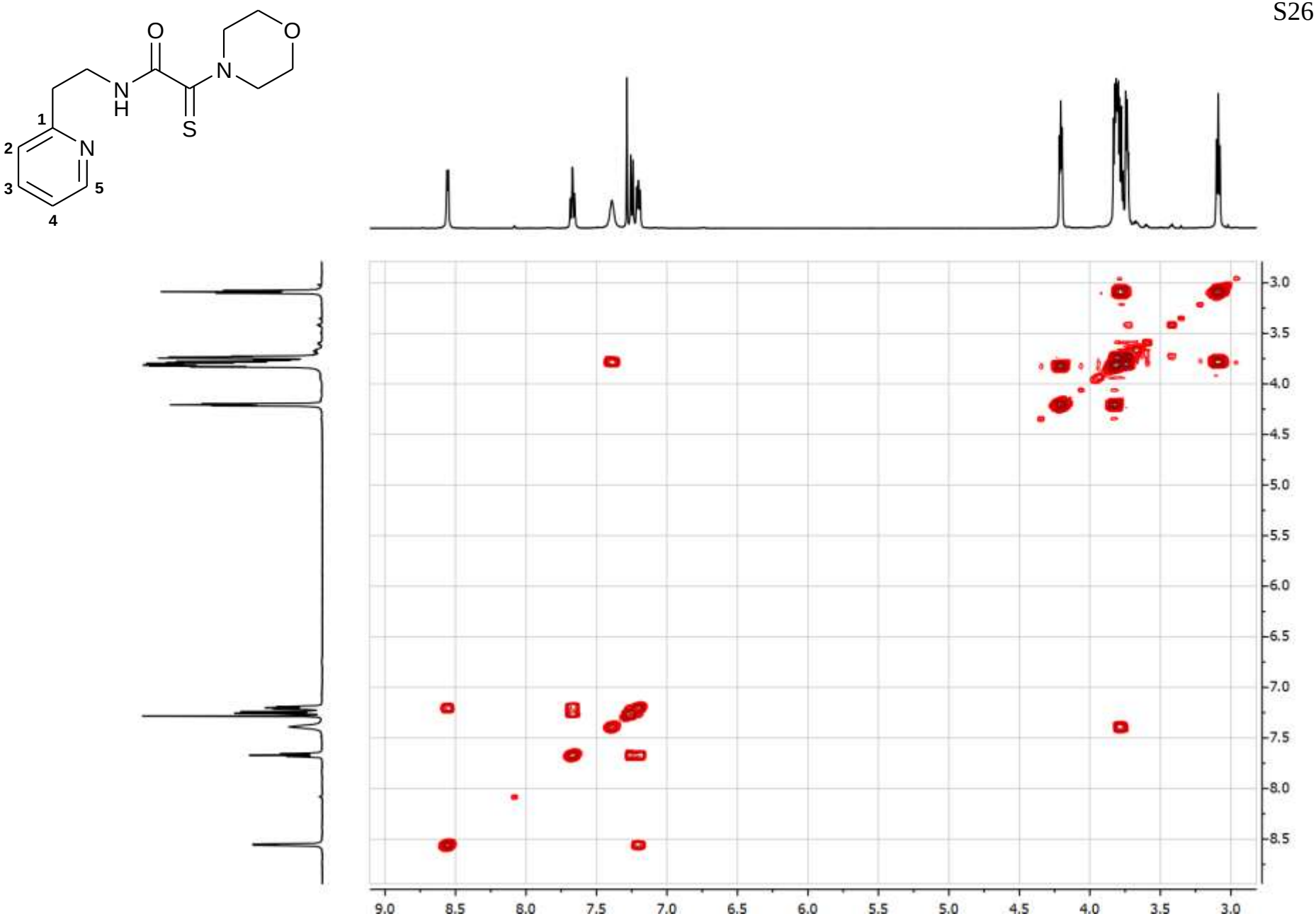

Fig. S8. $^{1}H-^{1}H$ COSY spectrum of ligand **2** (500.13 MHz, $CDCl_3$)

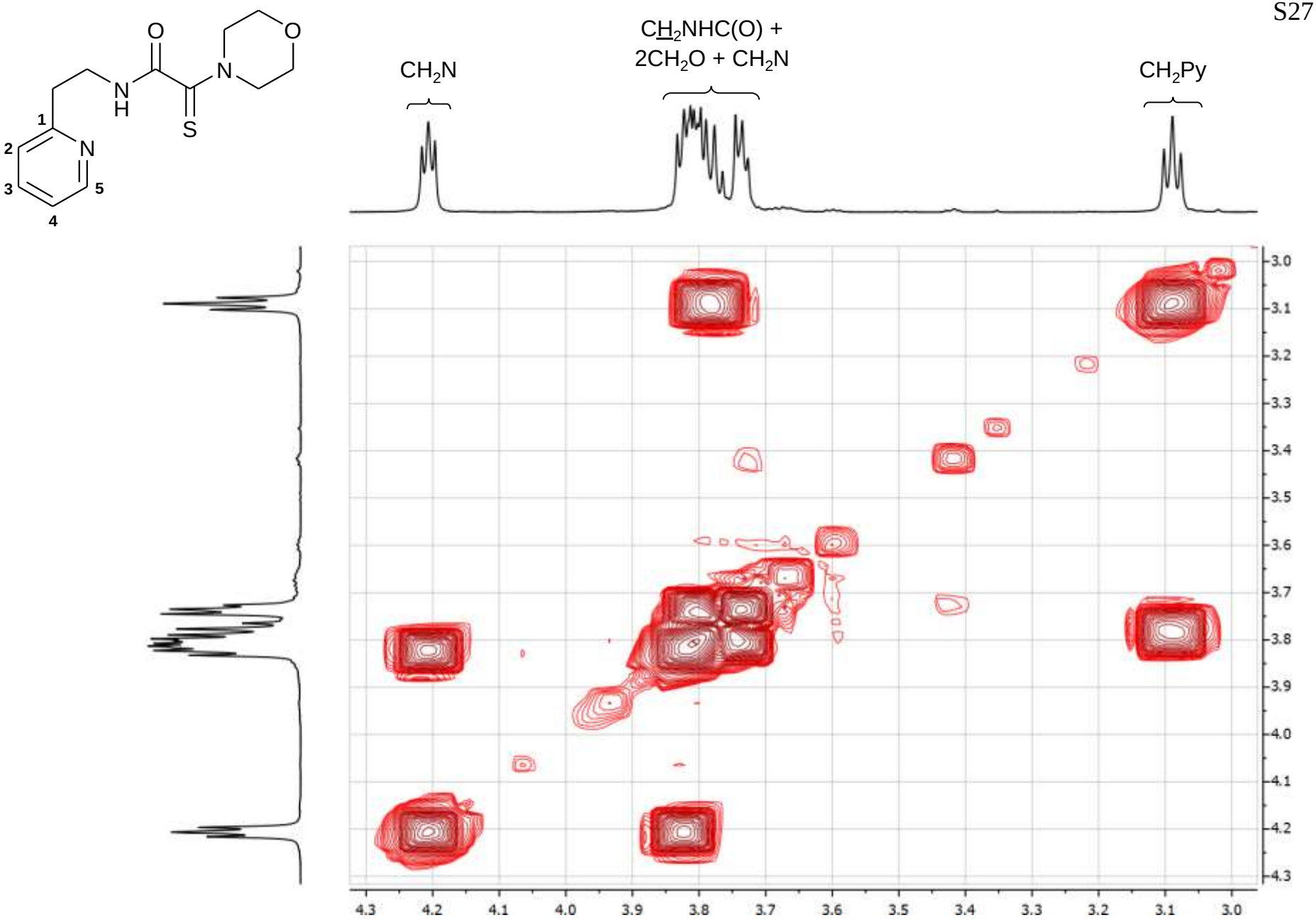

Fig. S9. Extended fragment of the $^{1}H-^{1}H$ COSY spectrum of ligand **2** (aliphatic proton region; 500.13 MHz, $CDCl_3$)

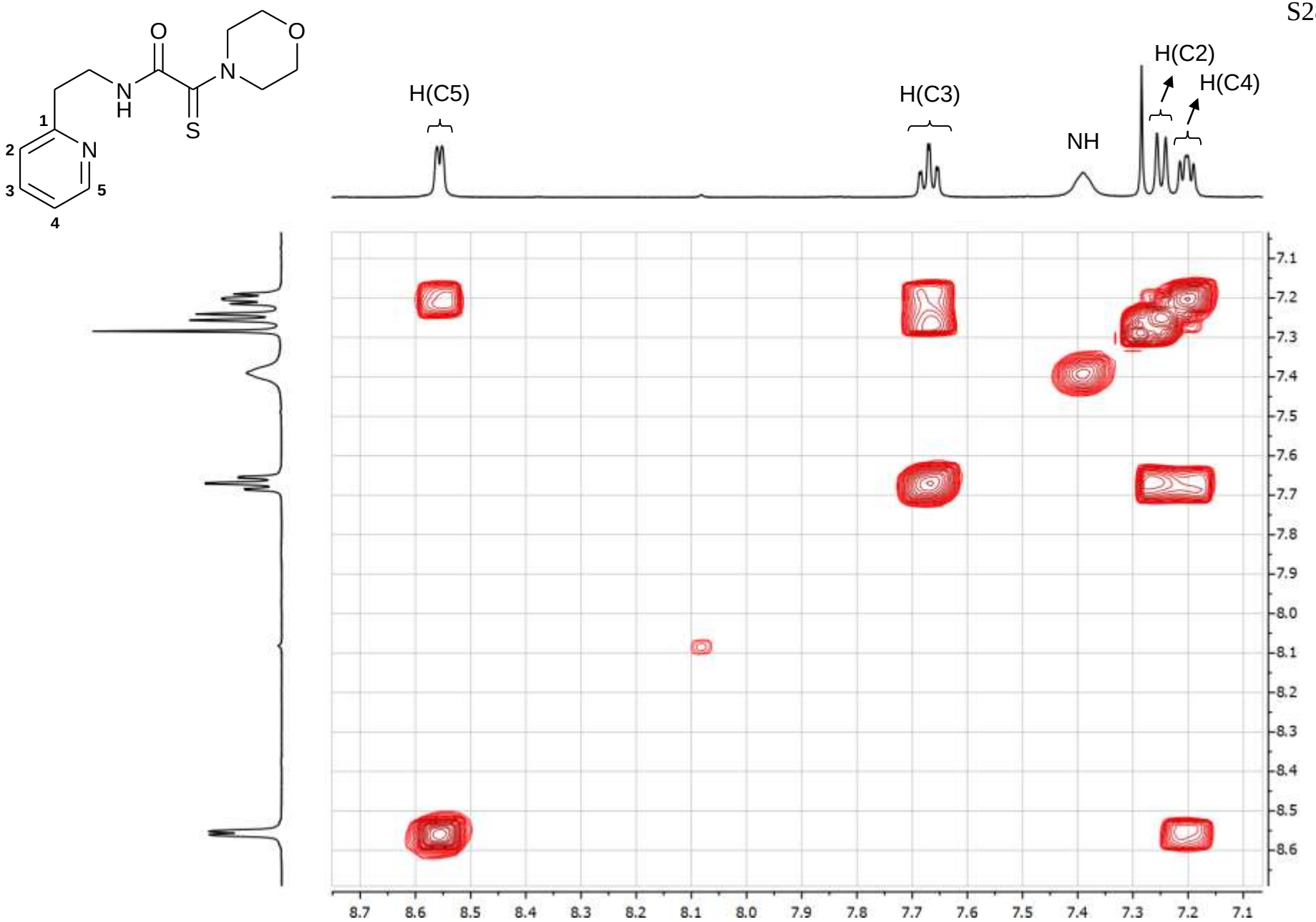

Fig. S10. Extended fragment of the $^{1}H-^{1}H$ COSY spectrum of ligand **2** (aromatic and NH proton regions; 500.13 MHz, $CDCl_3$)

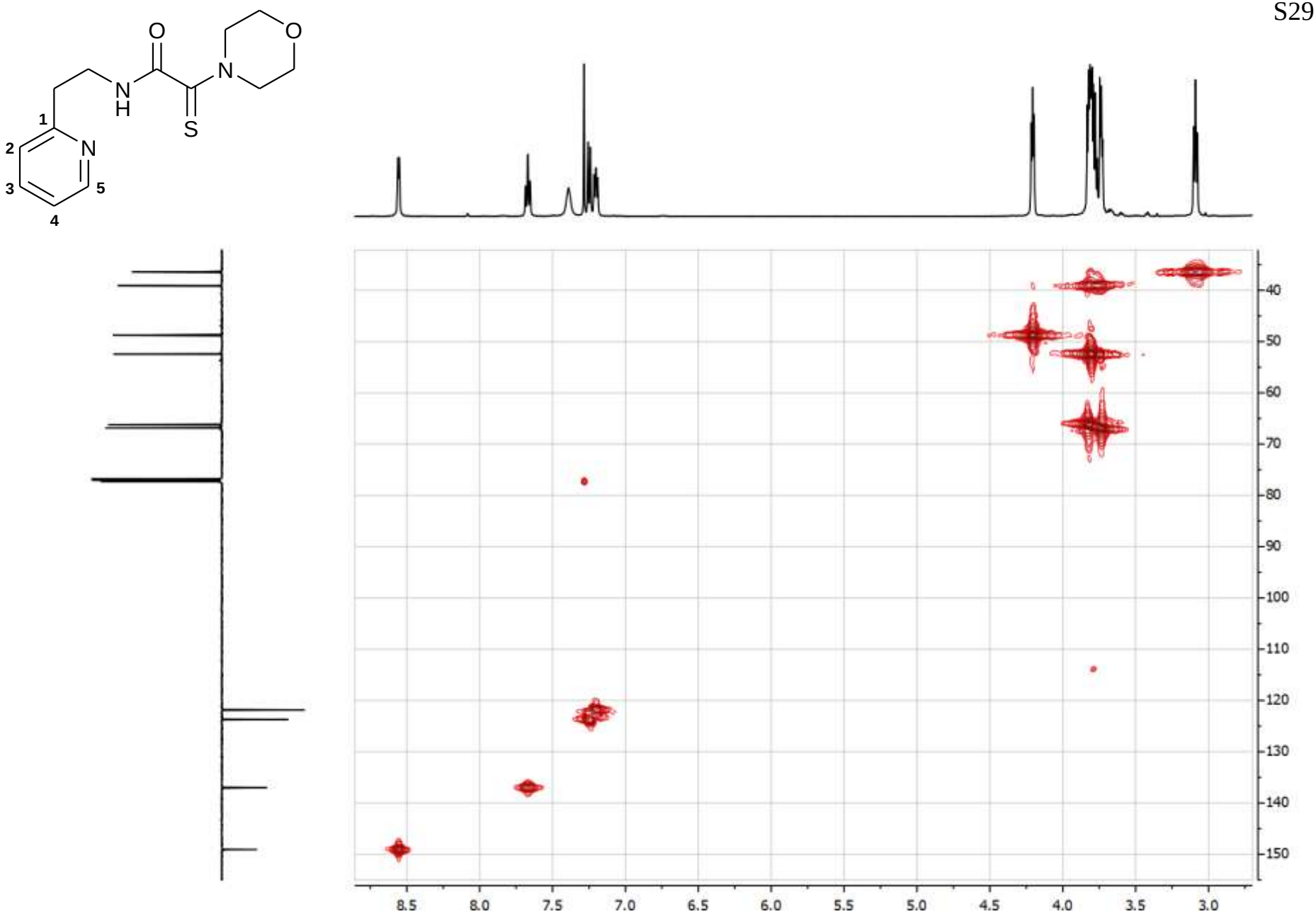

Fig. S11. HMQC spectrum of ligand **2** ($CDCl_3$)

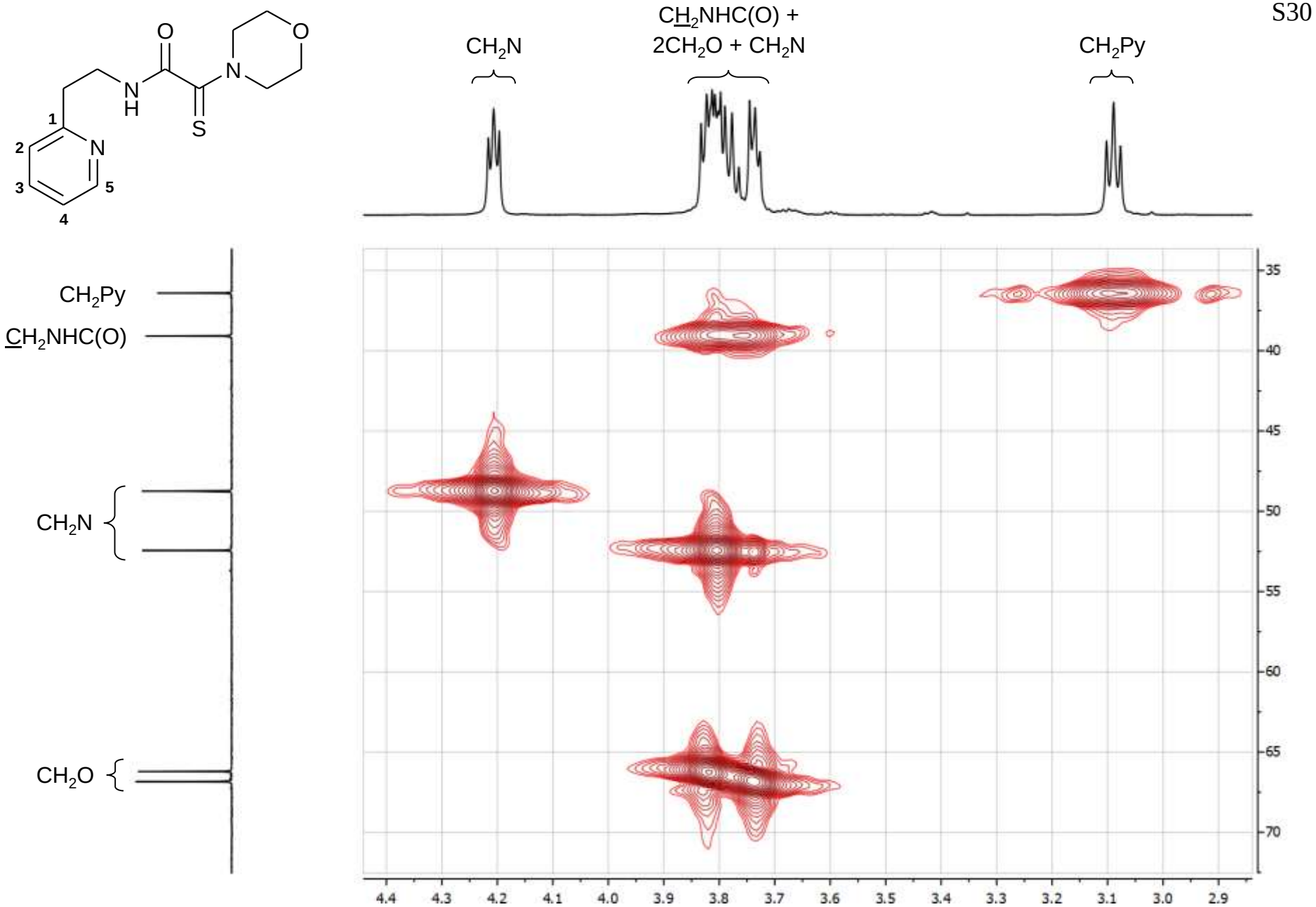

Fig. S12. Extended fragment of the HMQC spectrum of ligand **2** (aliphatic carbon and hydrogen nuclei; $CDCl_3$)

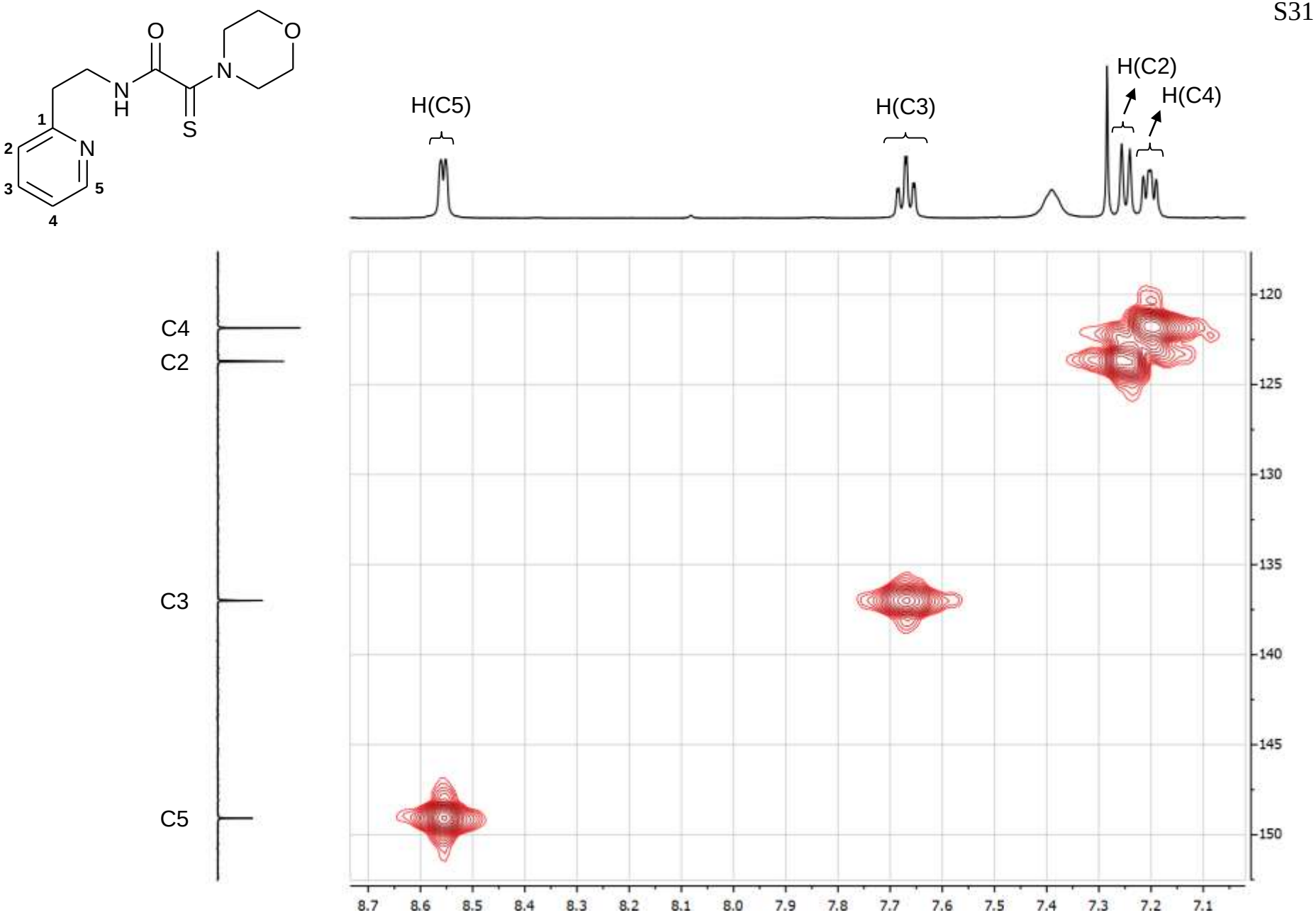

Fig. S13. Extended fragment of the HMQC spectrum of ligand **2** (aromatic carbon and hydrogen nuclei; $CDCl_3$)

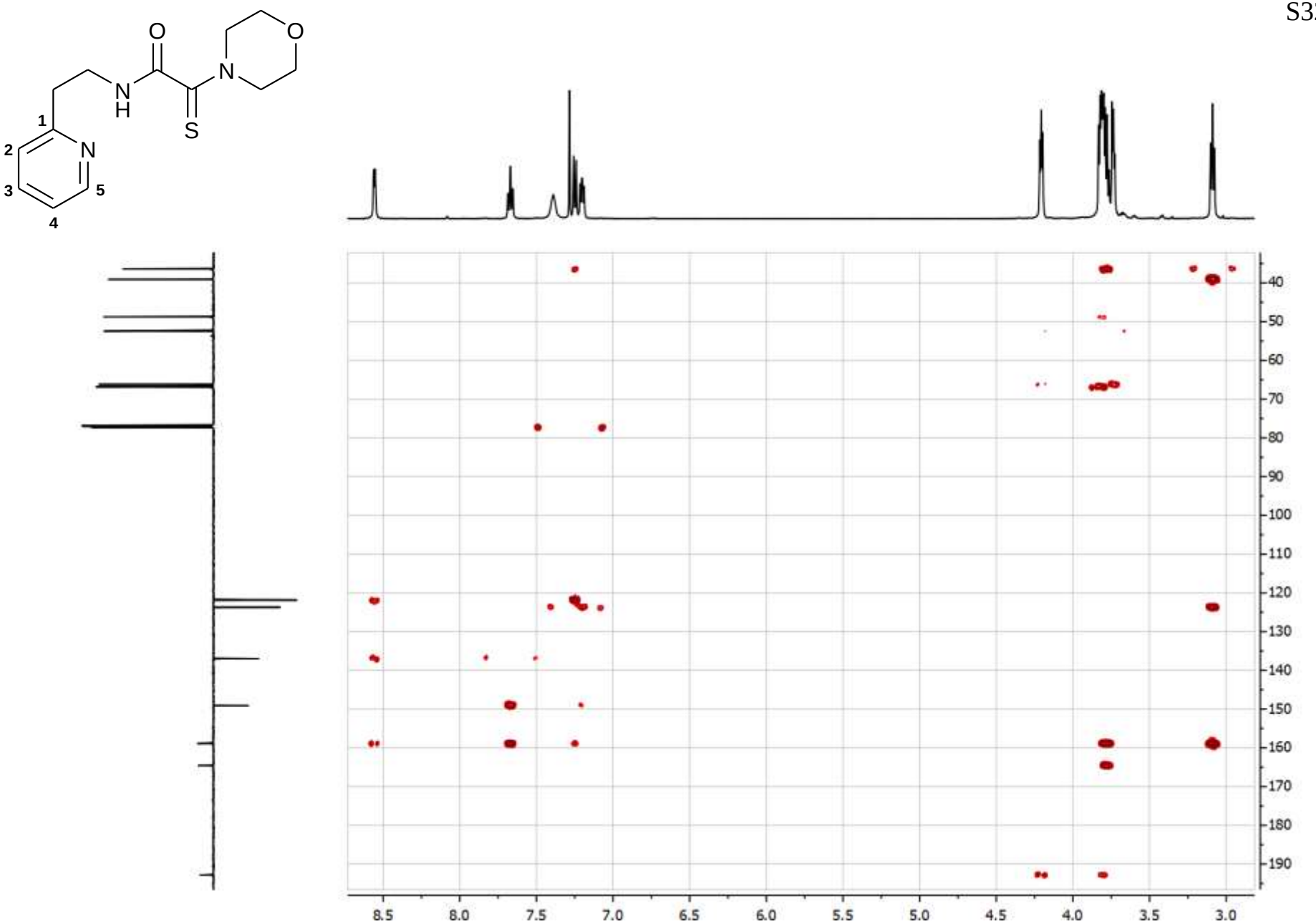

Fig. S14. ^{1}H–^{13}C HMBC spectrum of ligand **2** ($CDCl_3$)

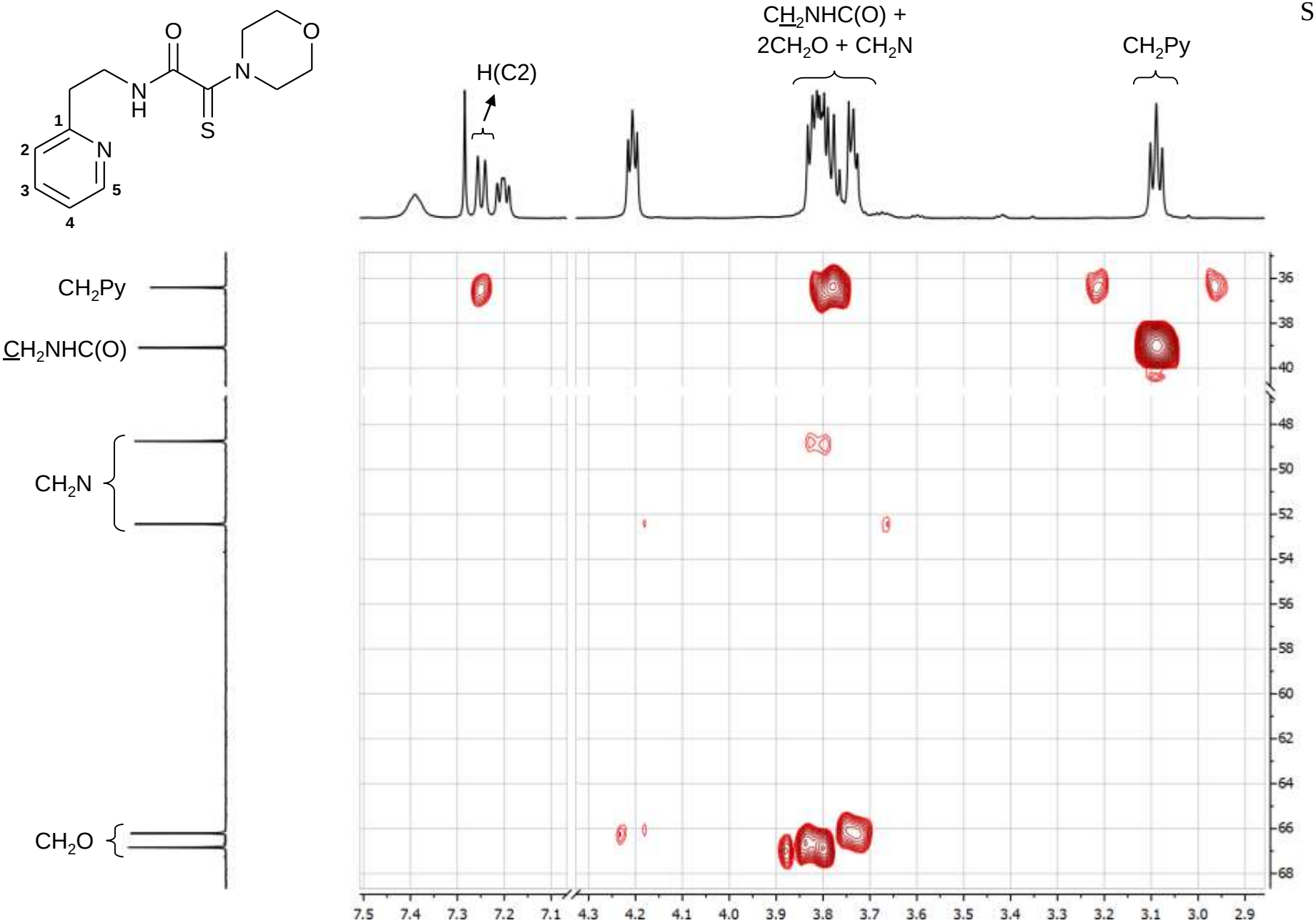

Fig. S15. Extended fragment of the ^{1}H–^{13}C HMBC spectrum of ligand **2** (aliphatic carbon nuclei; $CDCl_3$)

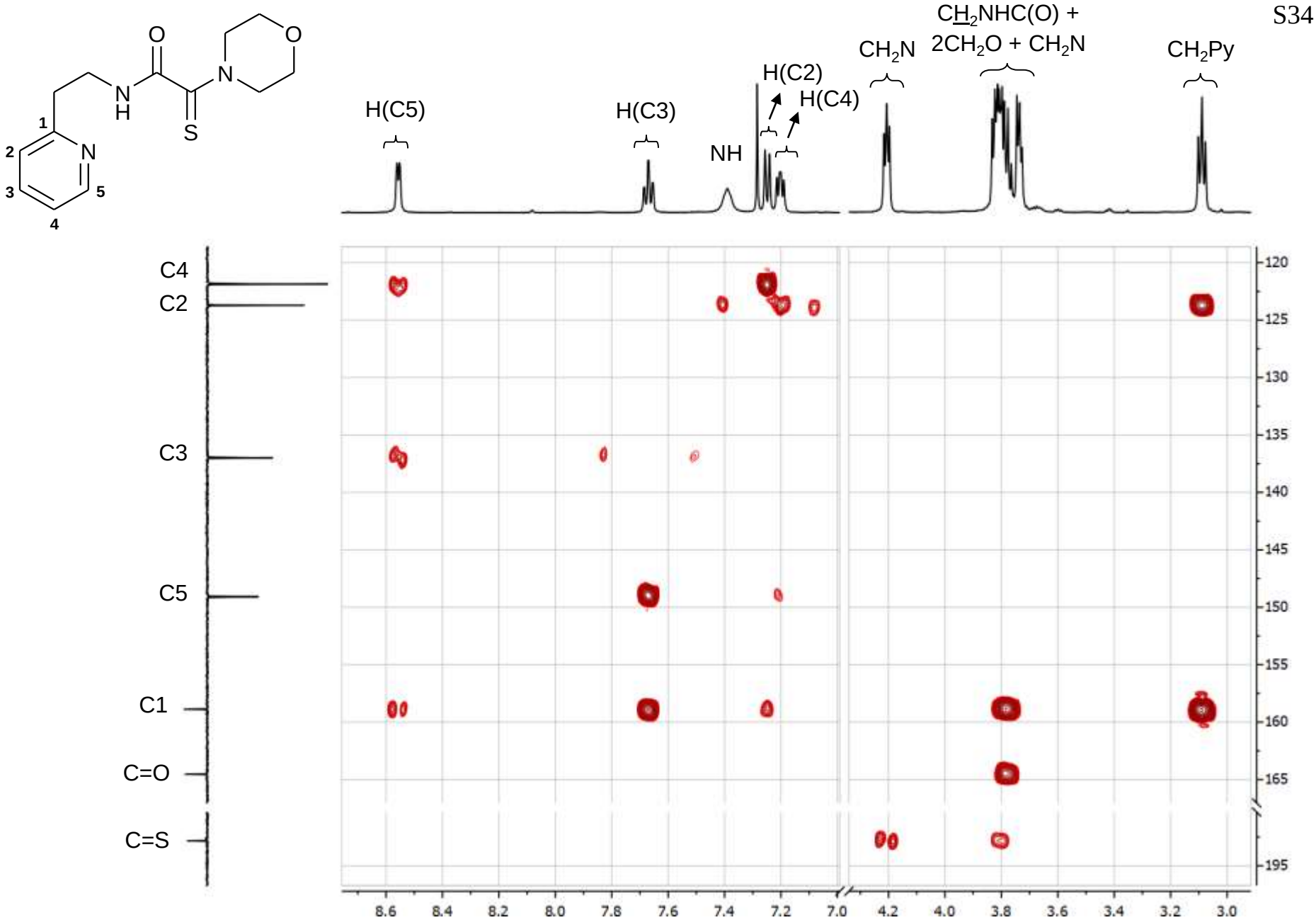

Fig. S16. Extended fragment of the $^{1}H–^{13}C$ HMBC spectrum of ligand **2** (aromatic and (thio)carbonyl carbon nuclei; $CDCl_3$)

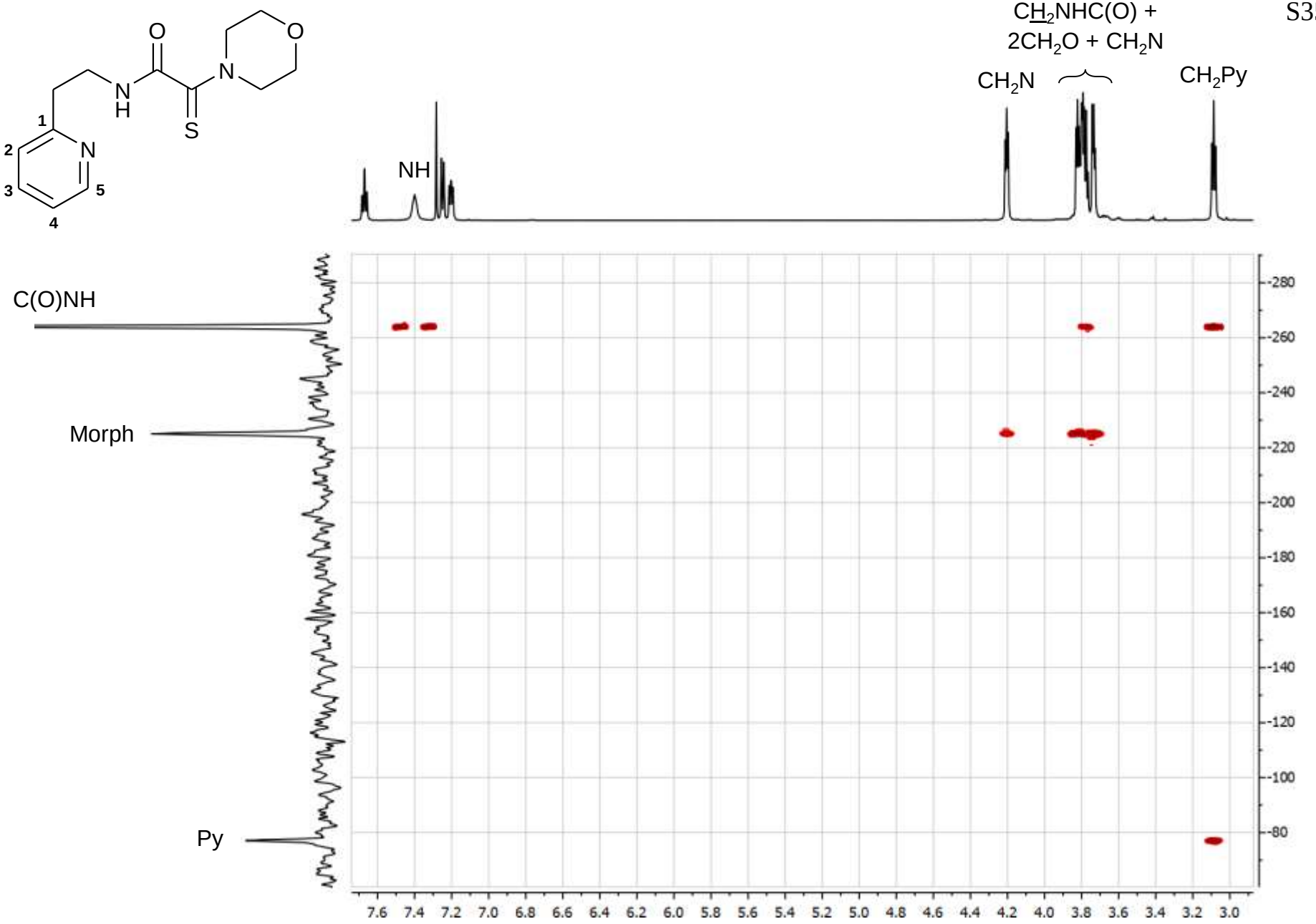

Fig. S17. $^{1}H–^{15}N$ HMBC spectrum of ligand **2** ($CDCl_3$)

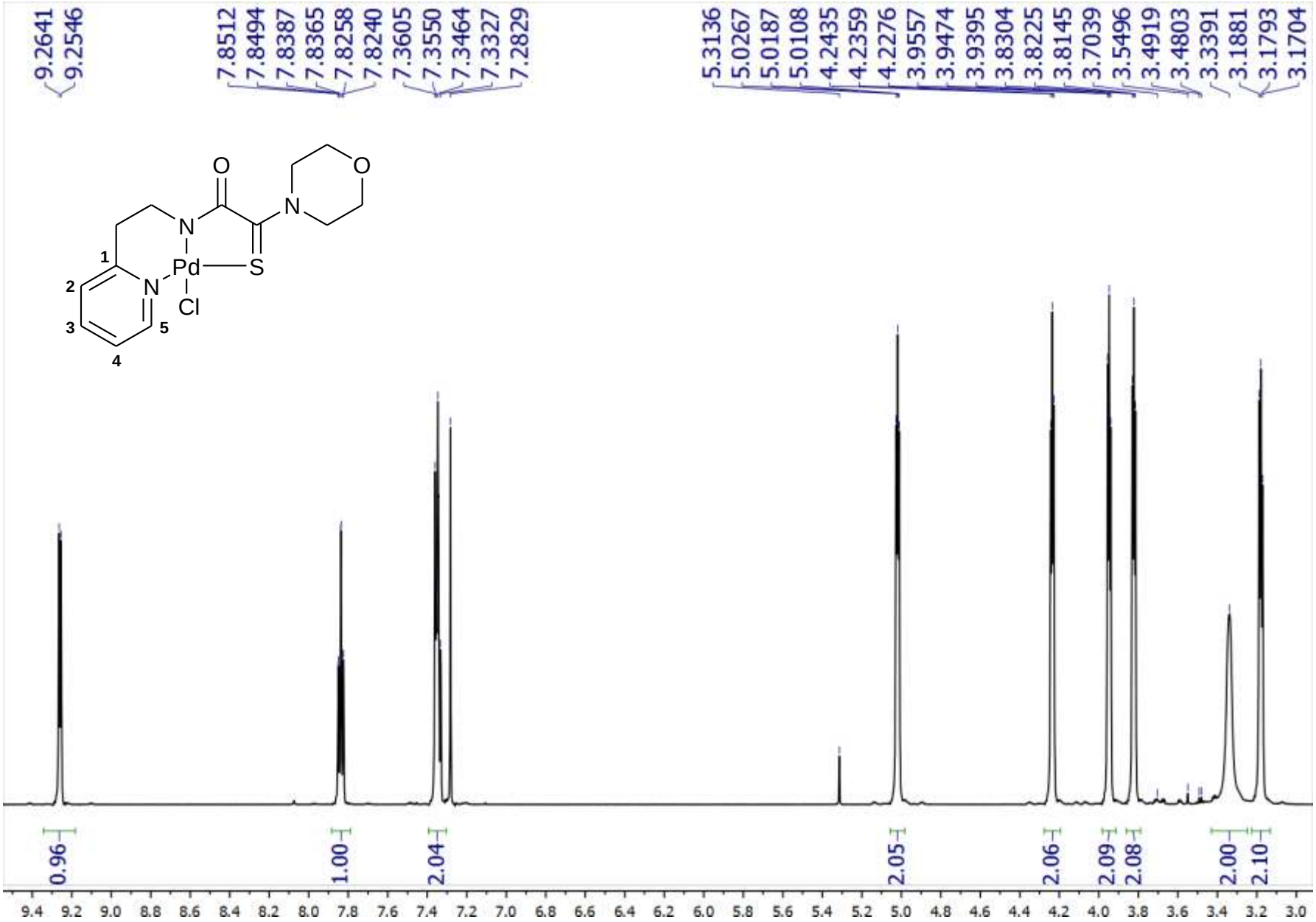

Fig. S18. ^{1}H NMR spectrum of complex **9** (600.22 MHz, $CDCl_3$)

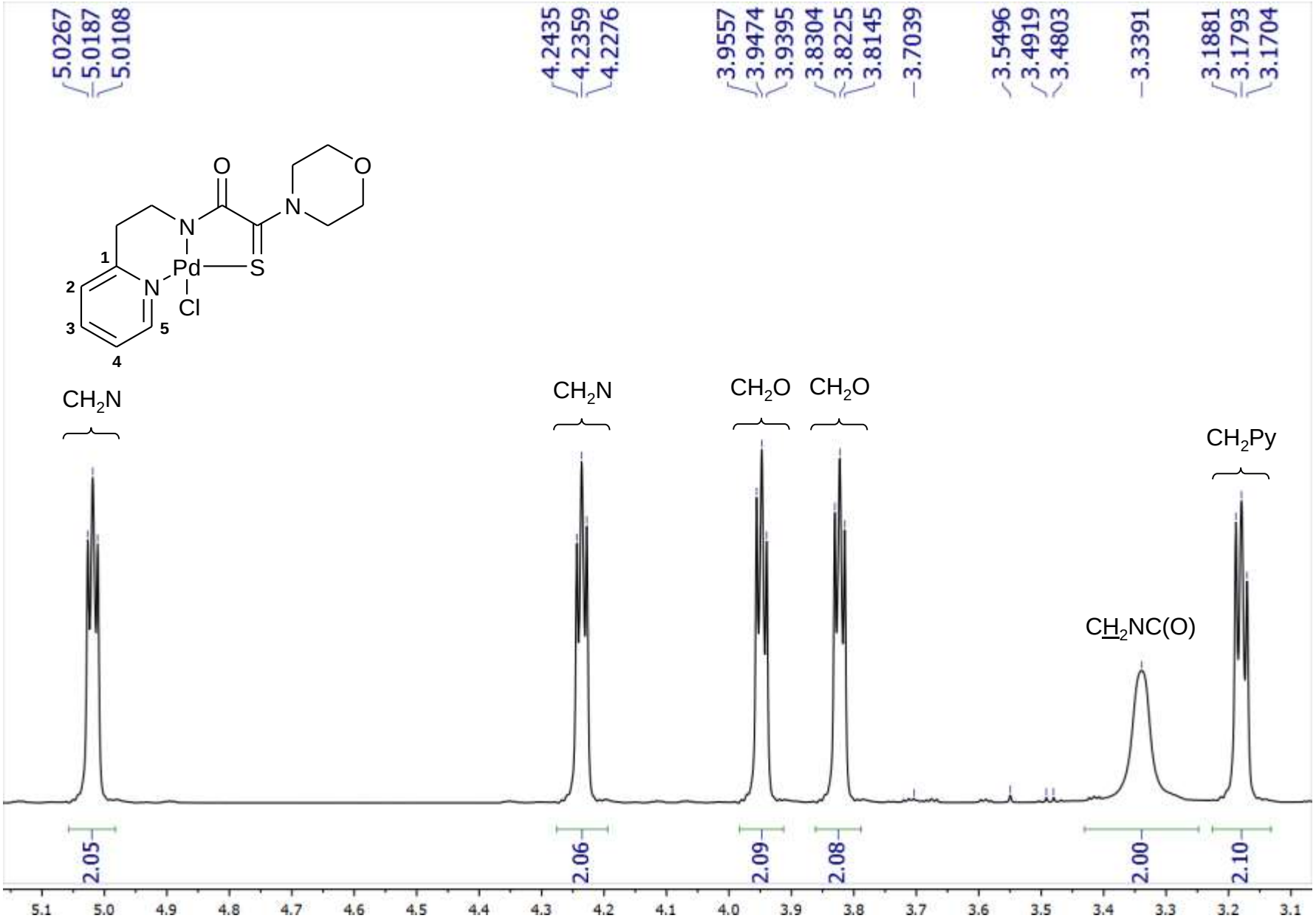

Fig. S19. Extended fragment of the ^{1}H NMR spectrum of complex **9** (aliphatic proton region; 600.22 MHz, $CDCl_3$)

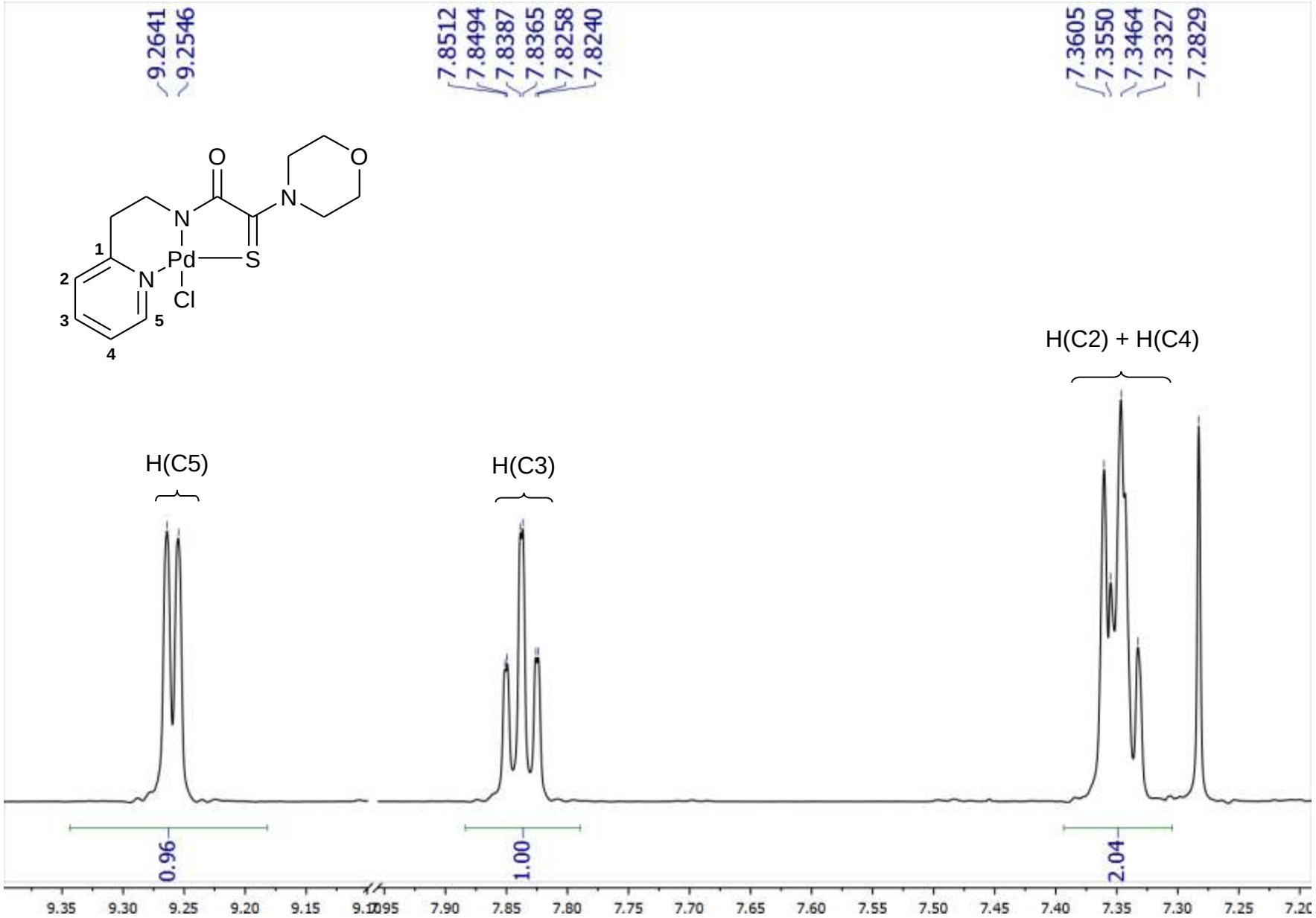

Fig. S20. Extended fragments of the ^{1}H NMR spectrum of complex **9** (aromatic proton region; 600.22 MHz, $CDCl_3$)

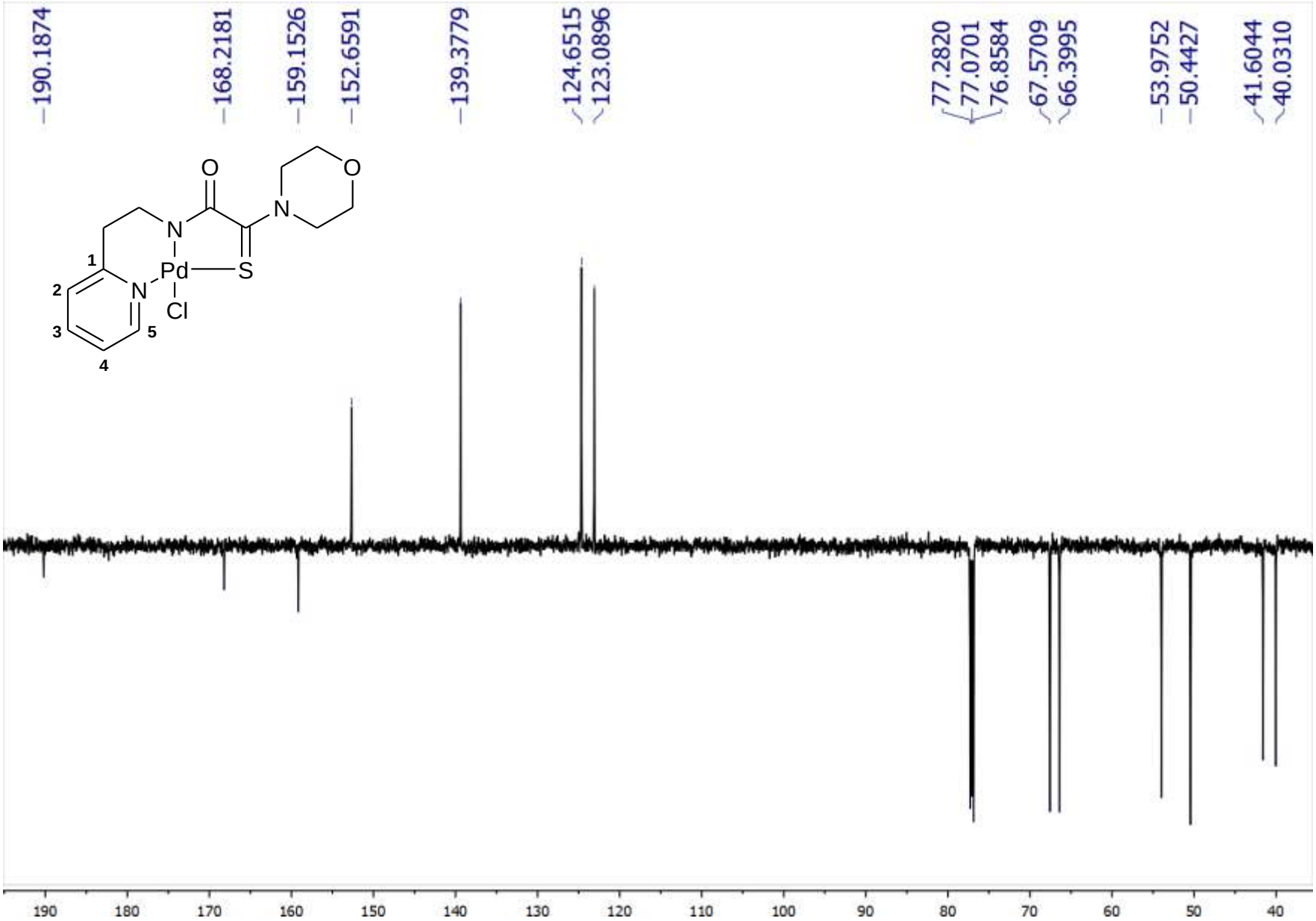

Fig. S21. $^{13}C\{^{1}H\}$ NMR spectrum of complex **9** (150.93 MHz, $CDCl_3$)

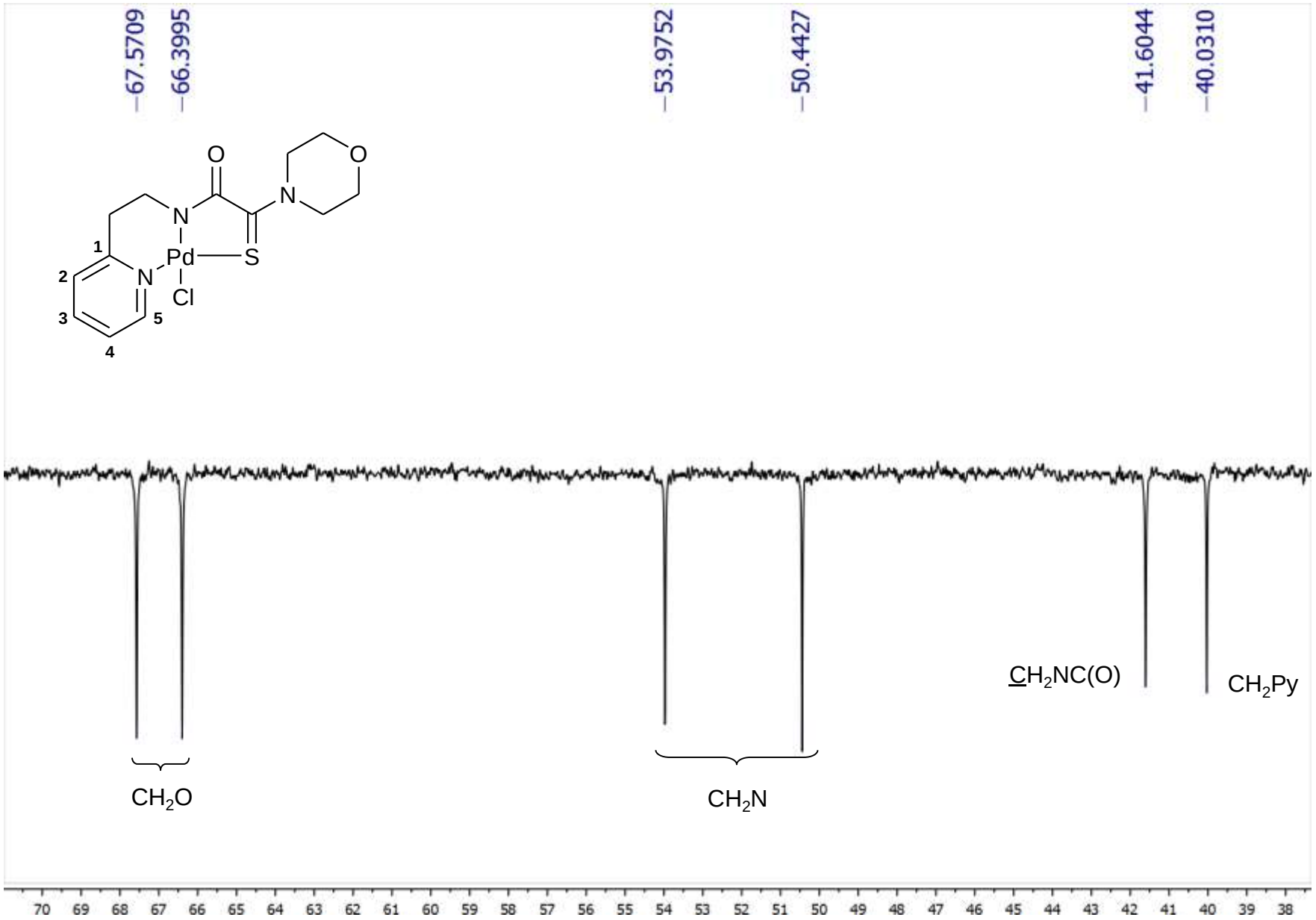

Fig. S22. Extended fragment of the $^{13}C\{^{1}H\}$ NMR spectrum of complex **9** (aliphatic carbon nuclei; 150.93 MHz, $CDCl_3$)

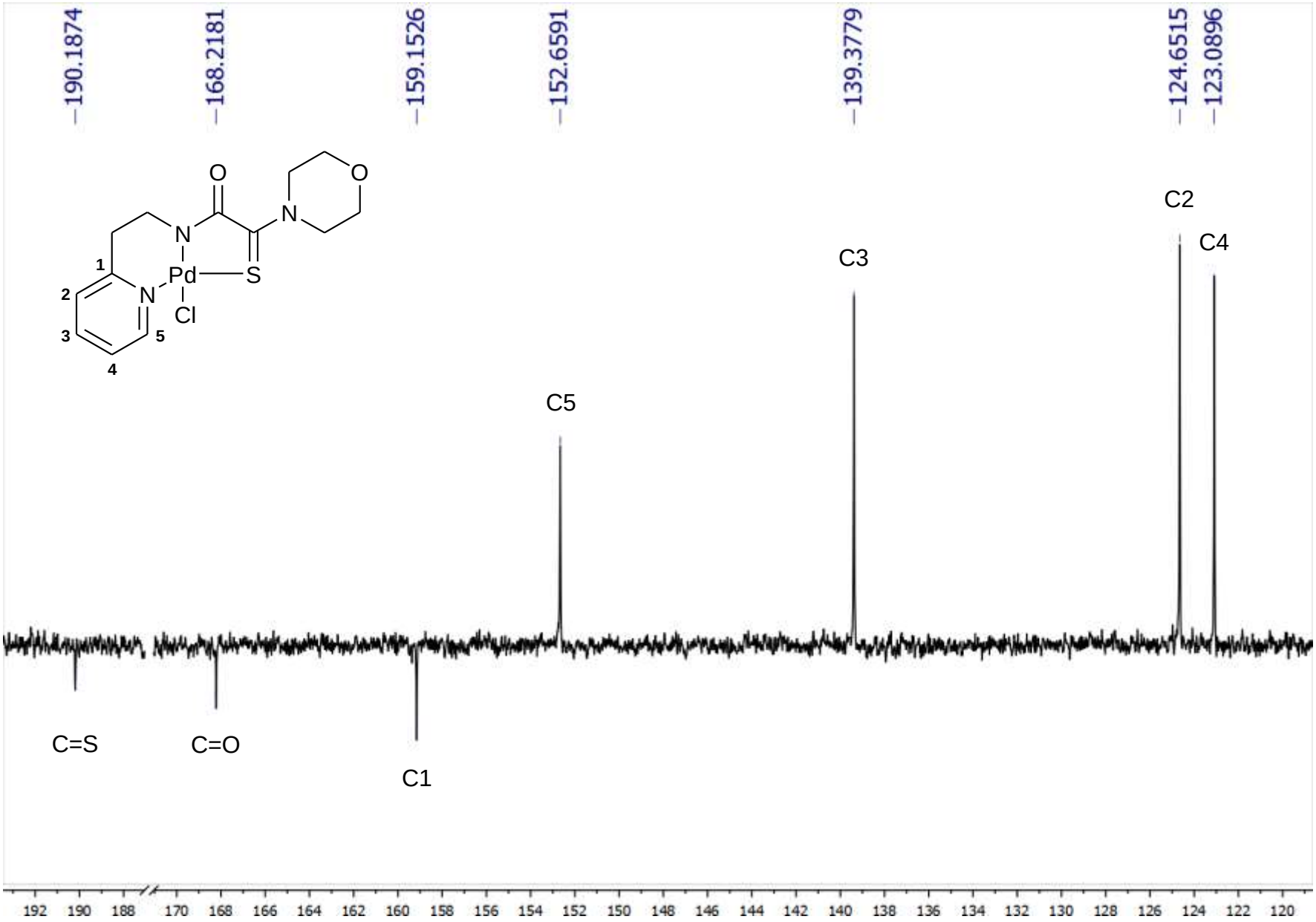

Fig. S23. Extended fragments of the $^{13}C\{^{1}H\}$ NMR spectrum of complex **9** (aromatic and (thio)carbonyl carbon nuclei; 150.93 MHz, $CDCl_3$)

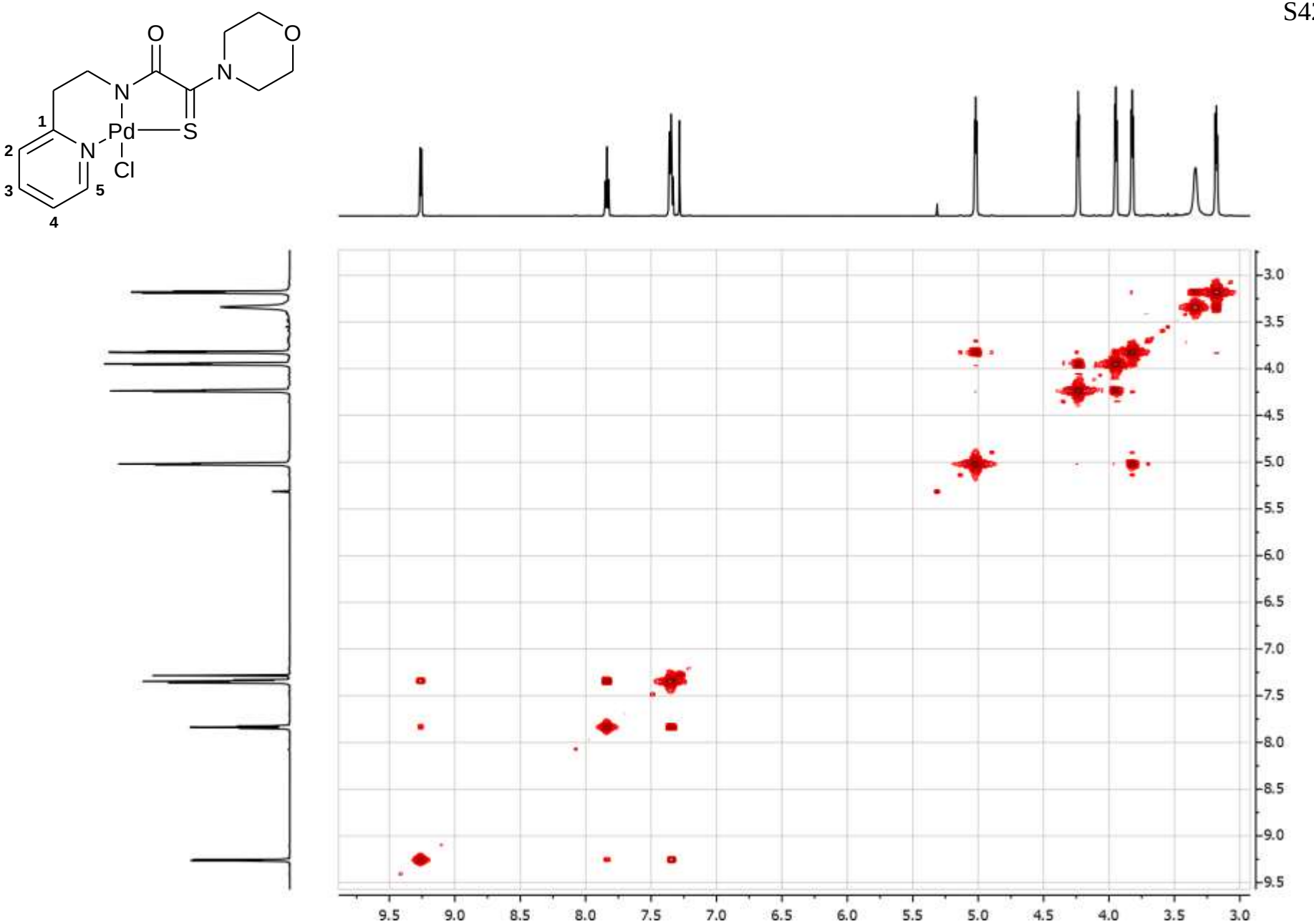

Fig. S24. $^{1}H-^{1}H$ COSY spectrum of complex **9** (600.22 MHz, $CDCl_3$)

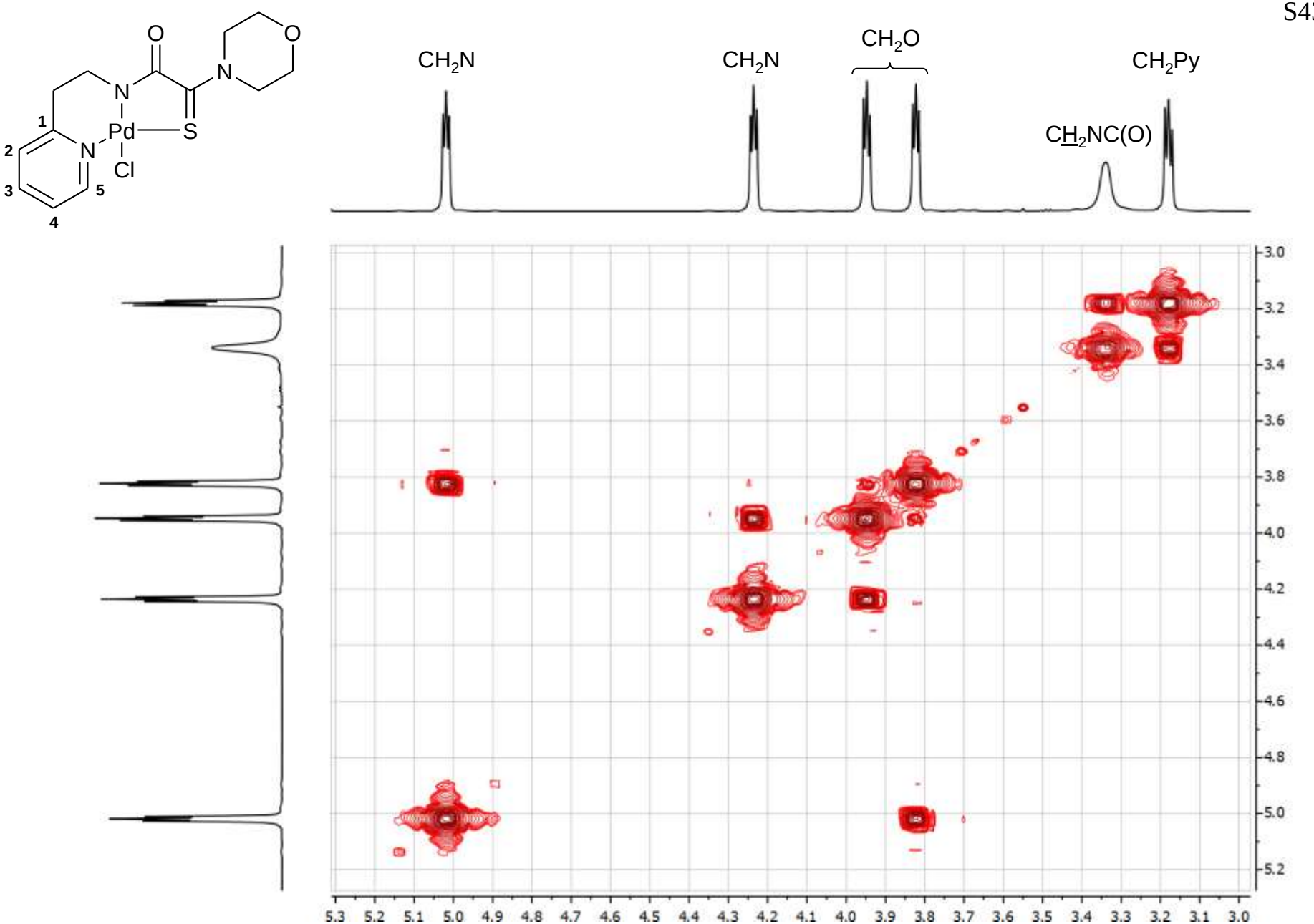

Fig. S25. Extended fragment of the $^{1}H-^{1}H$ COSY spectrum of complex **9** (aliphatic proton region; 600.22 MHz, $CDCl_3$)

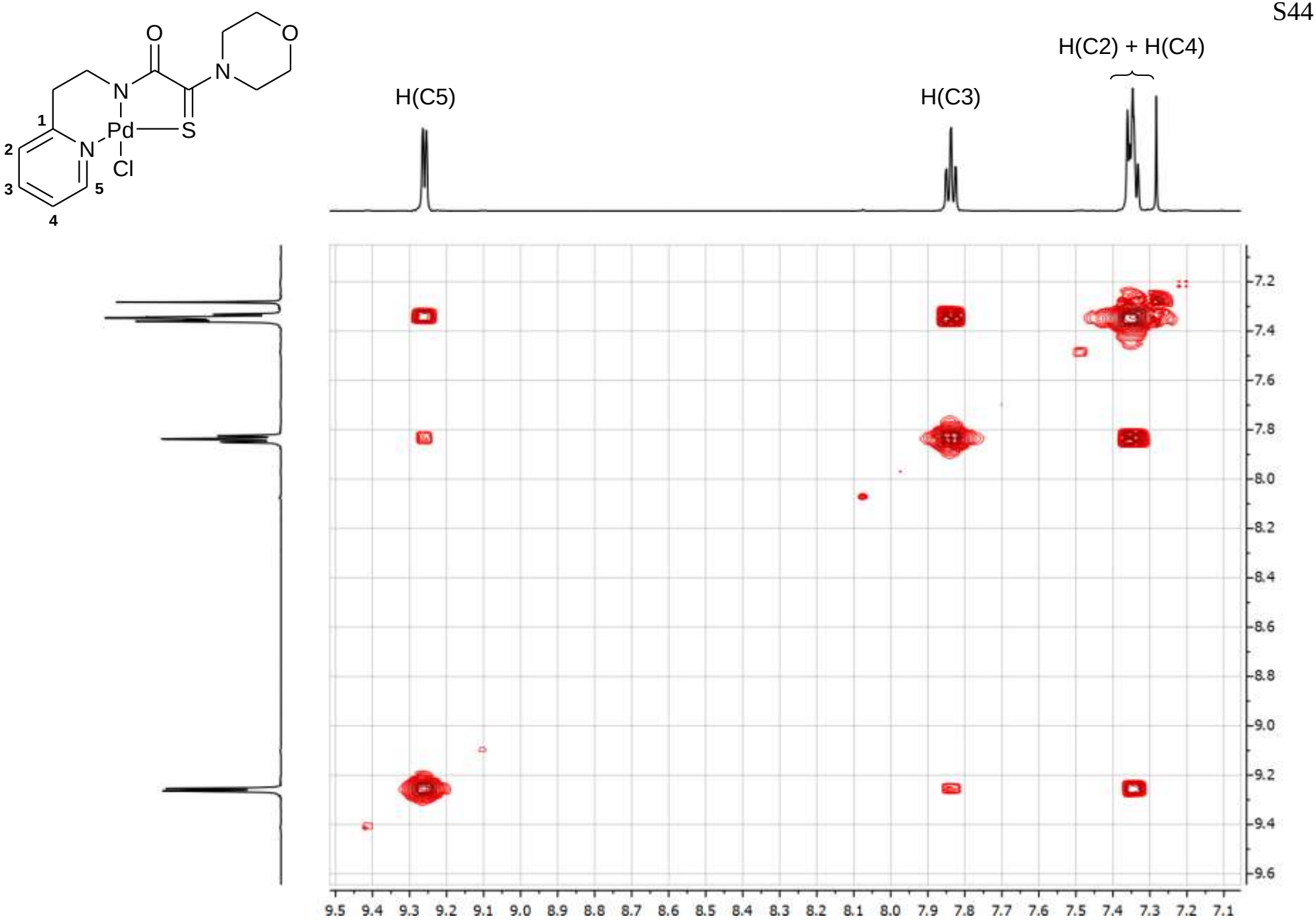

Fig. S26. Extended fragment of the $^{1}H-^{1}H$ COSY spectrum of complex **9** (aromatic proton region; 600.22 MHz, $CDCl_3$)

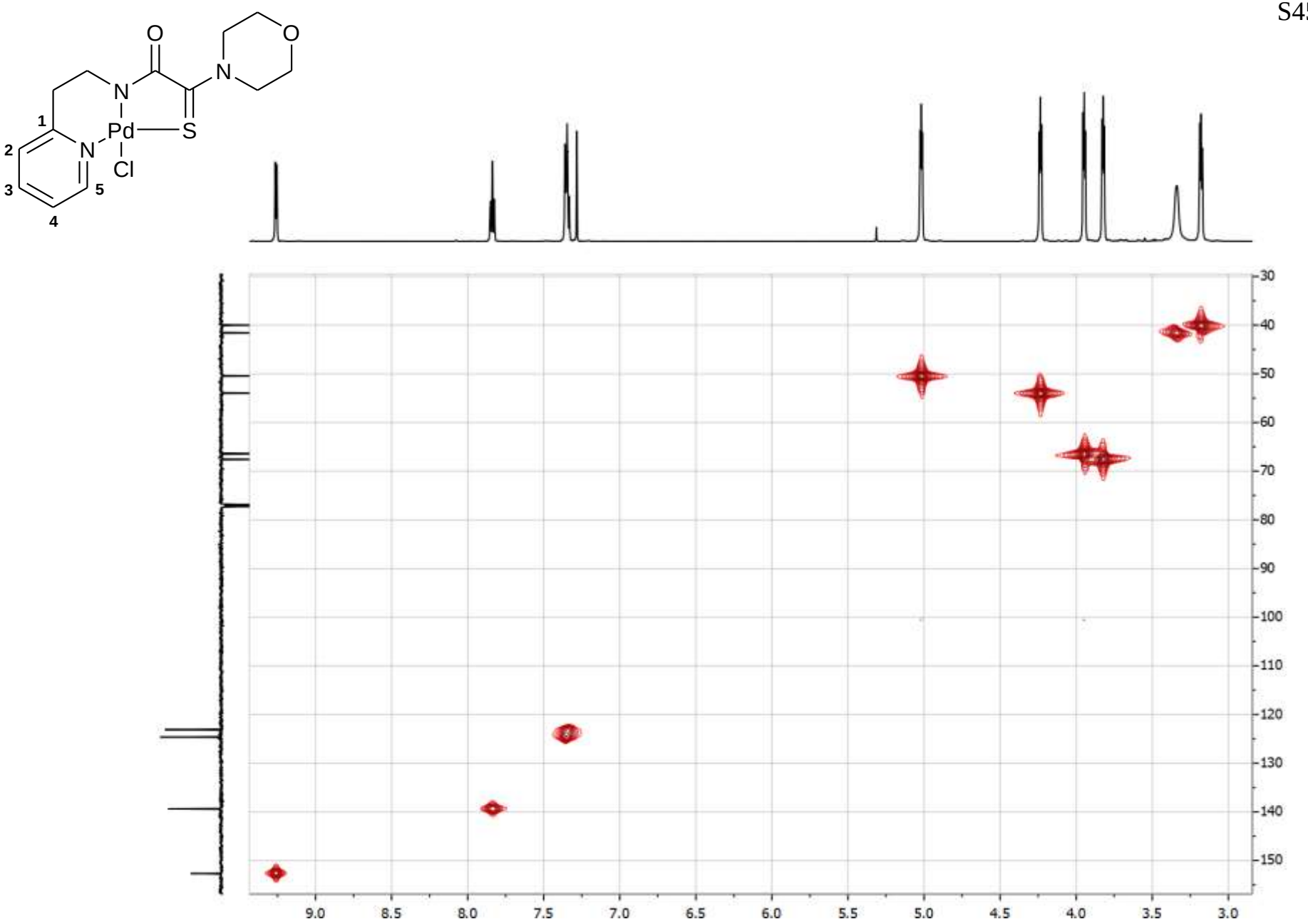

Fig. S27. HMQC spectrum of complex **9** ($CDCl_3$)

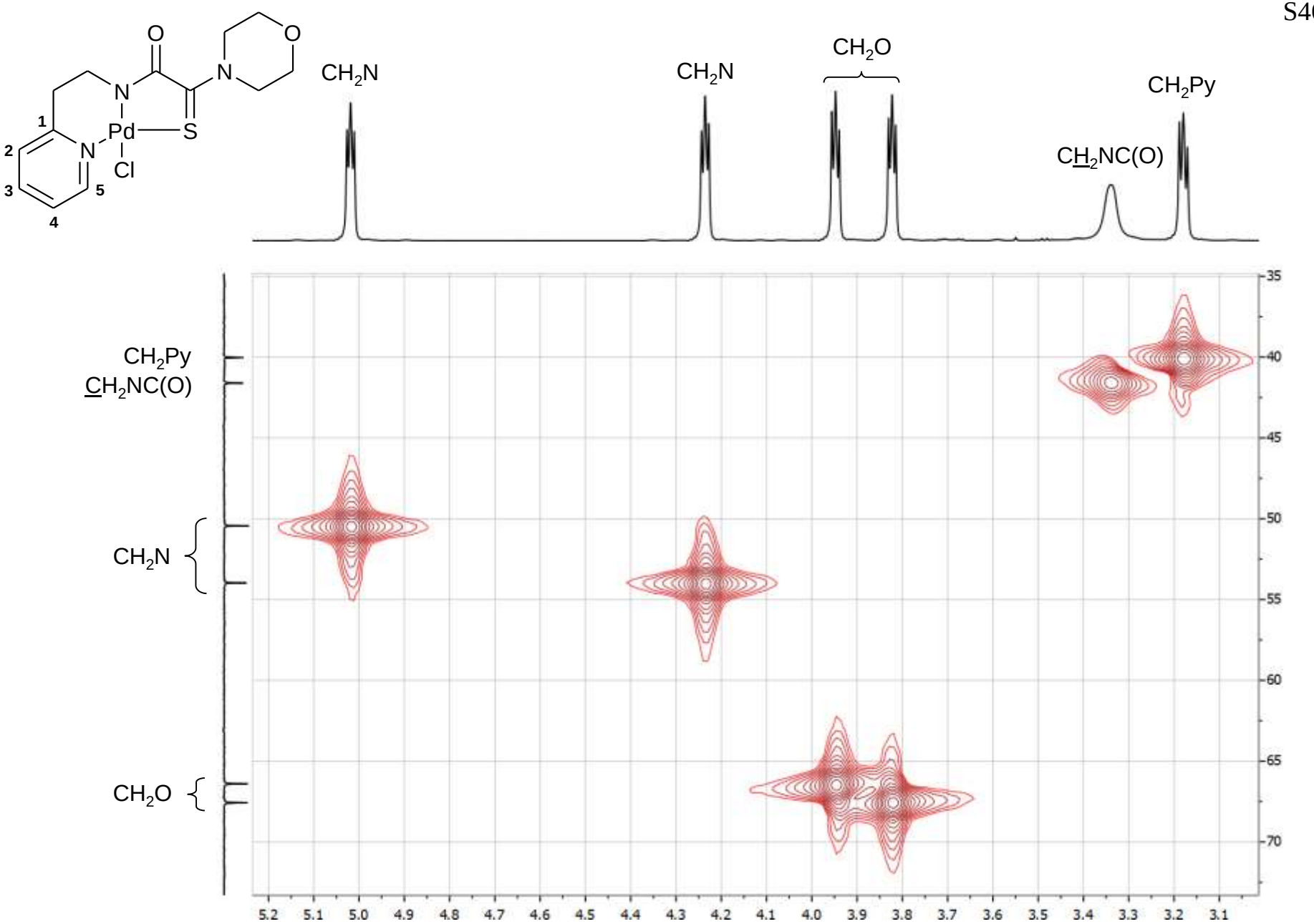

Fig. S28. Extended fragment of the HMQC spectrum of complex **9** (aliphatic carbon and hydrogen nuclei; $CDCl_3$)

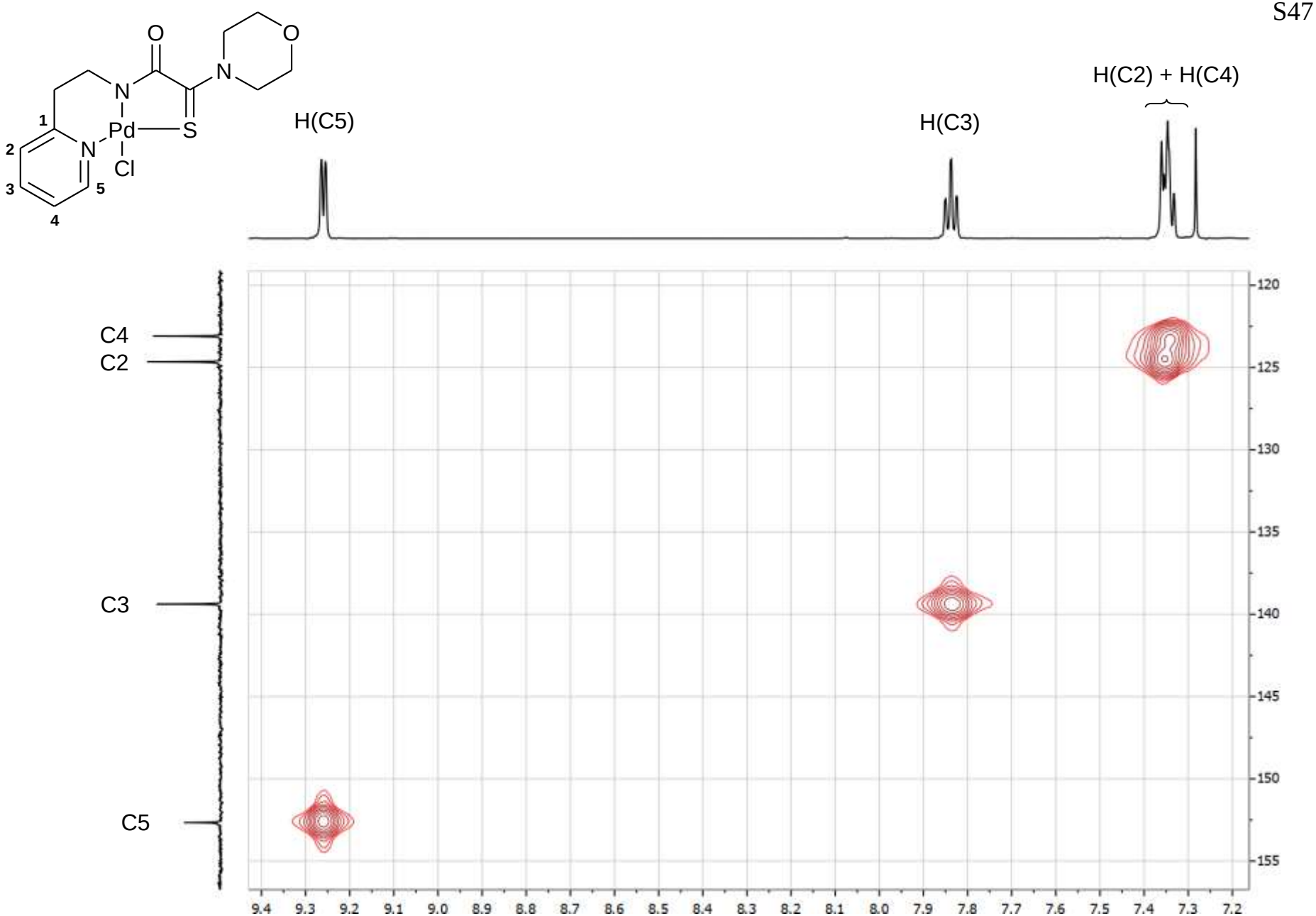

Fig. S29. Extended fragment of the HMQC spectrum of complex **9** (aromatic carbon and hydrogen nuclei; $CDCl_3$)

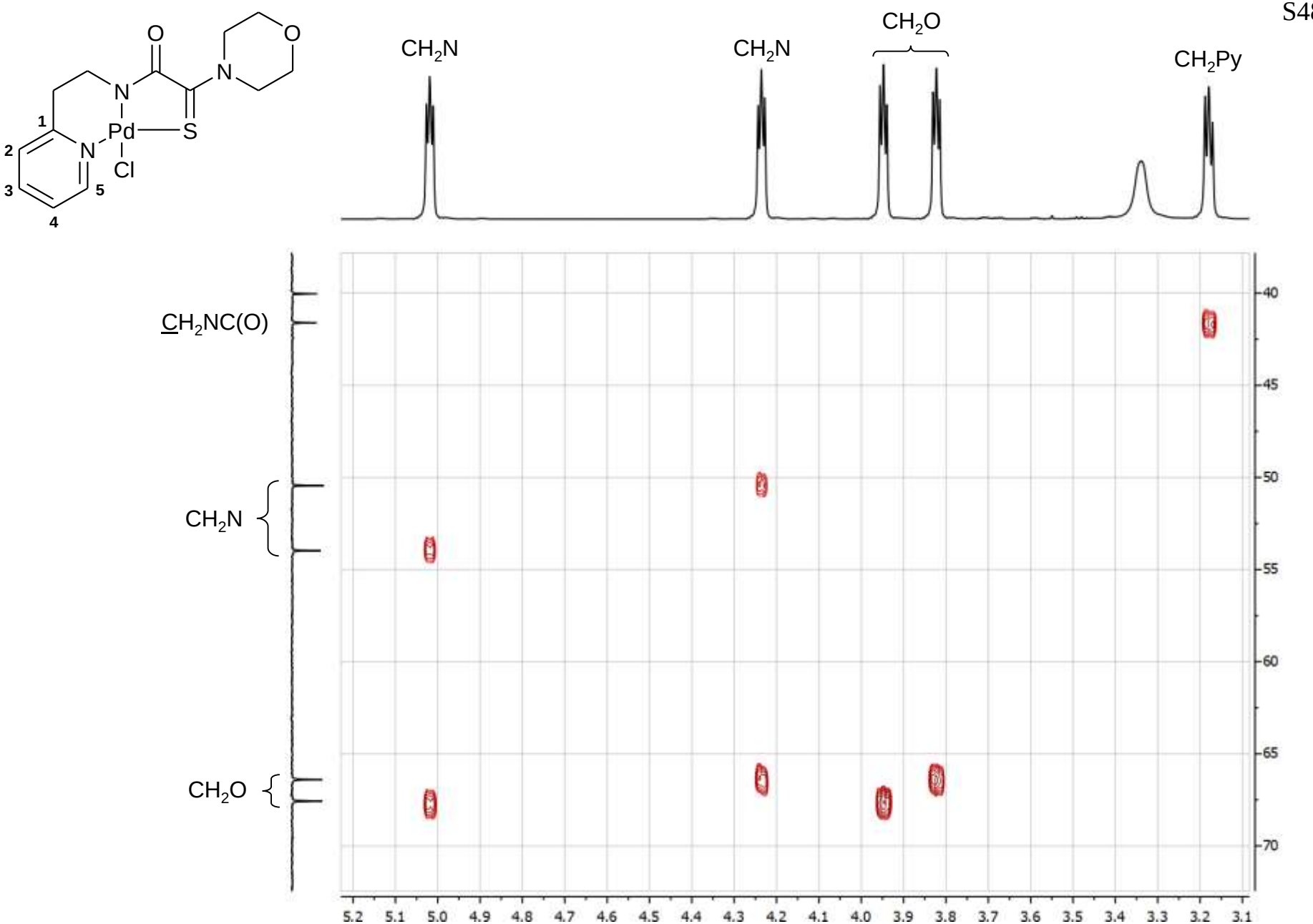

Fig. S30. Extended fragment of the ^{1}H–^{13}C HMBC spectrum of complex **9** (aliphatic carbon nuclei; $CDCl_3$)

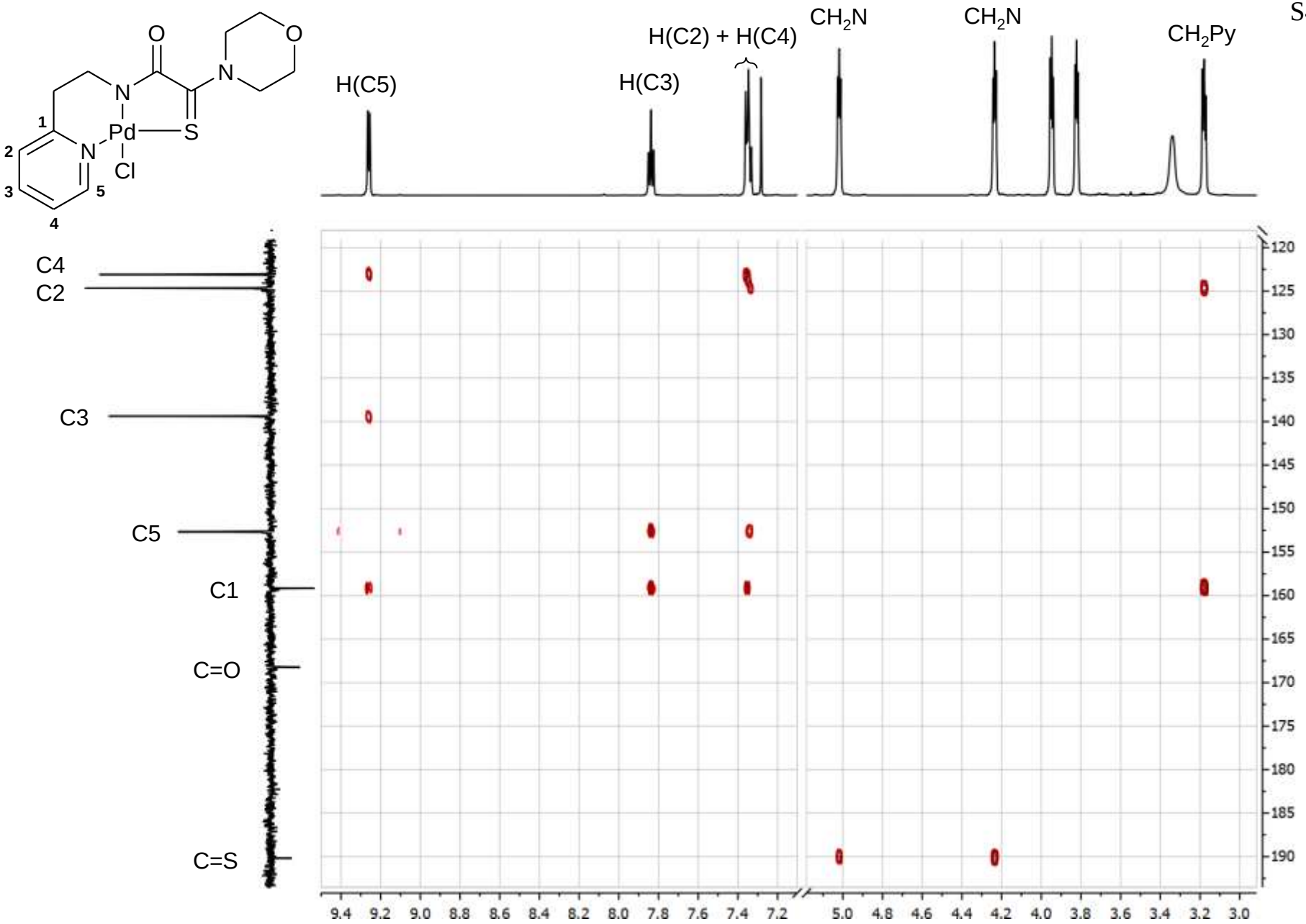

Fig. S31. Extended fragments of the ^{1}H–^{13}C HMBC spectrum of complex **9** (aromatic and (thio)carbonyl carbon nuclei; $CDCl_3$)

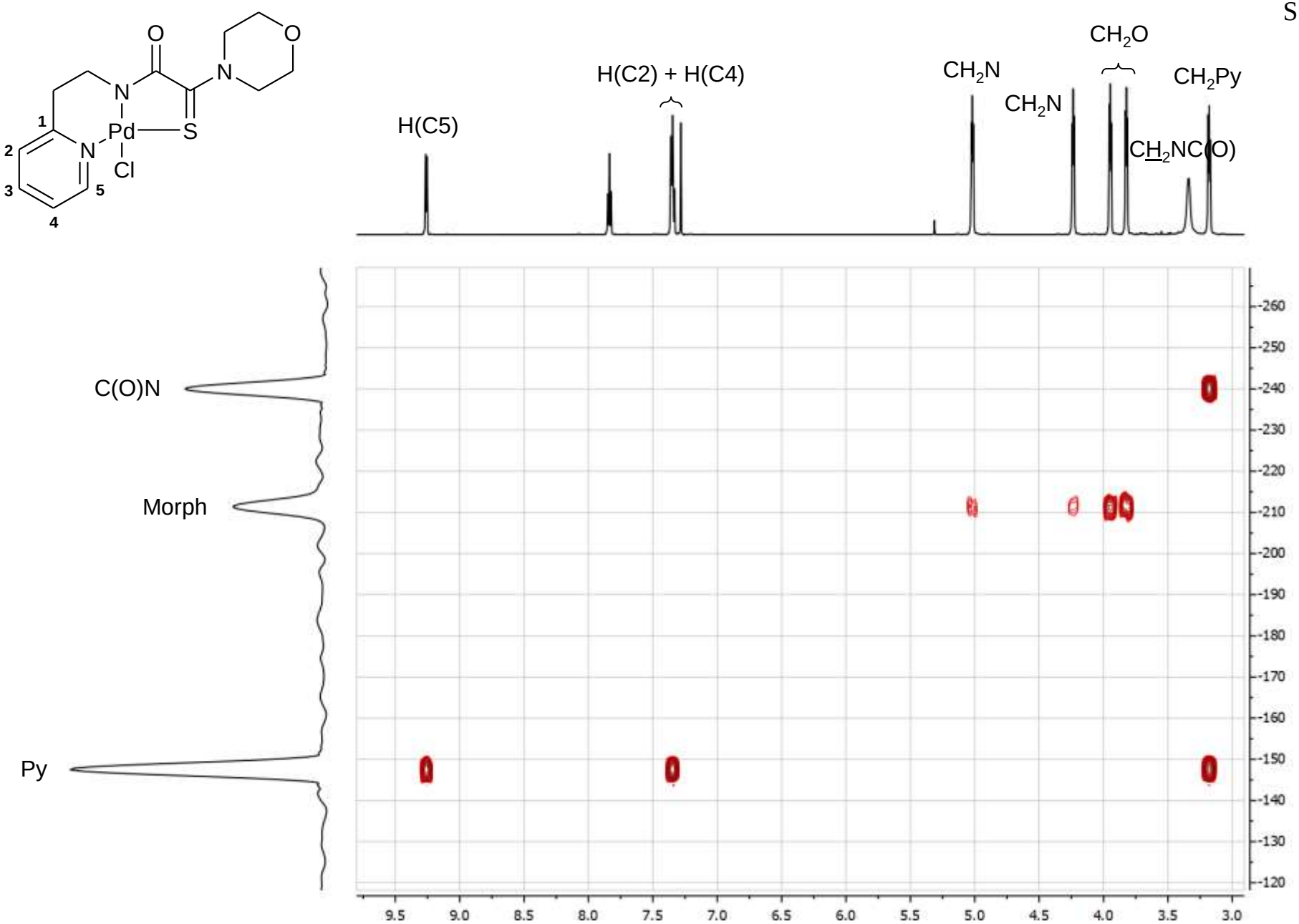

Fig. S32. $^{1}H–^{15}N$ HMBC spectrum of complex **9** ($CDCl_3$)

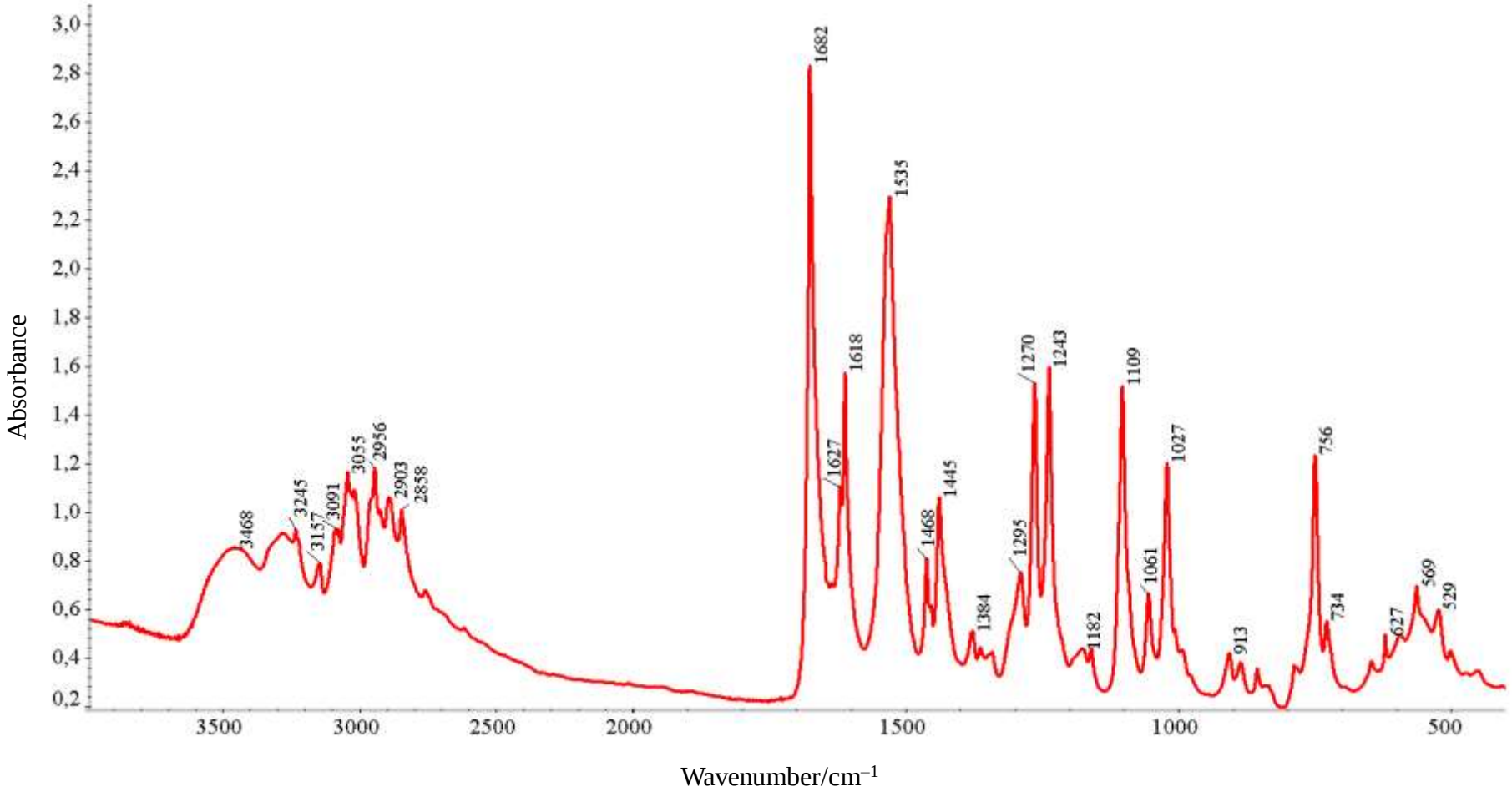

Fig. S33. IR spectrum of complex **15** (dark-red crystals)

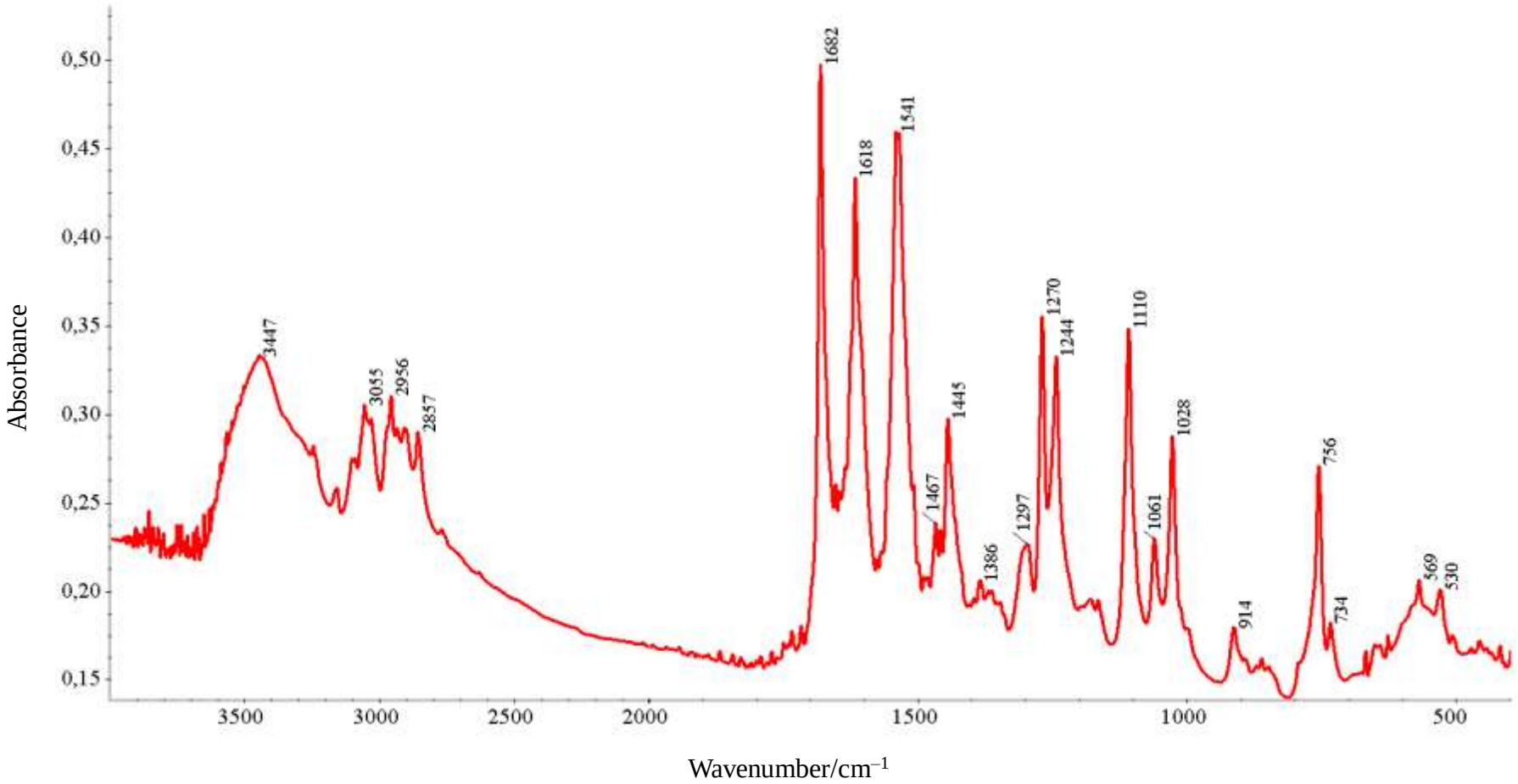

Fig. S34. IR spectrum of complex **15** (beige powder)

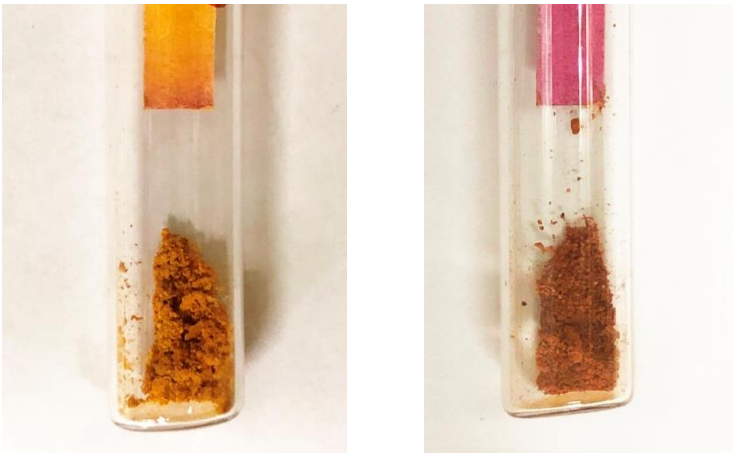

a ***b***

Fig. S35. Solid-phase cyclopalladation of functionalized monothiooxamide **2** under the action of $PdCl_2(NCPh)_2$: (***a***) a mixture of the reactants immediately after grinding in a mortar; (***b***) reaction mixture in 1 day

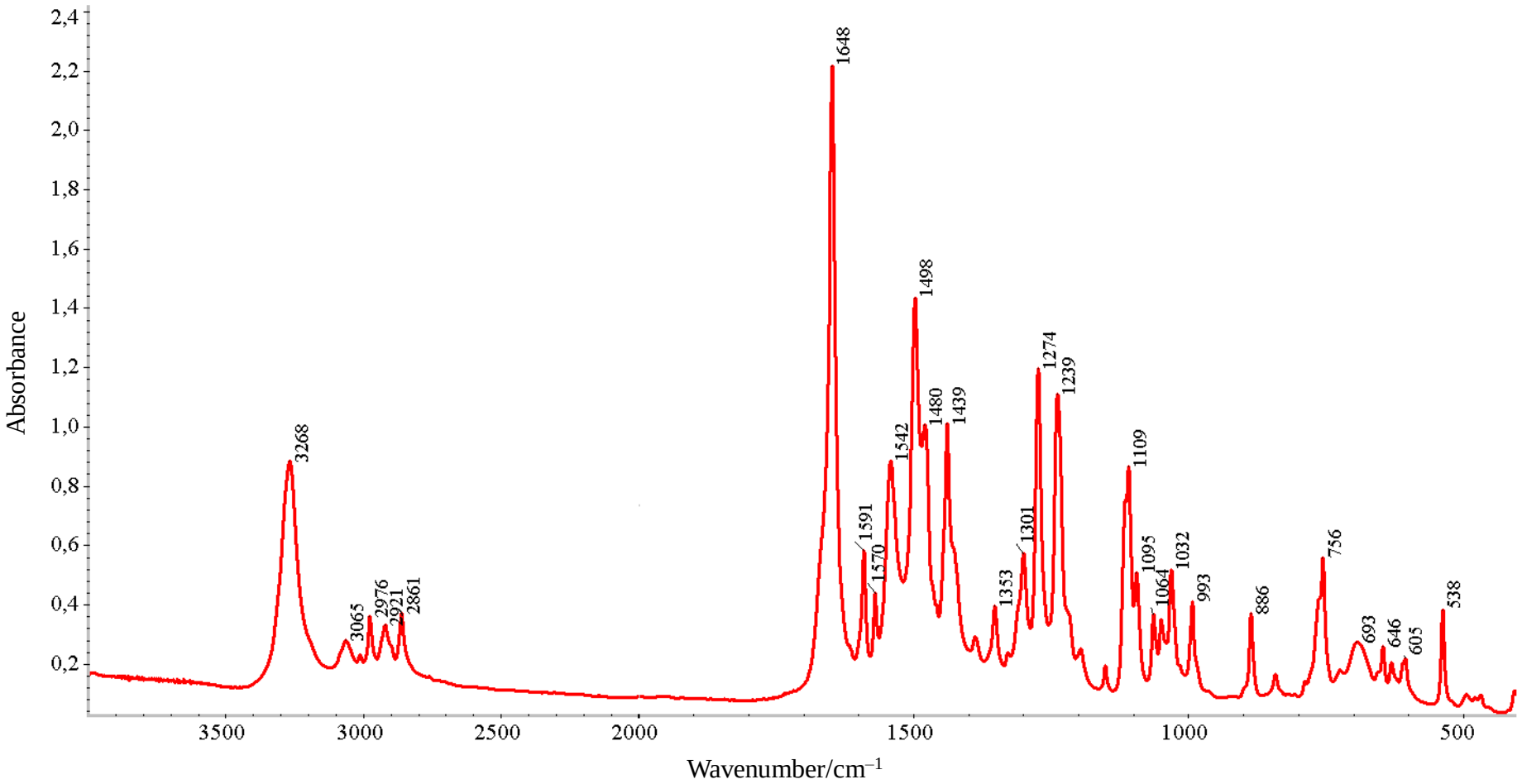

Fig. S36. IR spectrum of ligand **1**

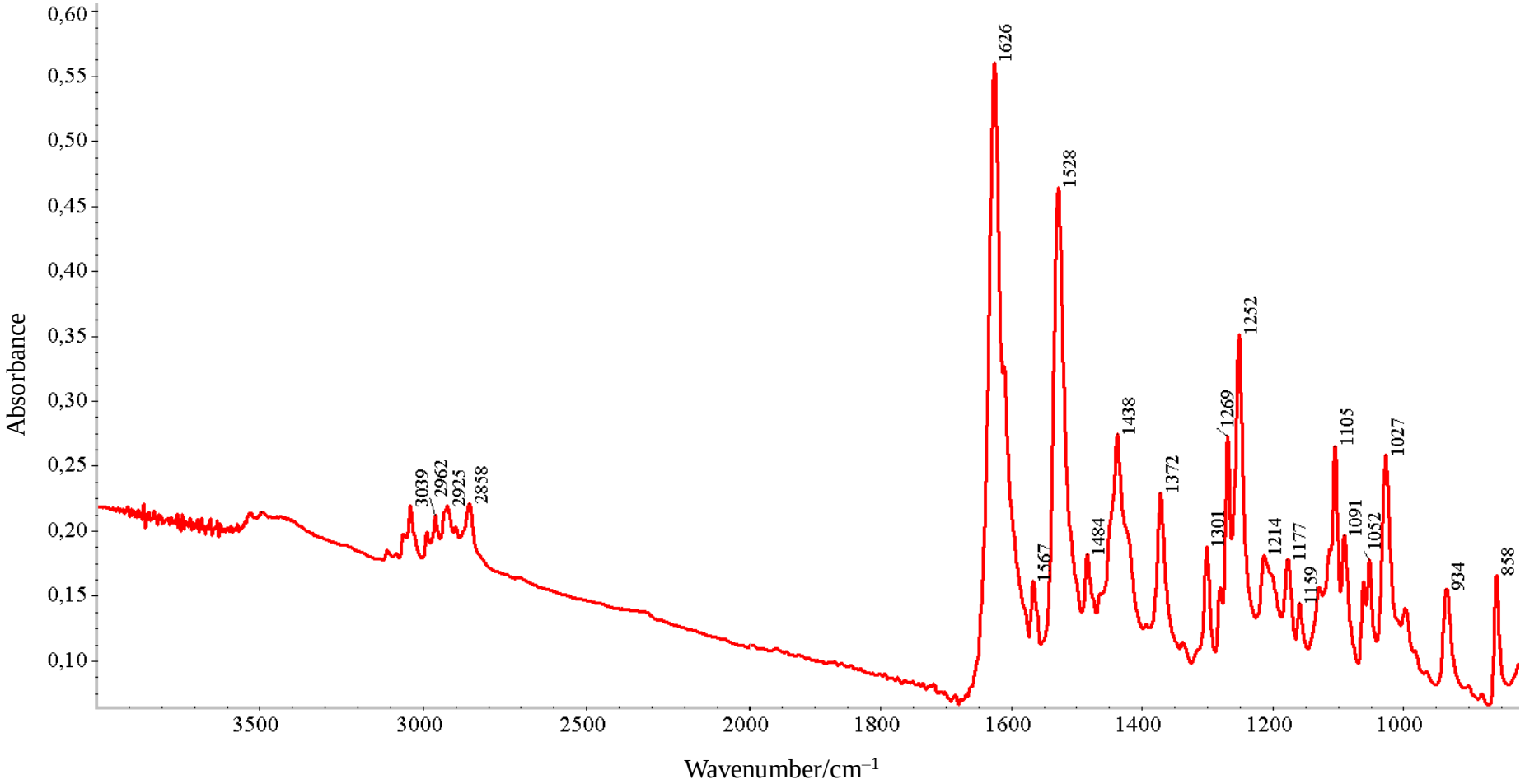

Fig. S37. IR spectrum of complex **8**

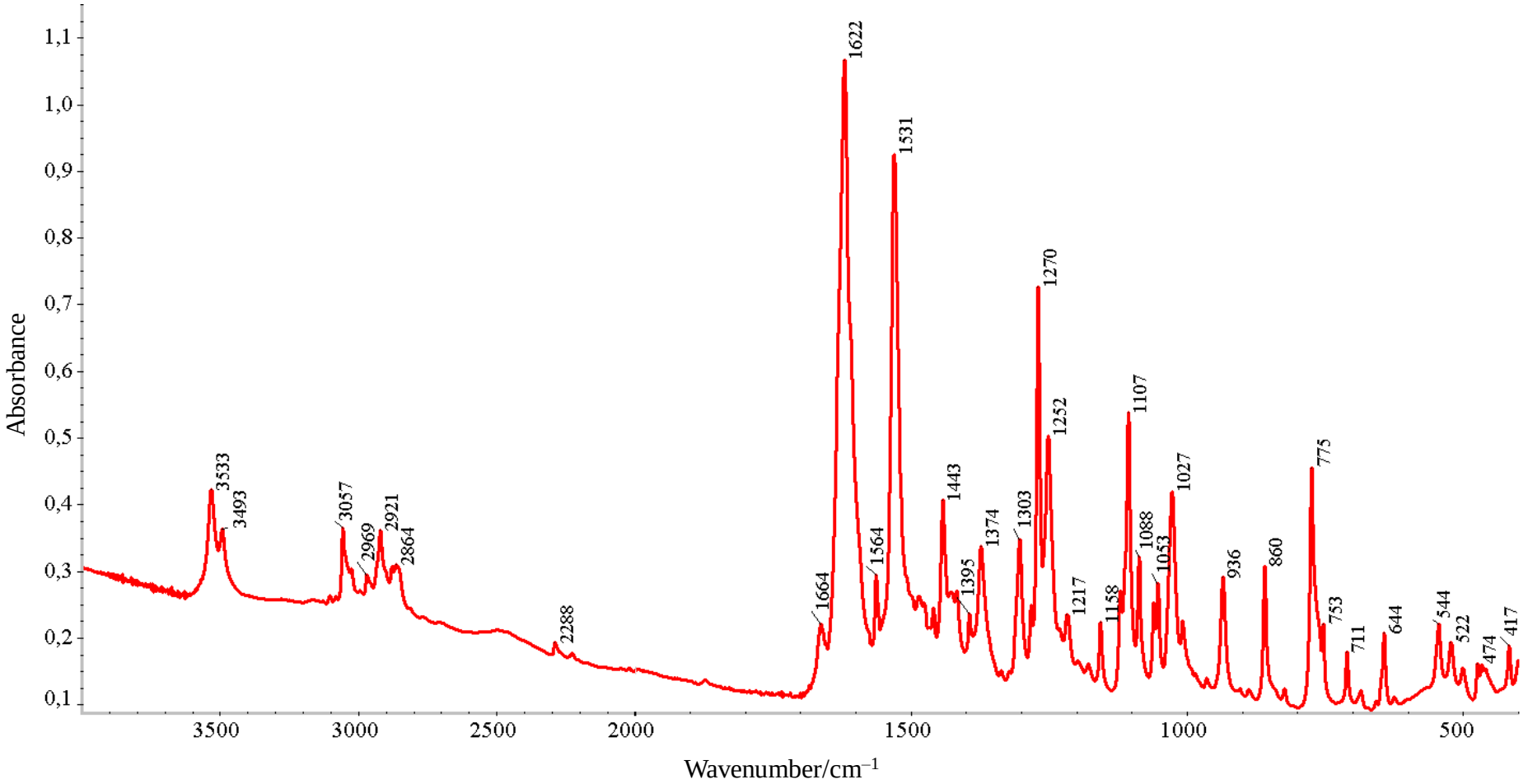

Fig. S38. IR spectrum of the residue obtained after a solid-phase reaction of ligand **1** with $PdCl_2(NCPh)_2$ promoted by manual grinding of the reactants in a mortar

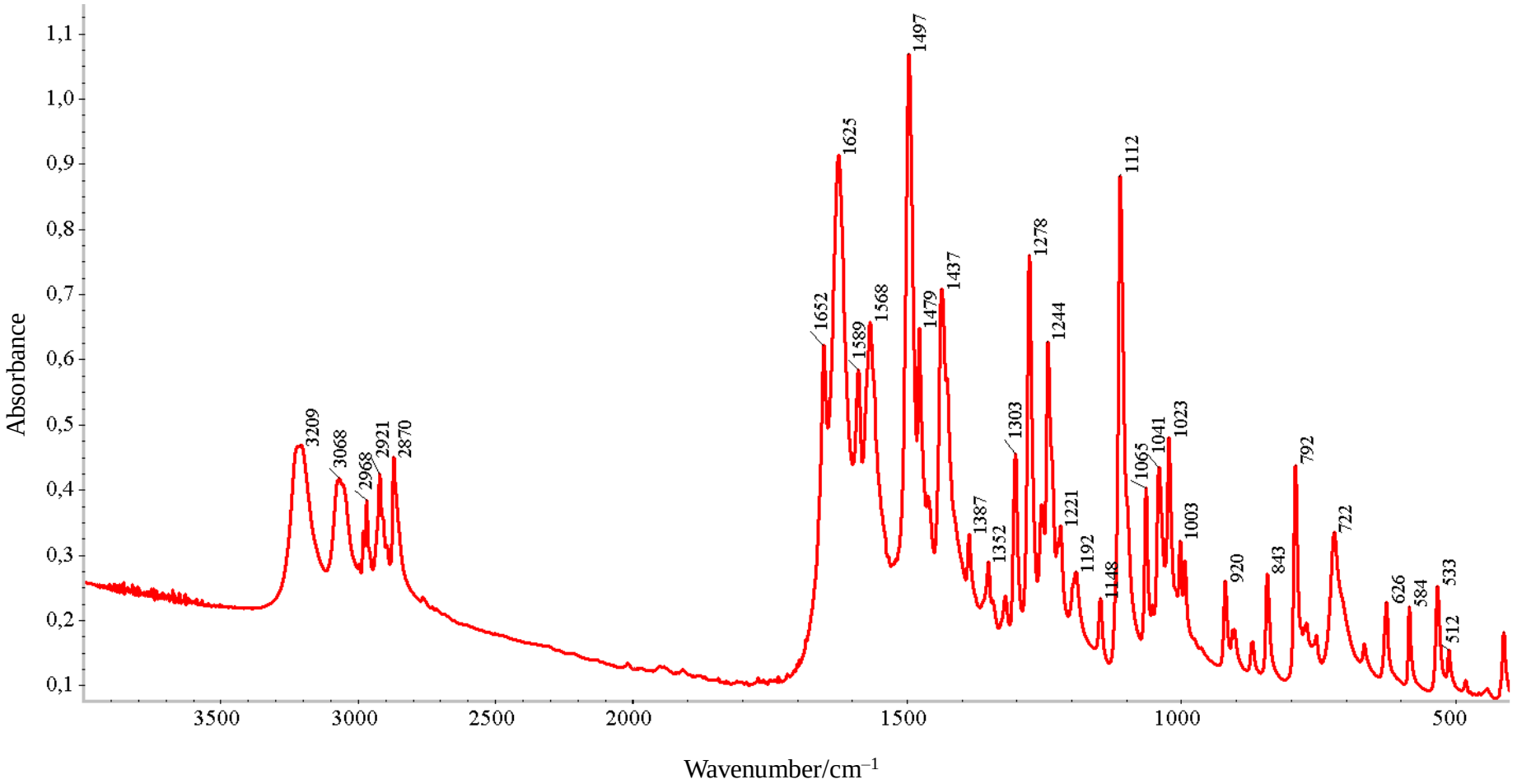

Fig. S39. IR spectrum of ligand **2**

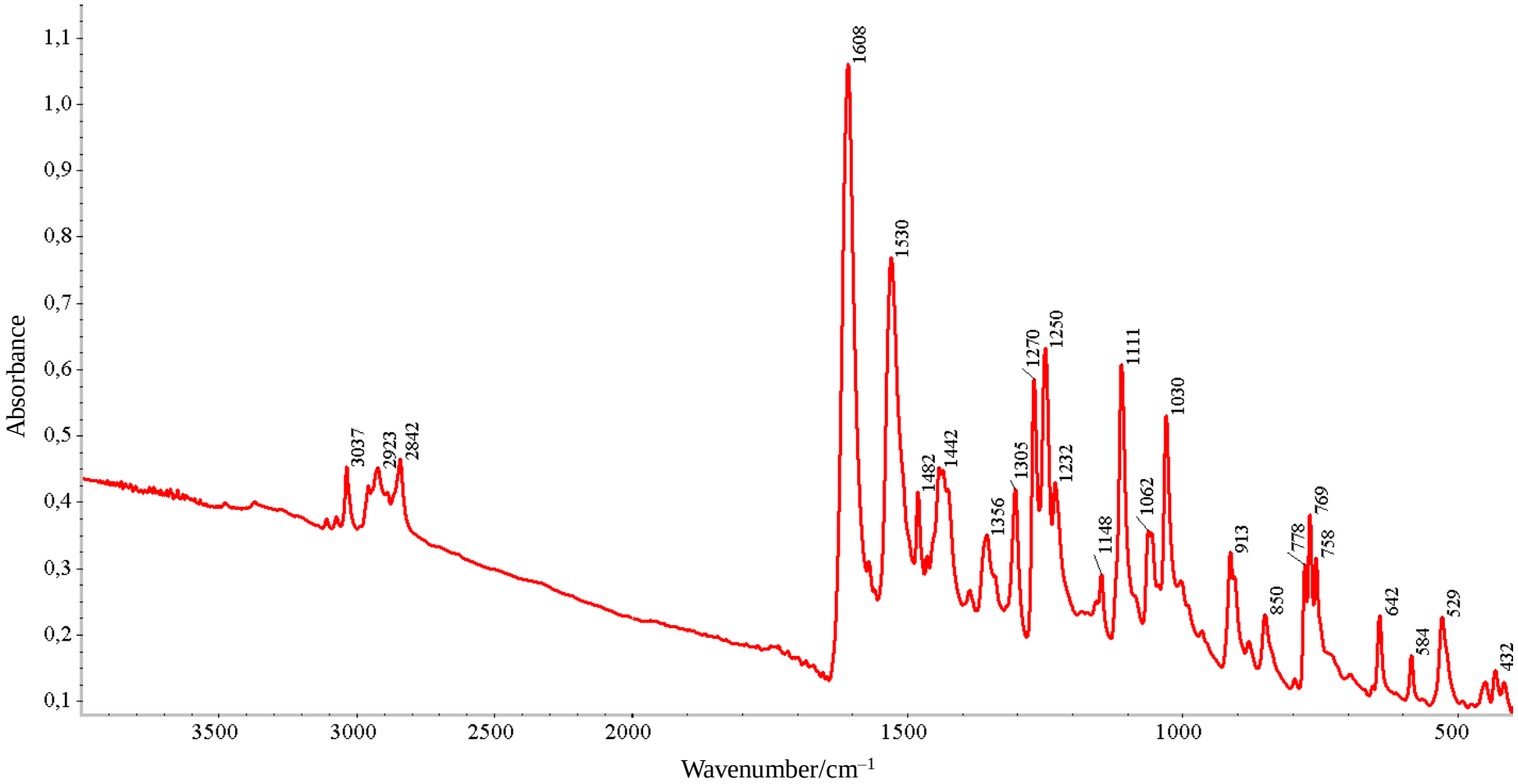

Fig. S40. IR spectrum of complex **9**

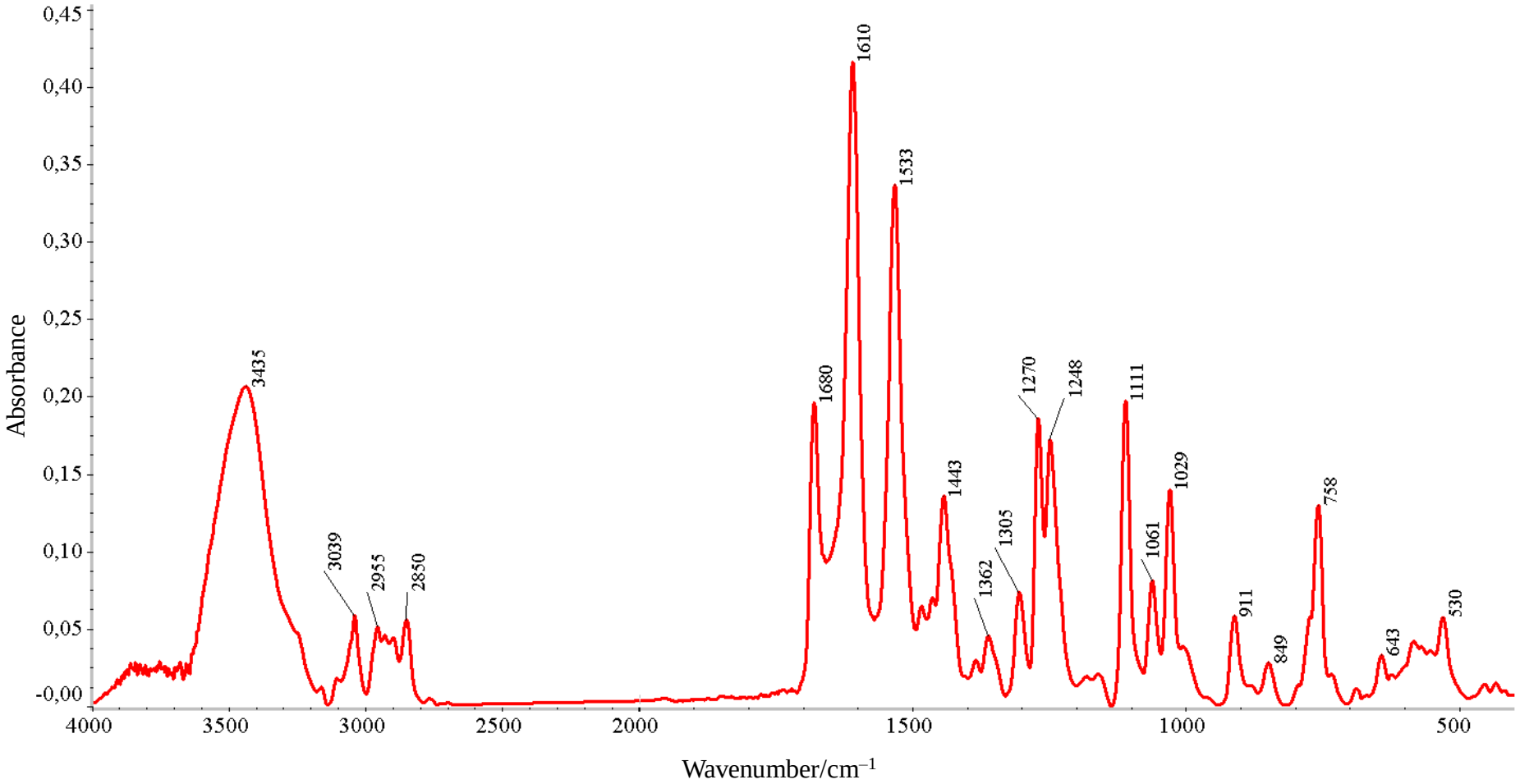

Fig. S41. IR spectrum of the residue obtained after a solid-phase reaction of ligand **2** with $PdCl_2(NCPh)_2$ promoted by manual grinding of the reactants in a mortar

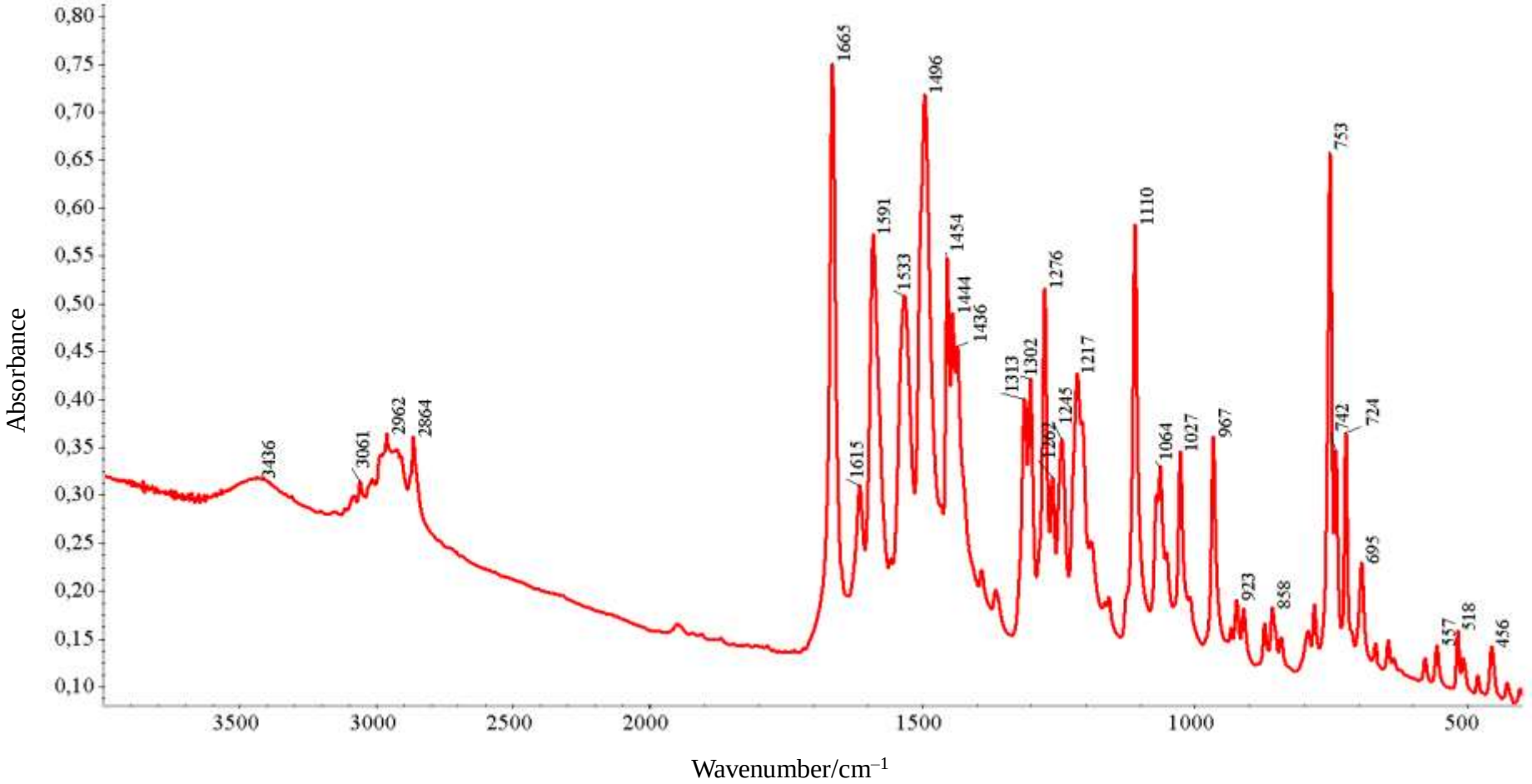

Fig. S42. IR spectrum of ligand **4**

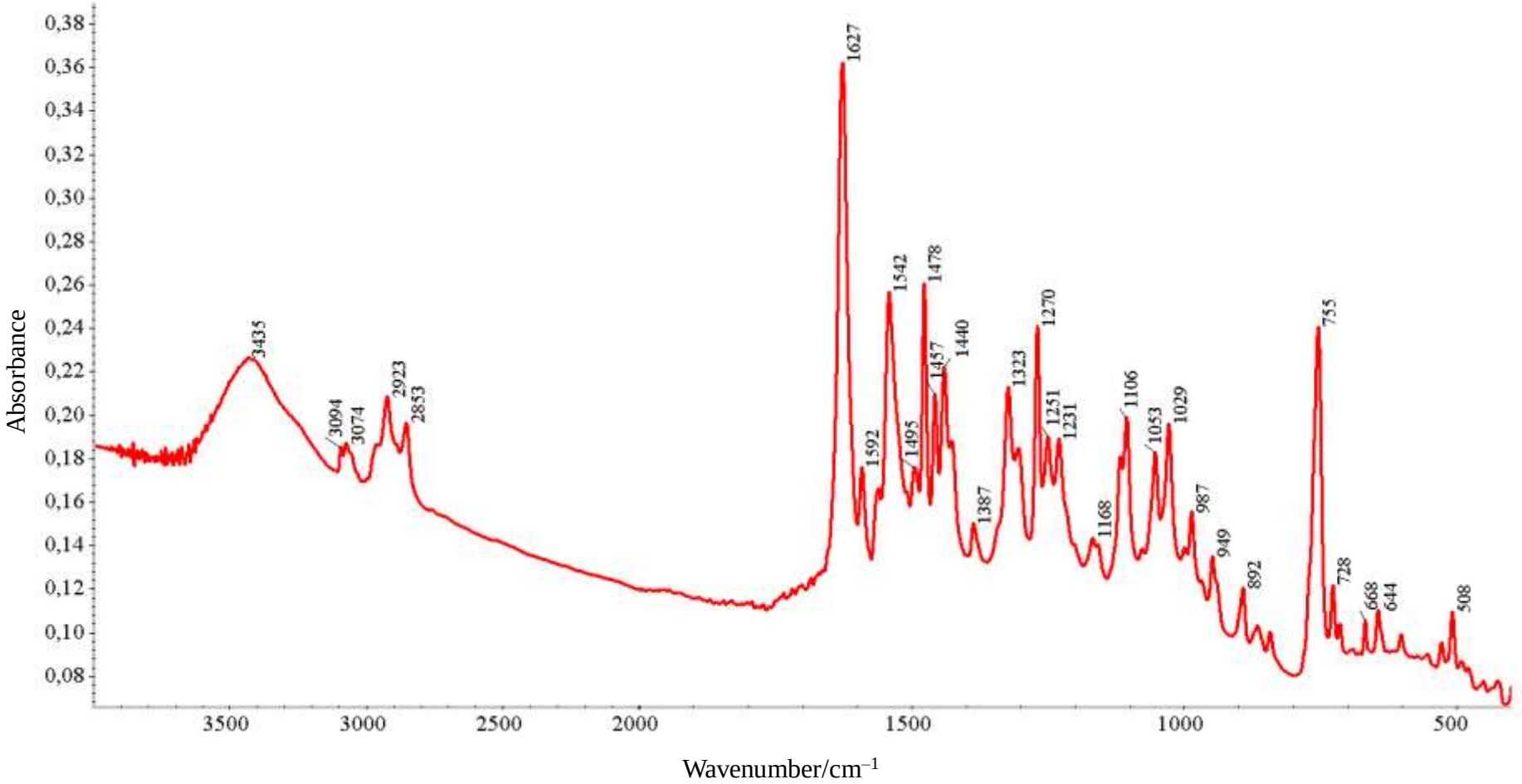

Fig. S43. IR spectrum of complex **12**

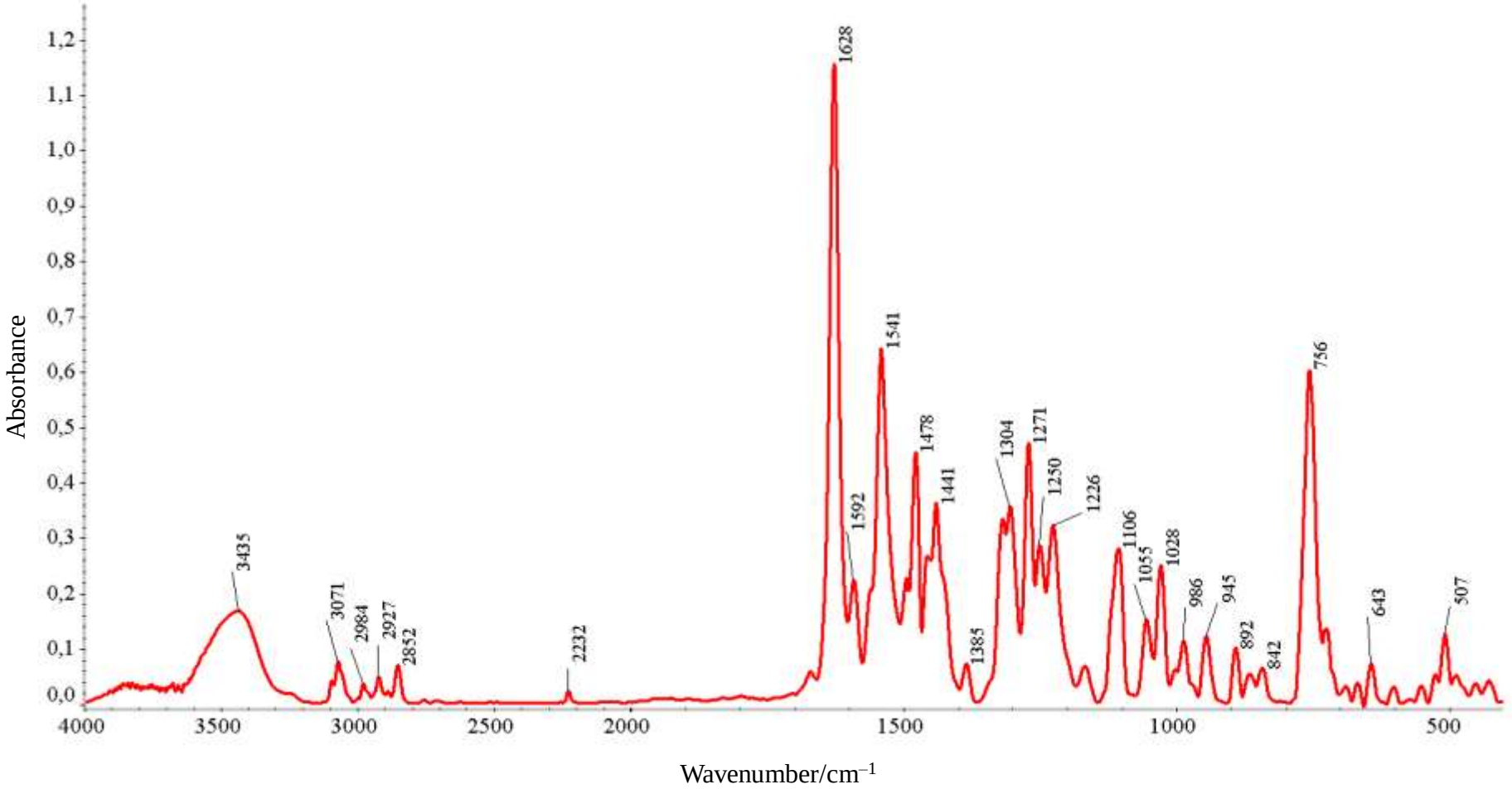

Fig. S44. IR spectrum of the residue obtained after a solid-phase reaction of ligand **4** with $PdCl_2(NCPh)_2$ promoted by manual grinding of the reactants in a mortar

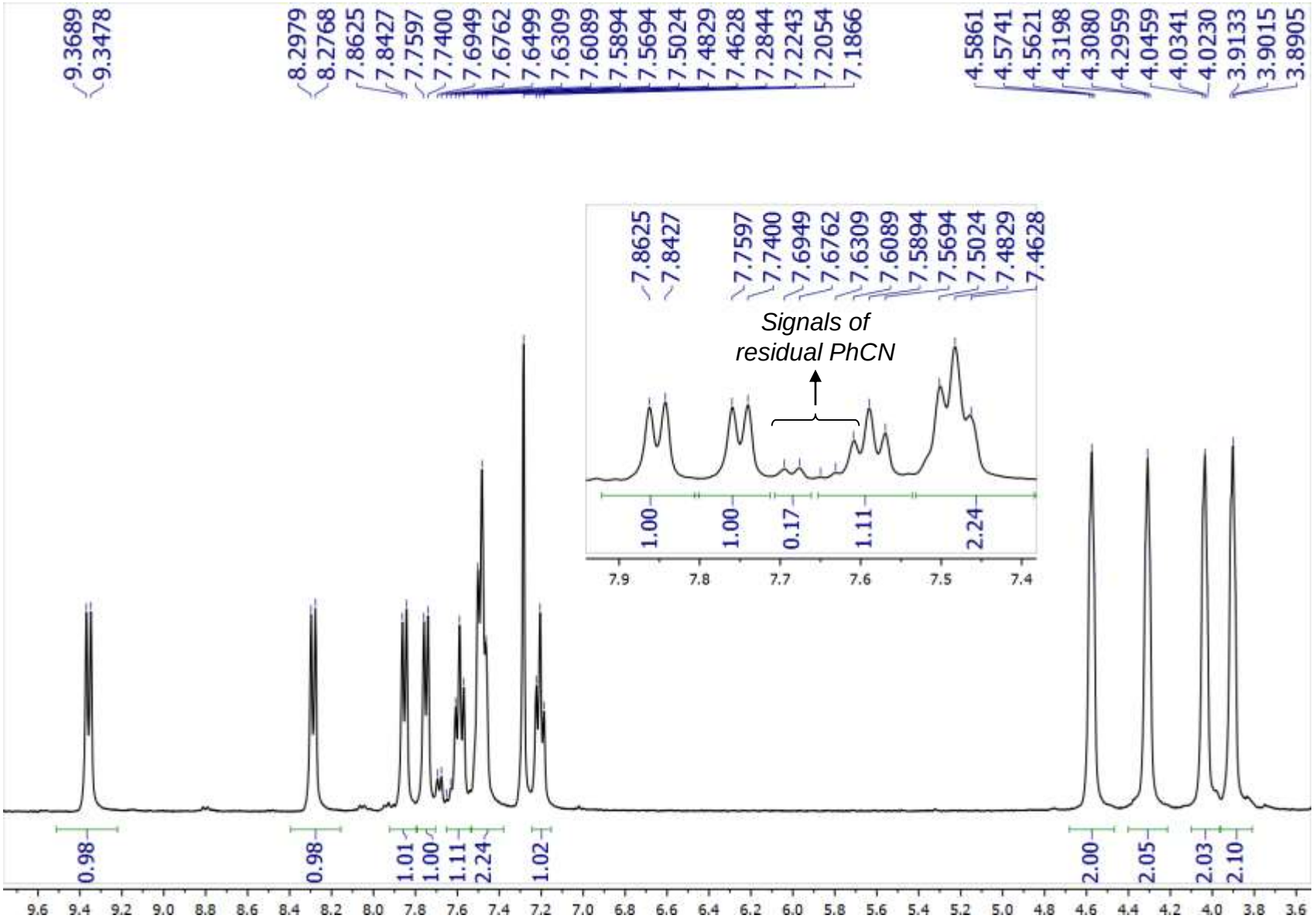

Fig. S45. ^{1}H NMR spectrum of the residue obtained after a solid-phase reaction of ligand **4** with $PdCl_2(NCPh)_2$ promoted by manual grinding of the reactants in a mortar and rinsed with hexane (400.13 MHz, $CDCl_3$)

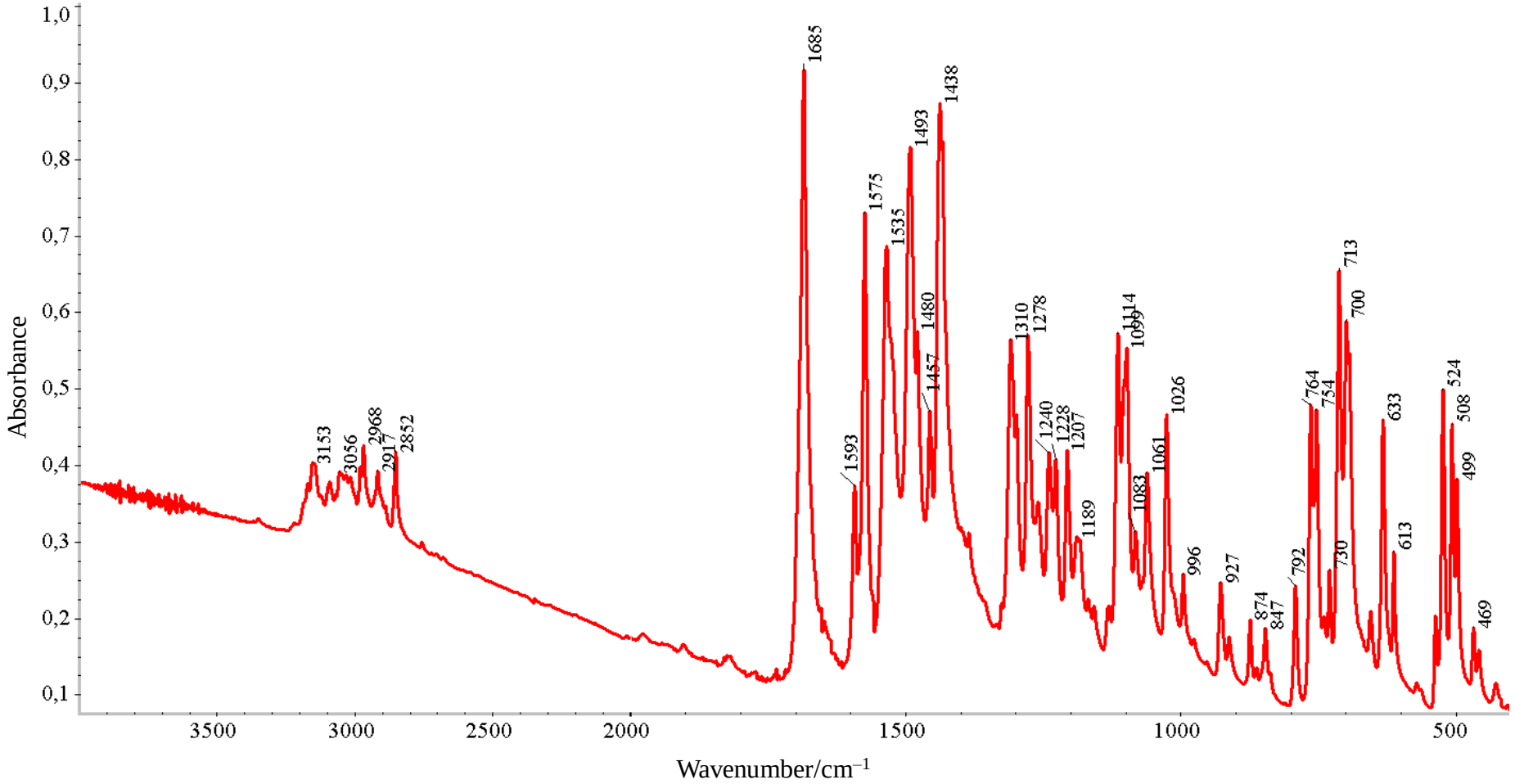

Fig. S46. IR spectrum of ligand **6**

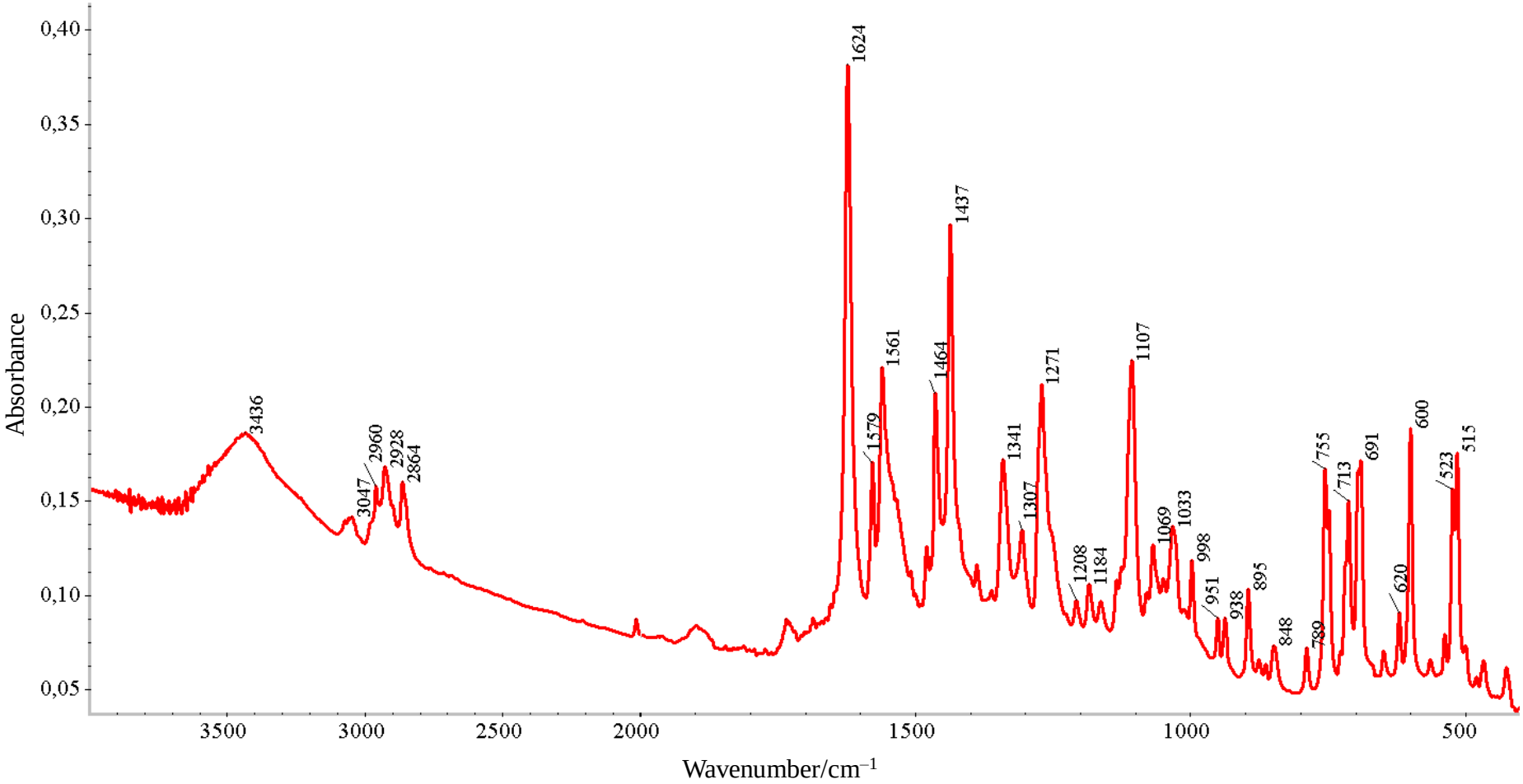

Fig. S47. IR spectrum of complex **14**

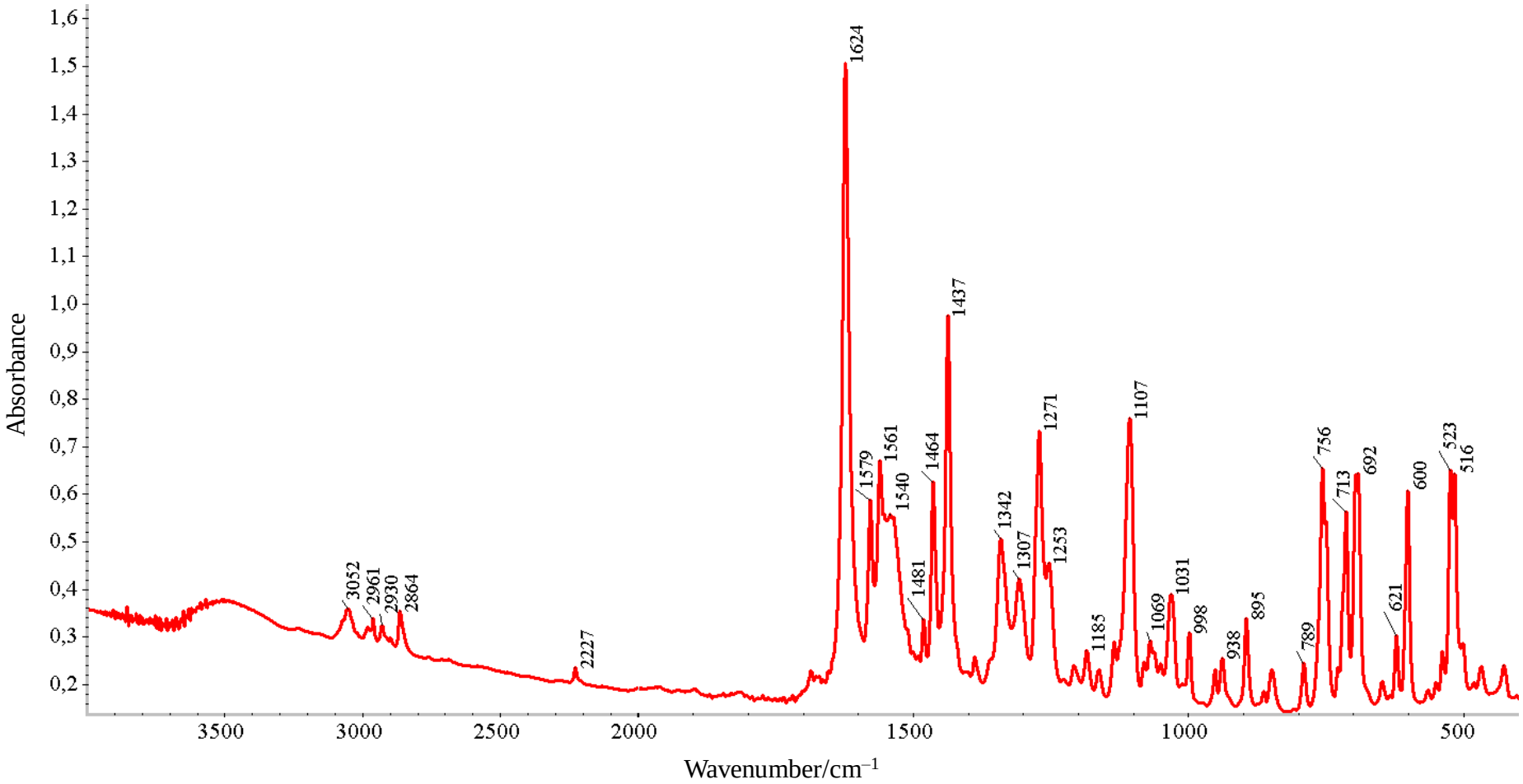

Fig. S48. IR spectrum of the residue obtained after a solid-phase reaction of ligand **6** with $PdCl_2(NCPh)_2$ promoted by manual grinding of the reactants in a mortar

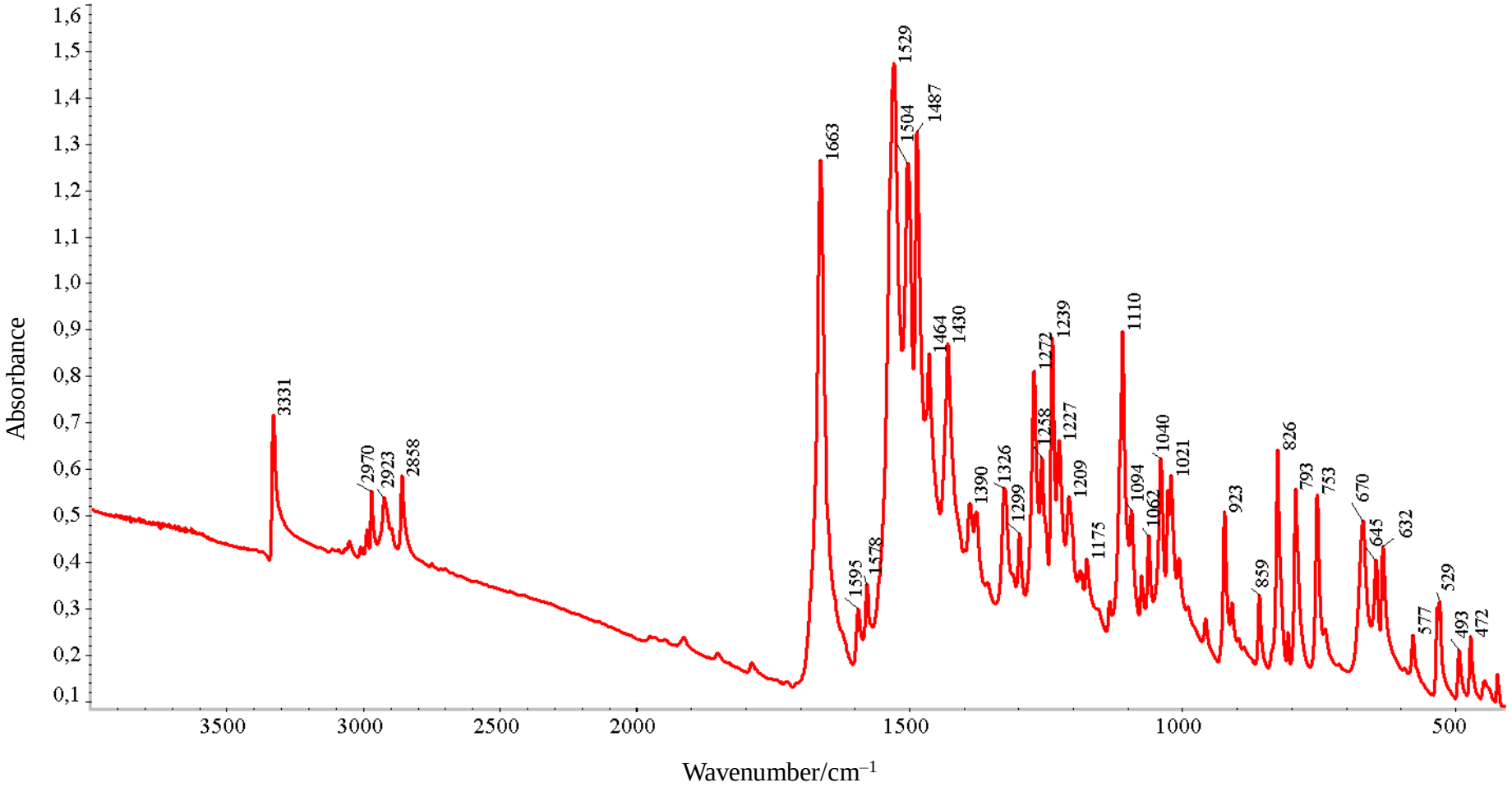

Fig. S49. IR spectrum of ligand **3**

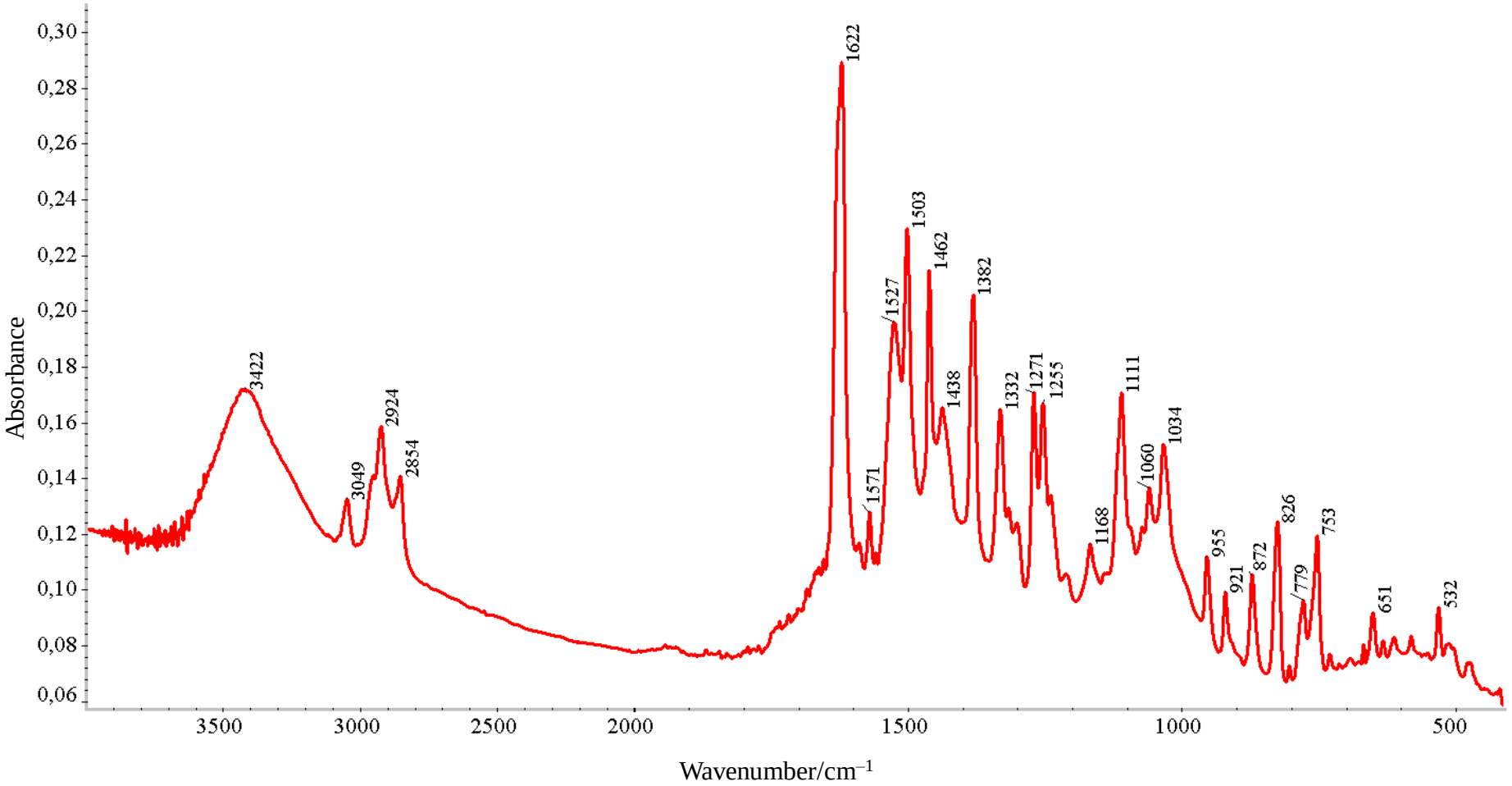

Fig. S50. IR spectrum of complex **10**

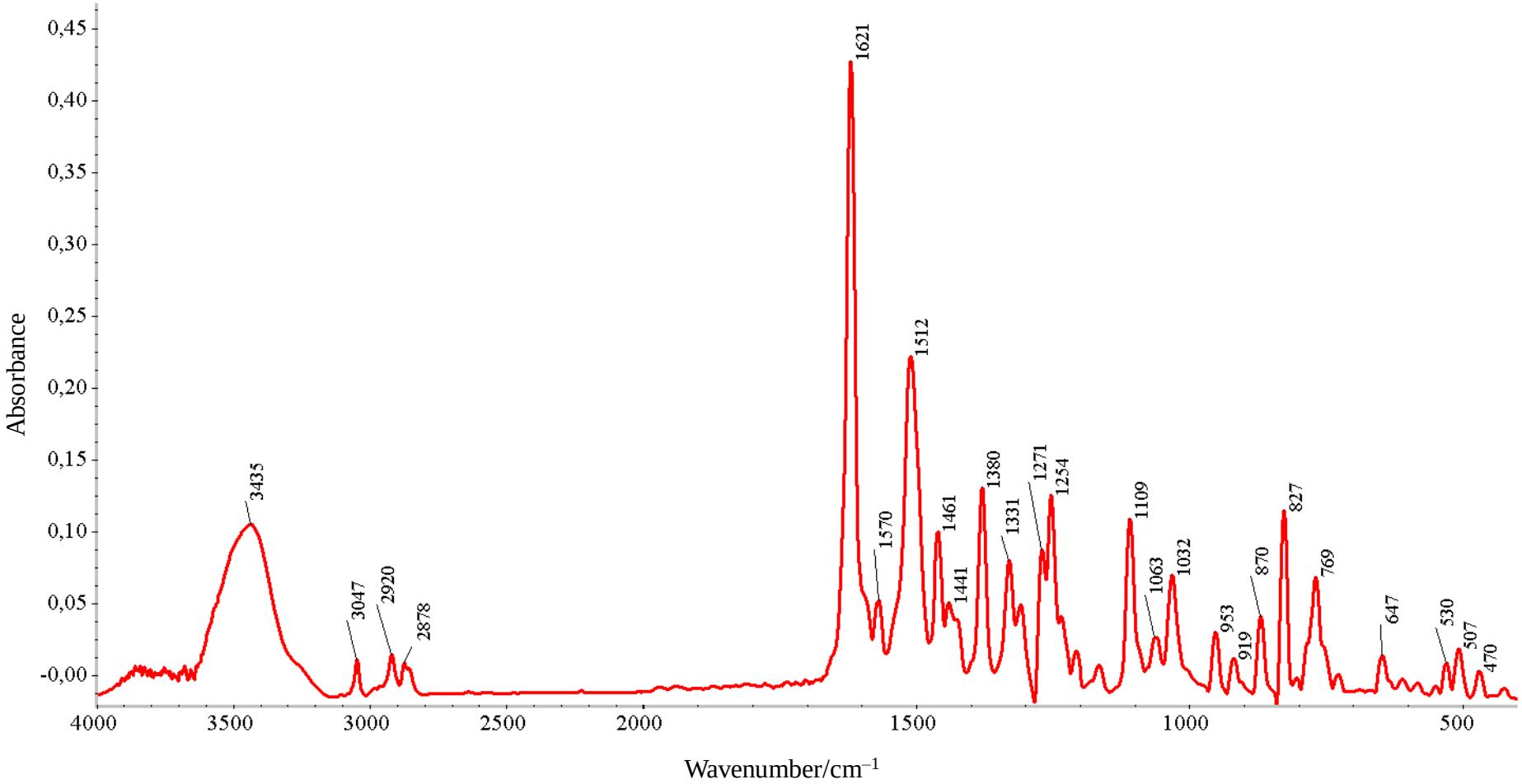

Fig. S51. IR spectrum of the residue obtained after a solid-phase reaction of ligand **3** with $PdCl_2(NCPh)_2$ in a mortar

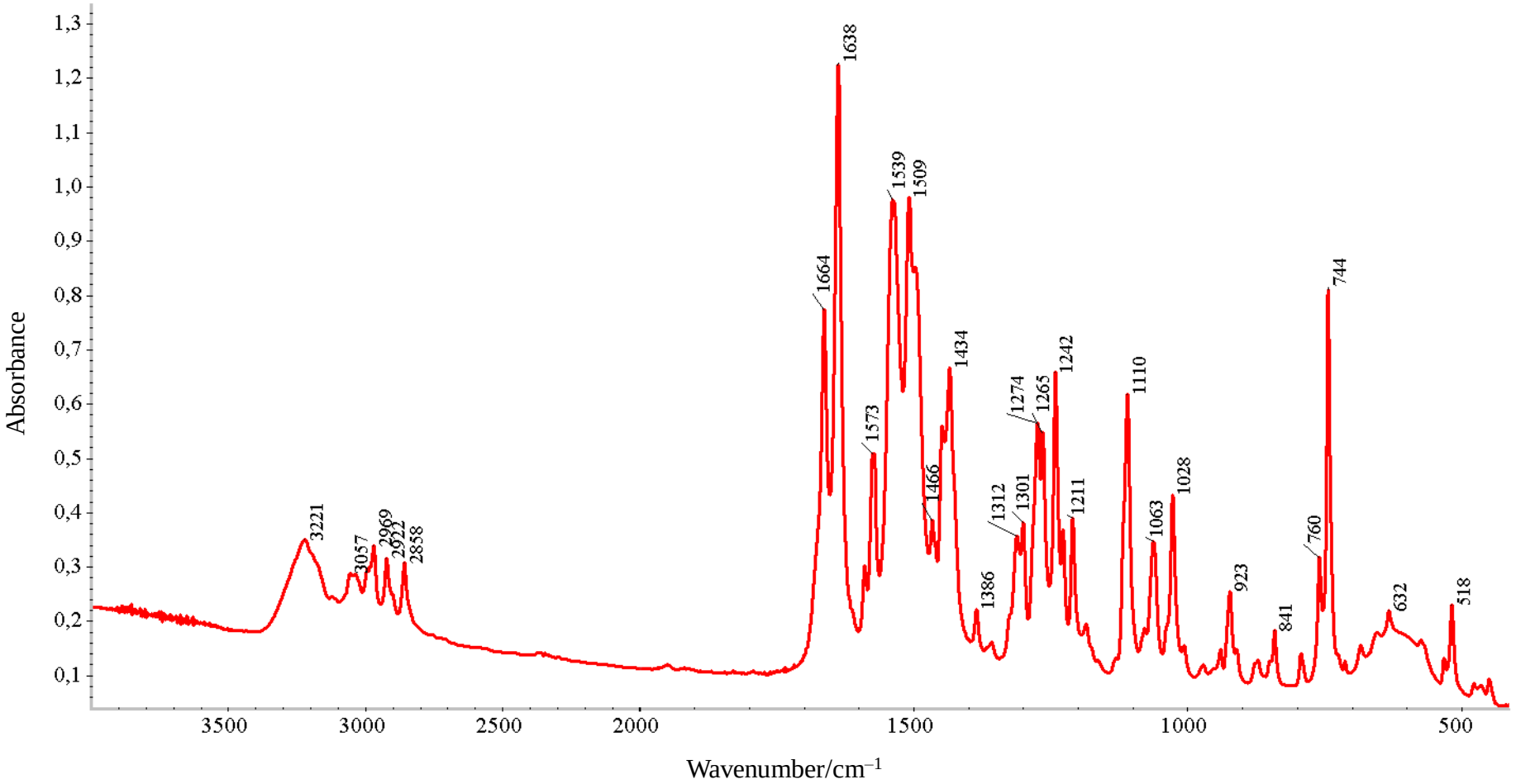

Fig. S52. IR spectrum of ligand **5**

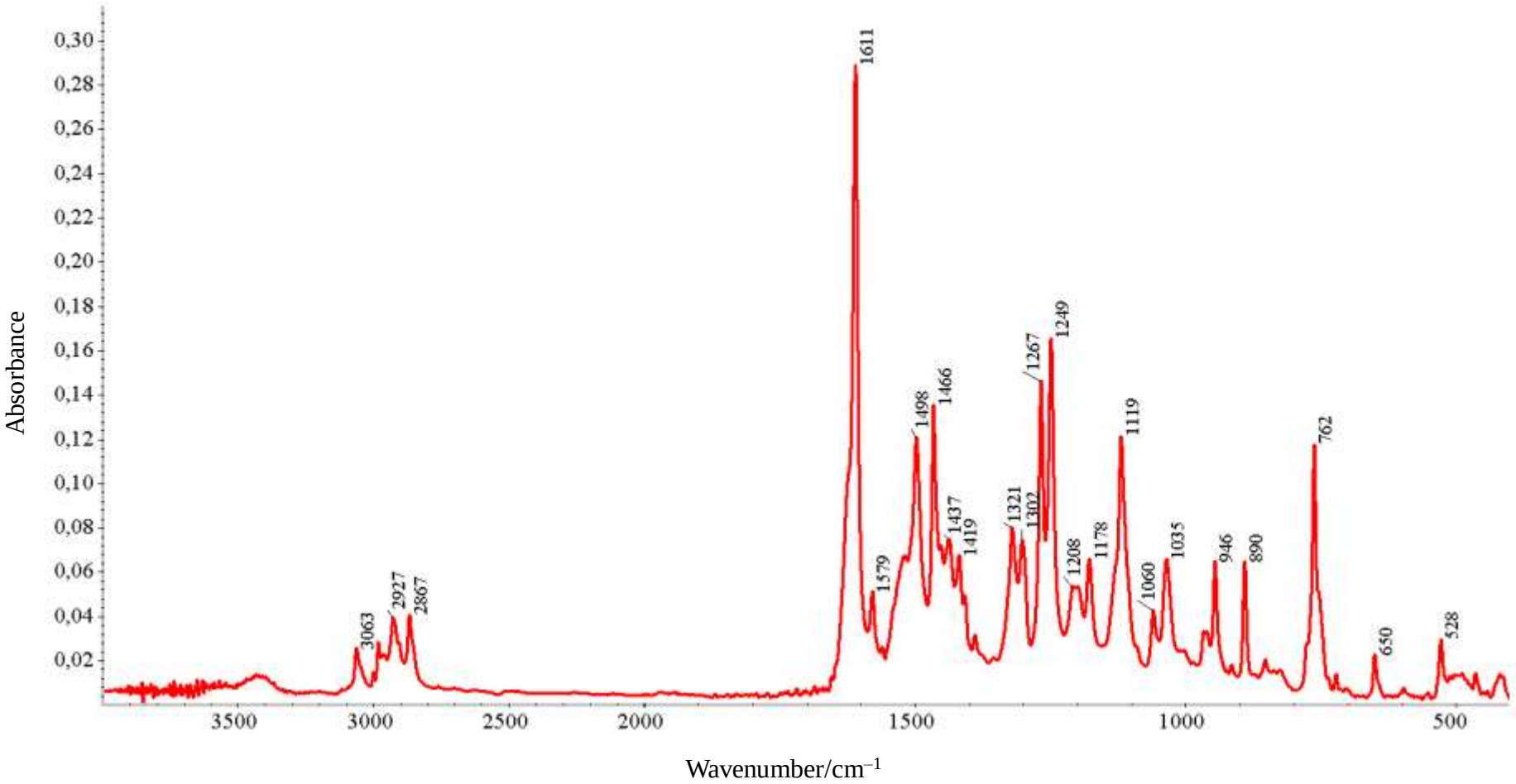

Fig. S53. IR spectrum of complex **13**

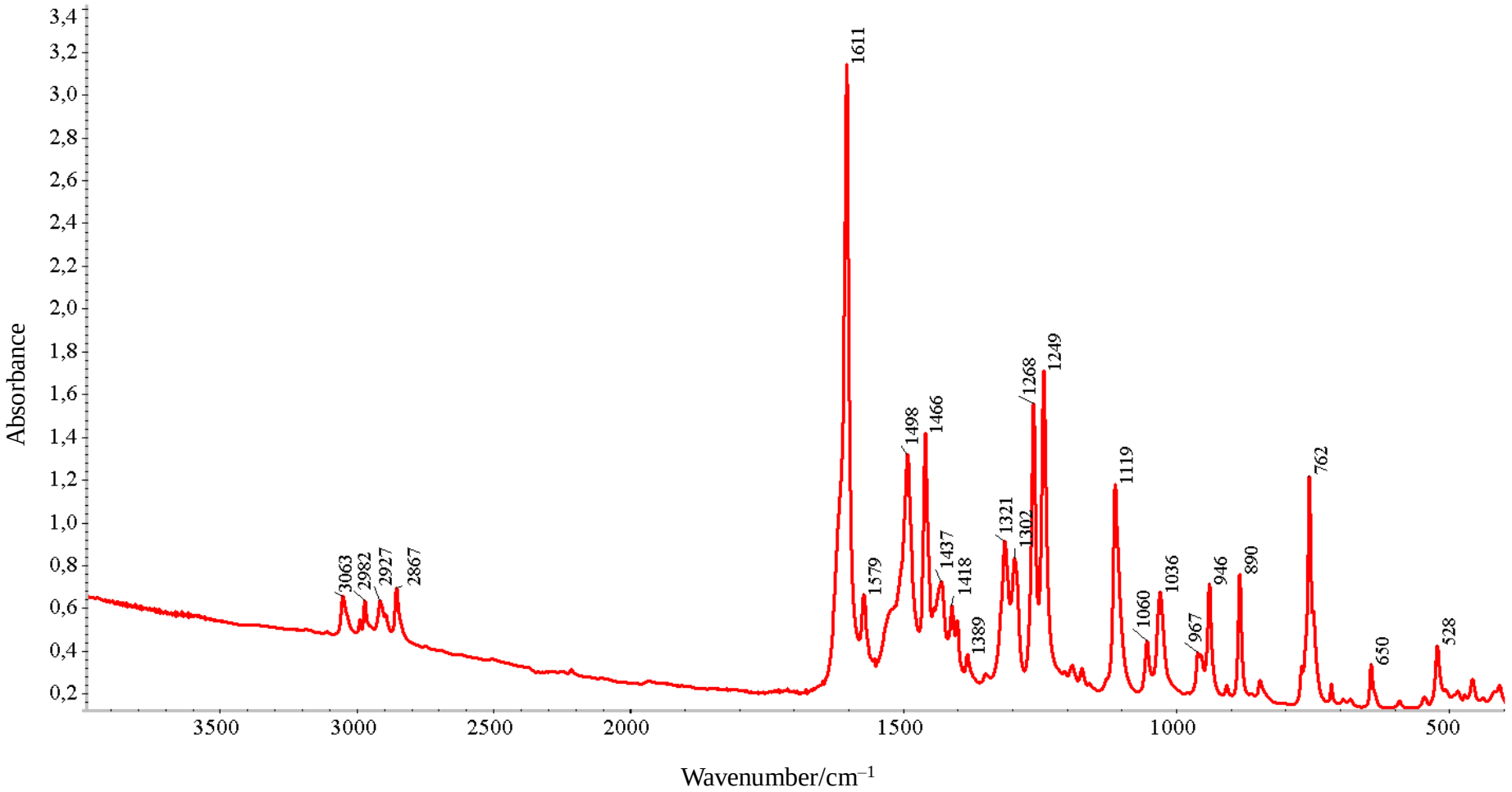

Fig. S54. IR spectrum of the paste-like residue obtained after a solid-phase reaction of ligand **5** with $PdCl_2(NCPh)_2$ in a mortar (registered in 30 min after the grinding cessation)

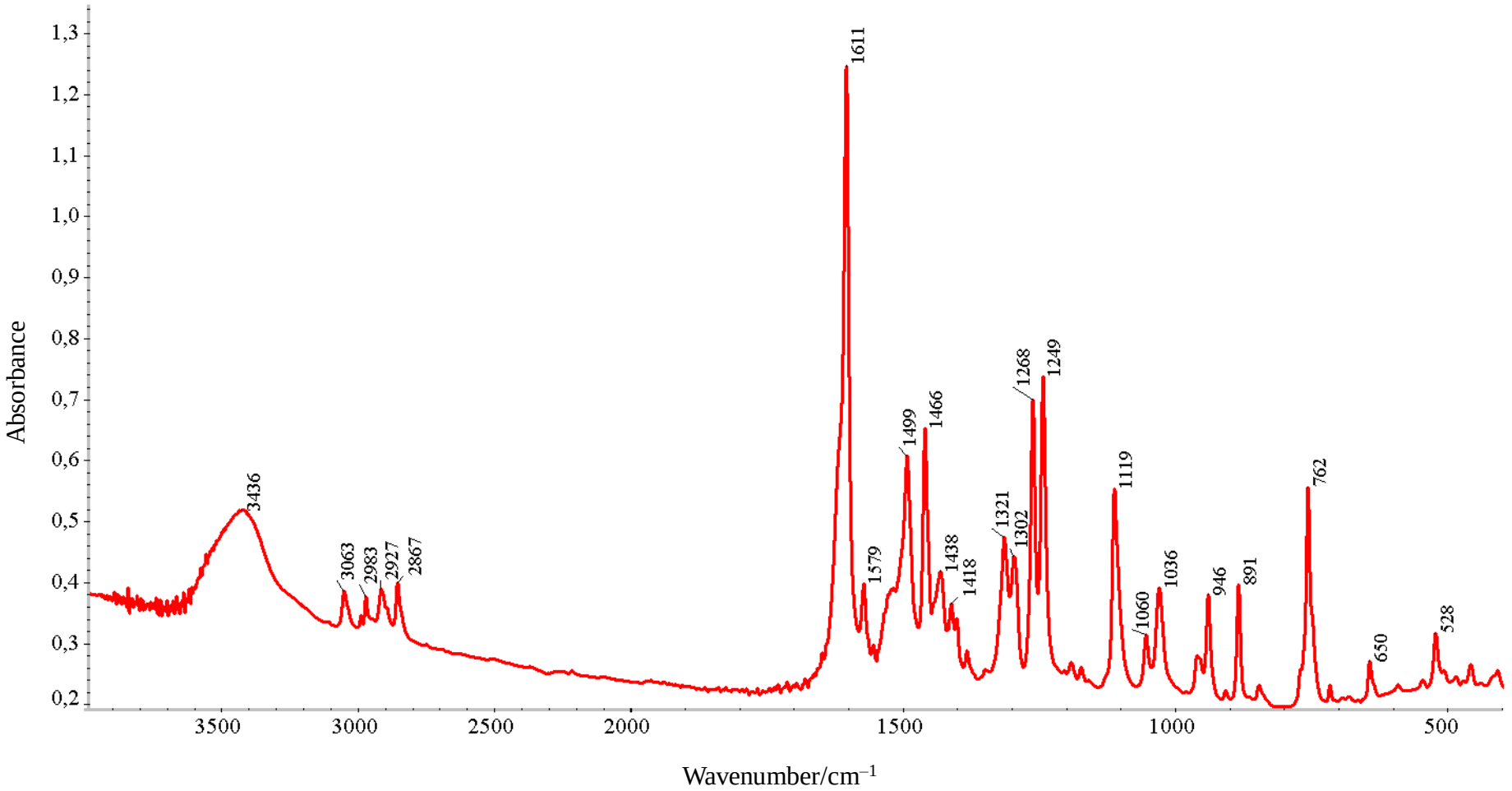

Fig. S55. IR spectrum of the powder obtained after a solid-phase reaction of ligand **5** with $PdCl_2(NCPh)_2$ in a mortar (registered in 2 h after the grinding cessation)

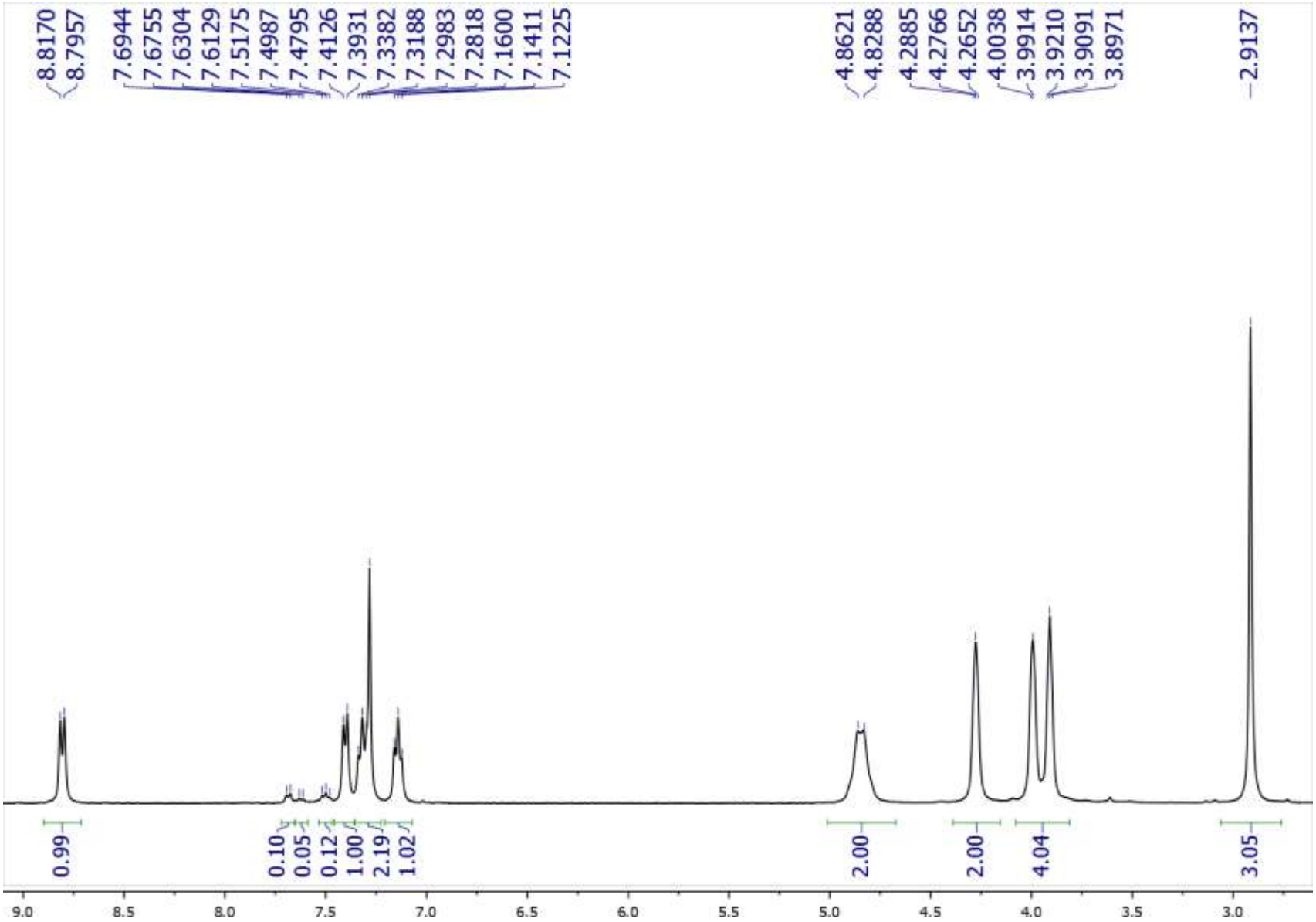

Fig. S56. ^{1}H NMR spectrum of the residue obtained after a solid-phase reaction of ligand **5** with $PdCl_2(NCPh)_2$ in a mortar and rinsed with hexane (400.13 MHz, $CDCl_3$)

Fig. S57. Narva DDR GM 9458 vibration ball mill with a custom-built agate insert

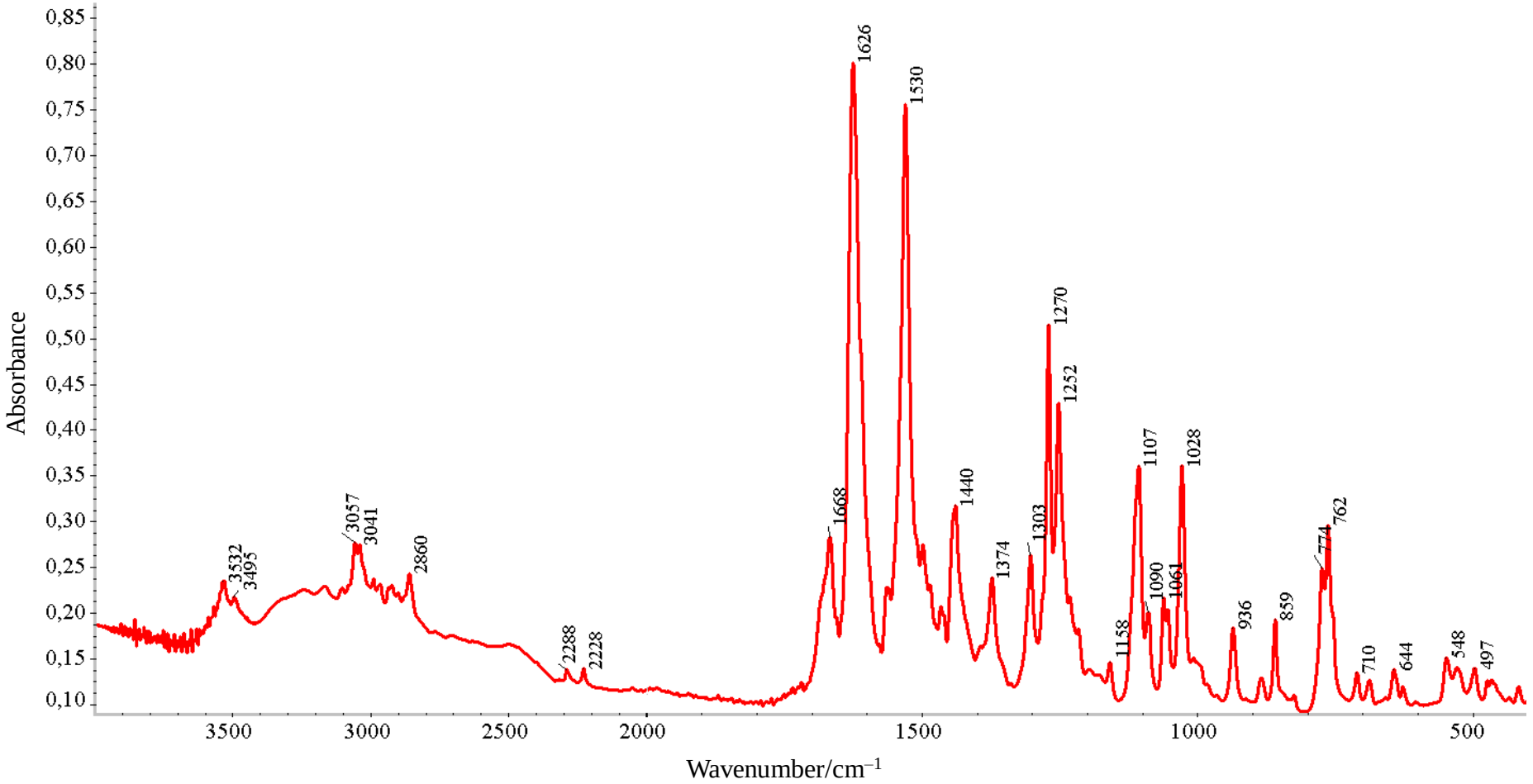

Fig. S58. IR spectrum of the residue obtained after a solid-phase reaction of ligand **1** with $PdCl_2(NCPh)_2$ in a vibration ball mill (registered in 30 min after the grinding cessation)

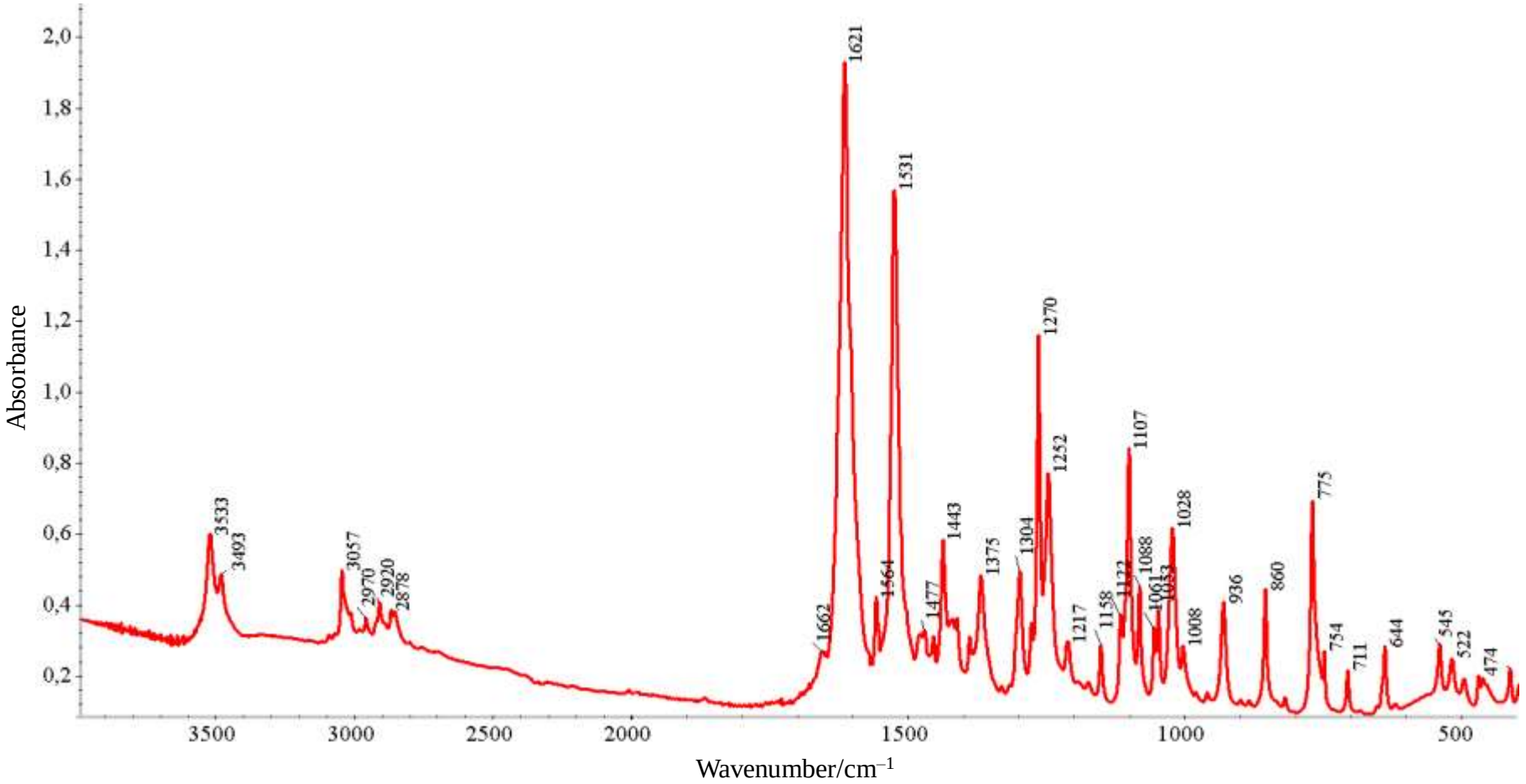

Fig. S59. IR spectrum of the residue obtained after a solid-phase reaction of ligand **1** with $PdCl_2(NCPh)_2$ in a vibration ball mill (registered in 2 weeks after the experiment)

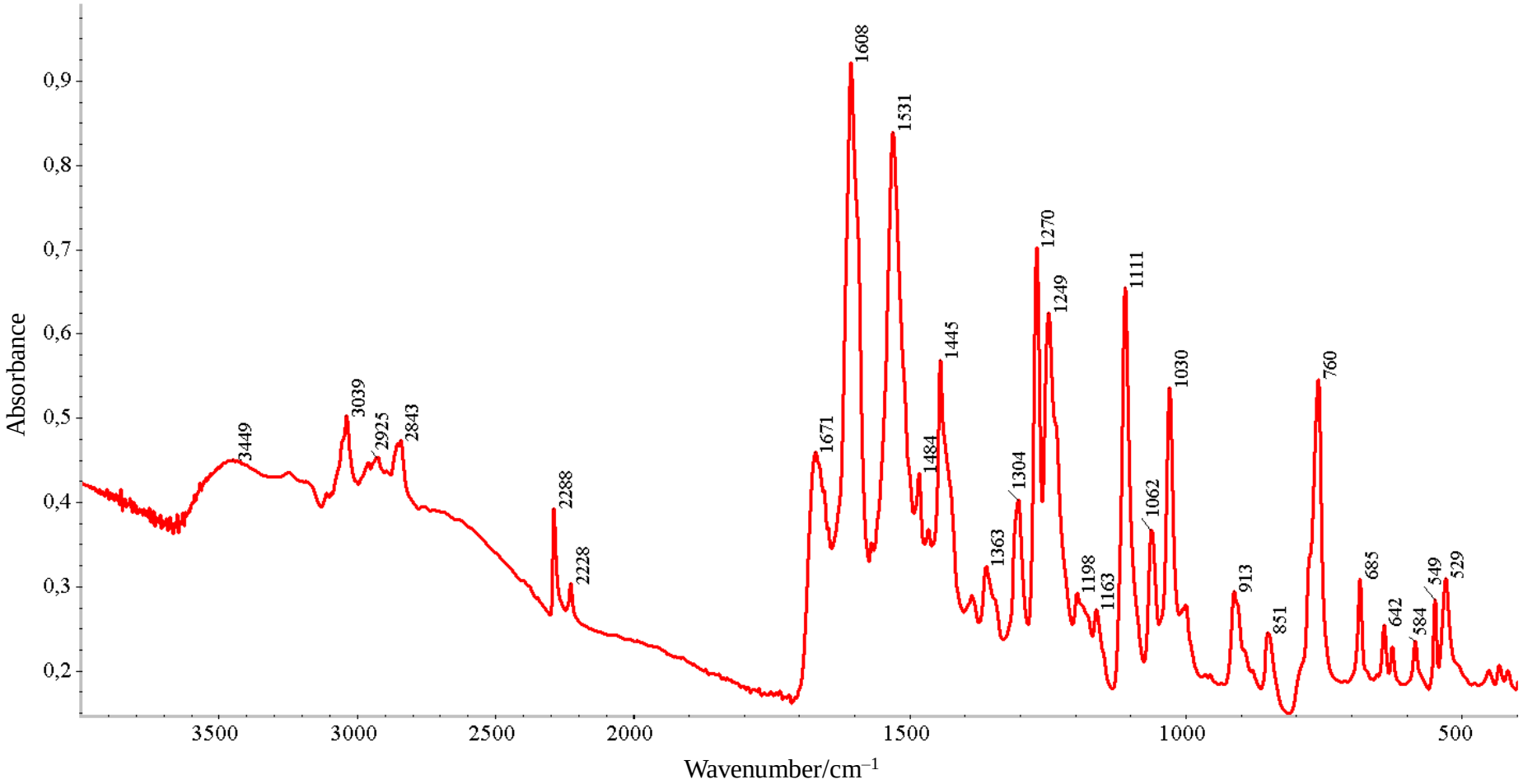

Fig. S60. IR spectrum of the residue obtained after a solid-phase reaction of ligand **2** with $PdCl_2(NCPh)_2$ in a vibration ball mill (registered in 1 h after the grinding cessation)

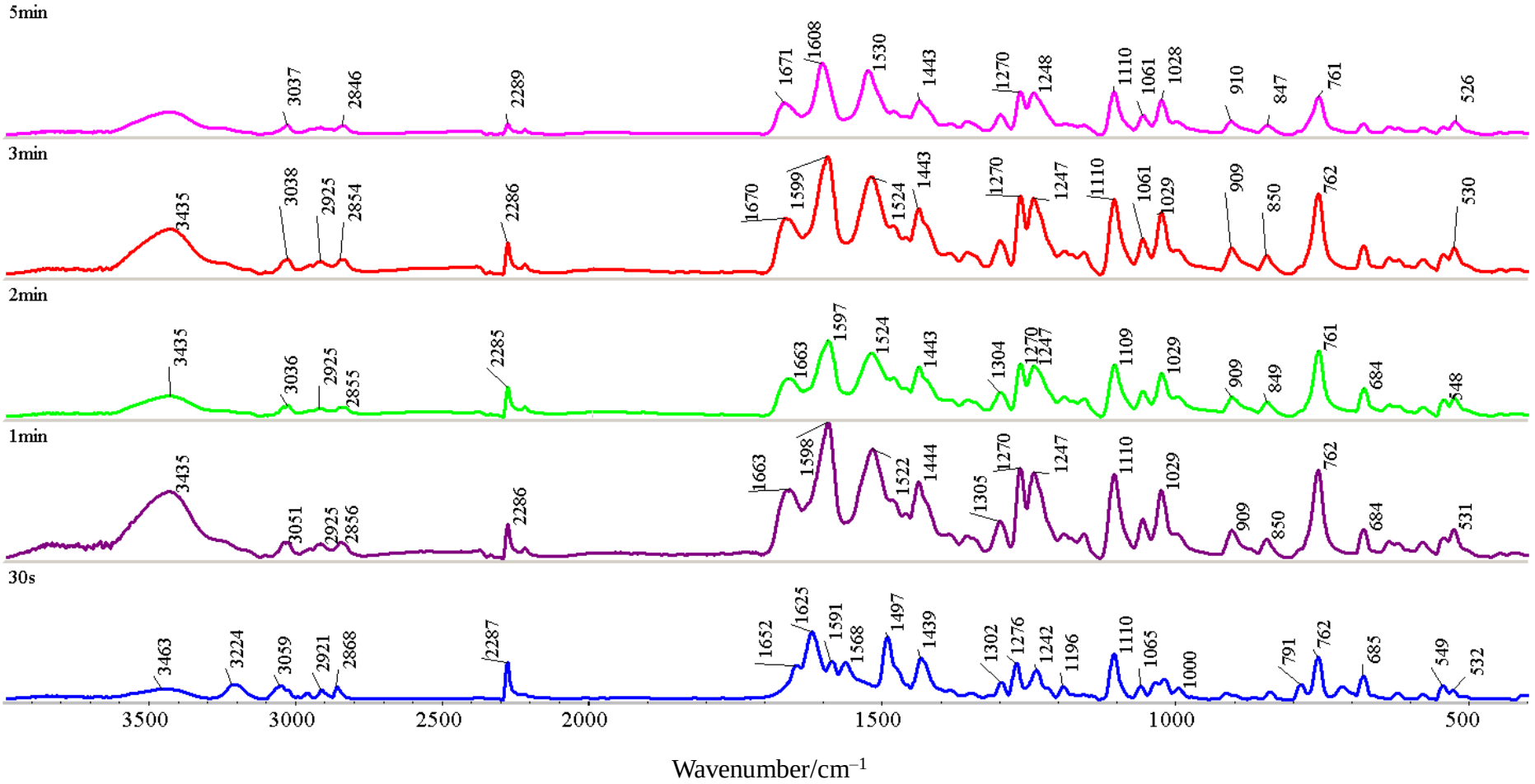

Fig. S61. IR spectroscopic monitoring of the reaction of ligand **2** with $PdCl_2(NCPh)_2$ in a vibration ball mill (the registration of all the spectra was completed in 2.5 h after the grinding cessation)

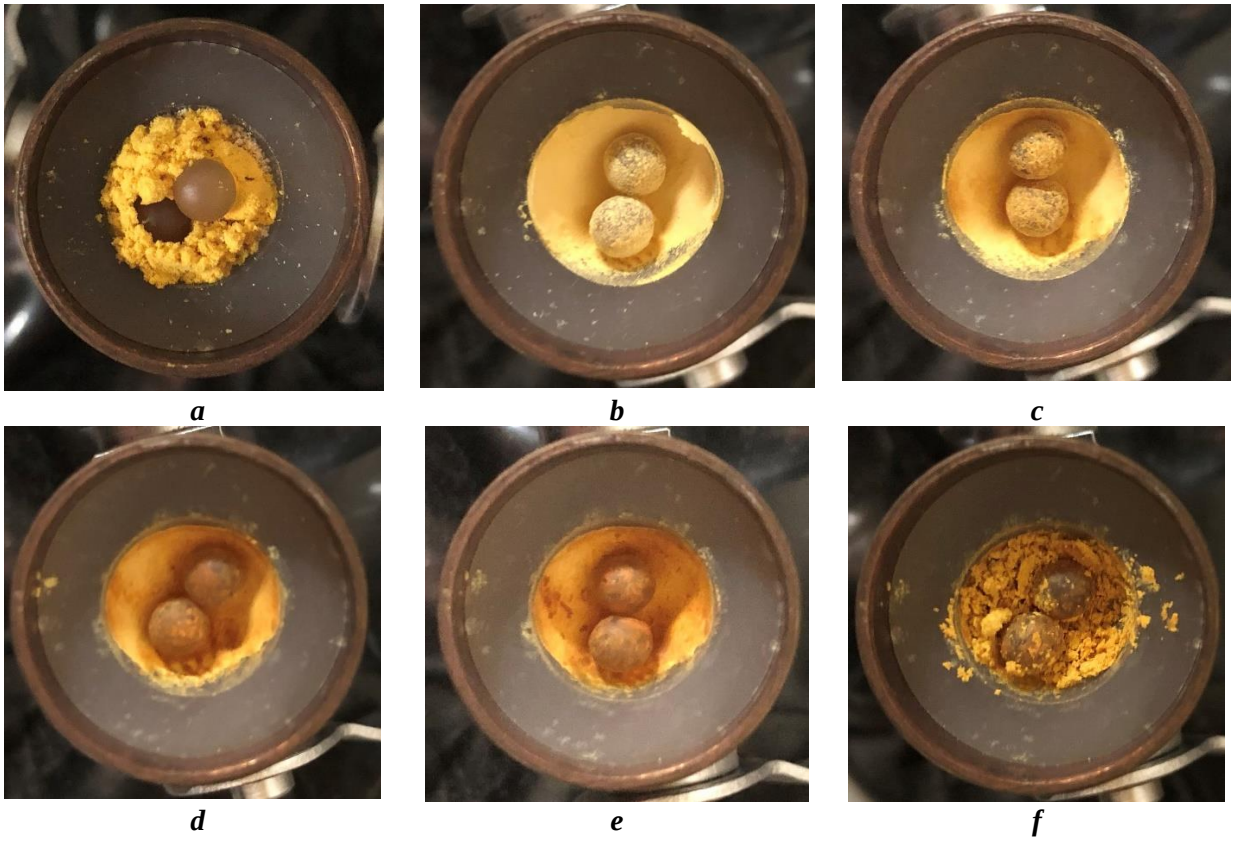

Fig. S62. Solid-phase reaction between ligand **2** and $PdCl_2(NCPh)_2$ in a vibration ball mill: a mixture of the reactants before grinding (***a***); grinding for 0.5 (***b***), 1 (***c***), 2 (***d***), 3 (***e***), and 5 (***f***) min

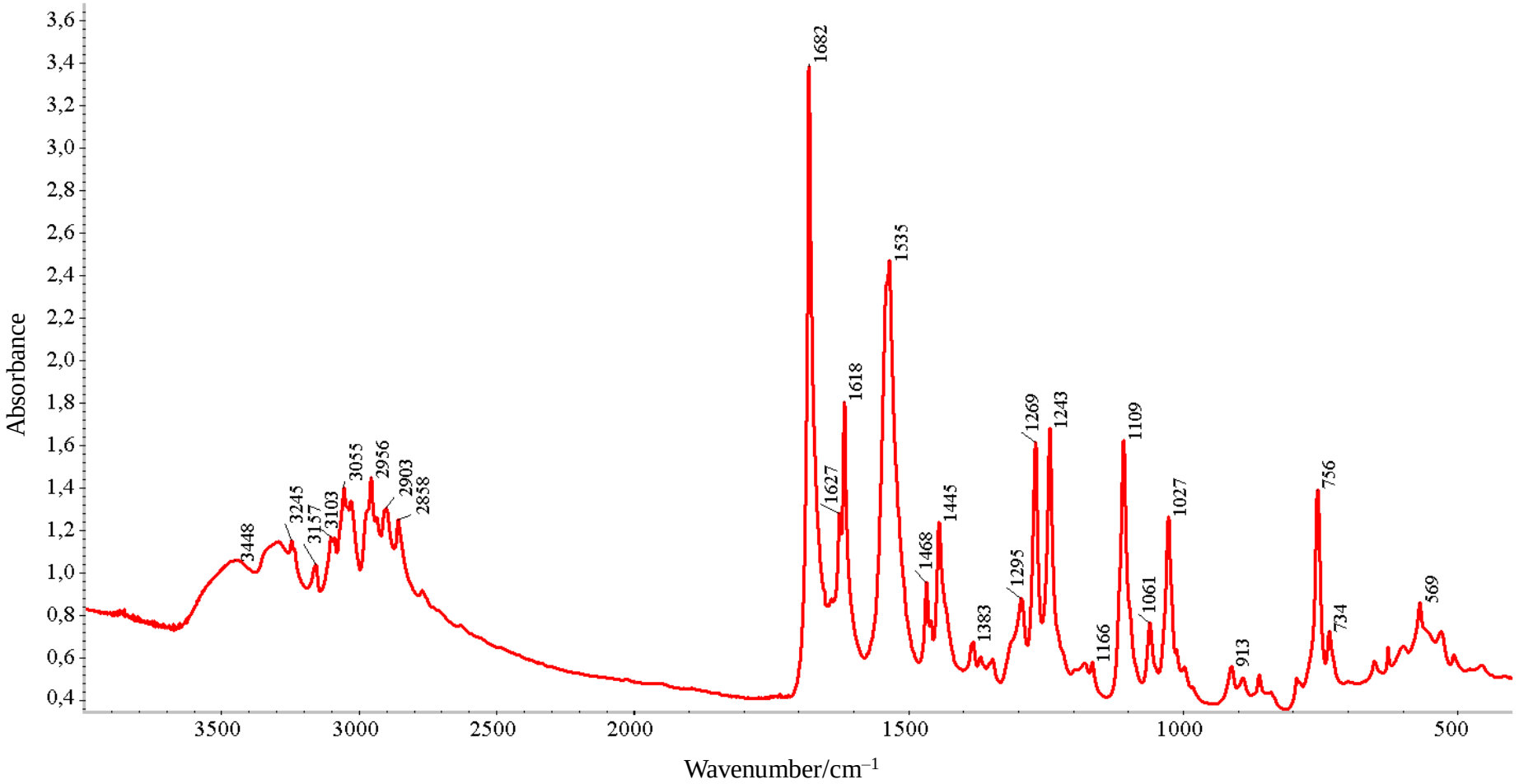

Fig. S63. IR spectrum of complex **15** isolated from a solid-phase reaction of ligand **2** with $PdCl_2(NCPh)_2$ in a vibration ball mill

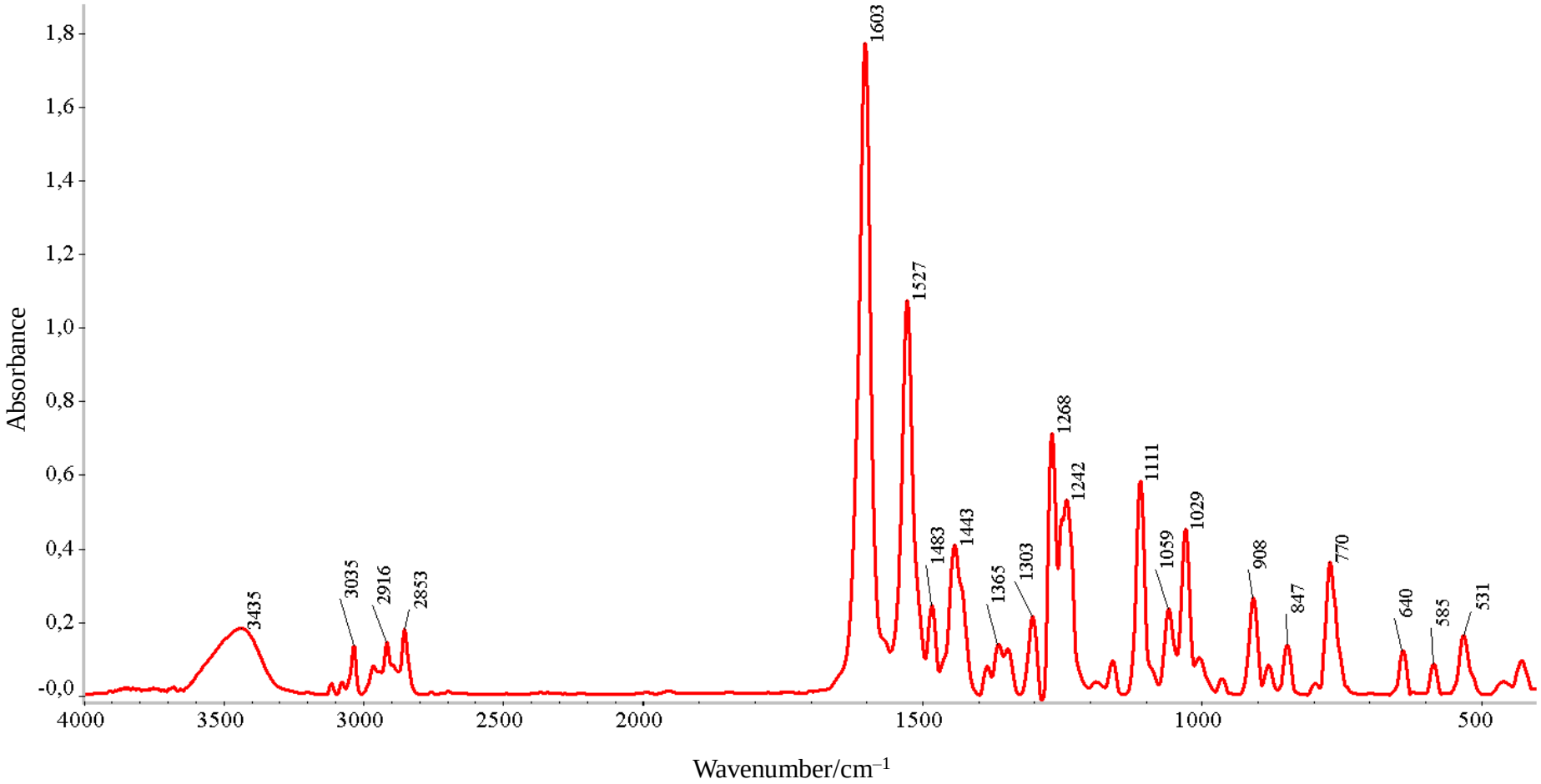

Fig. S64. IR spectrum of complex **9** after grinding in a vibration ball mill for 7 min
(Anal. Calcd for $C_{13}H_{16}ClN_3O_2PdS$: C, 37.16; H, 3.84; N, 10.00. Found: C, 37.11; H, 3.91; N, 10.08%)

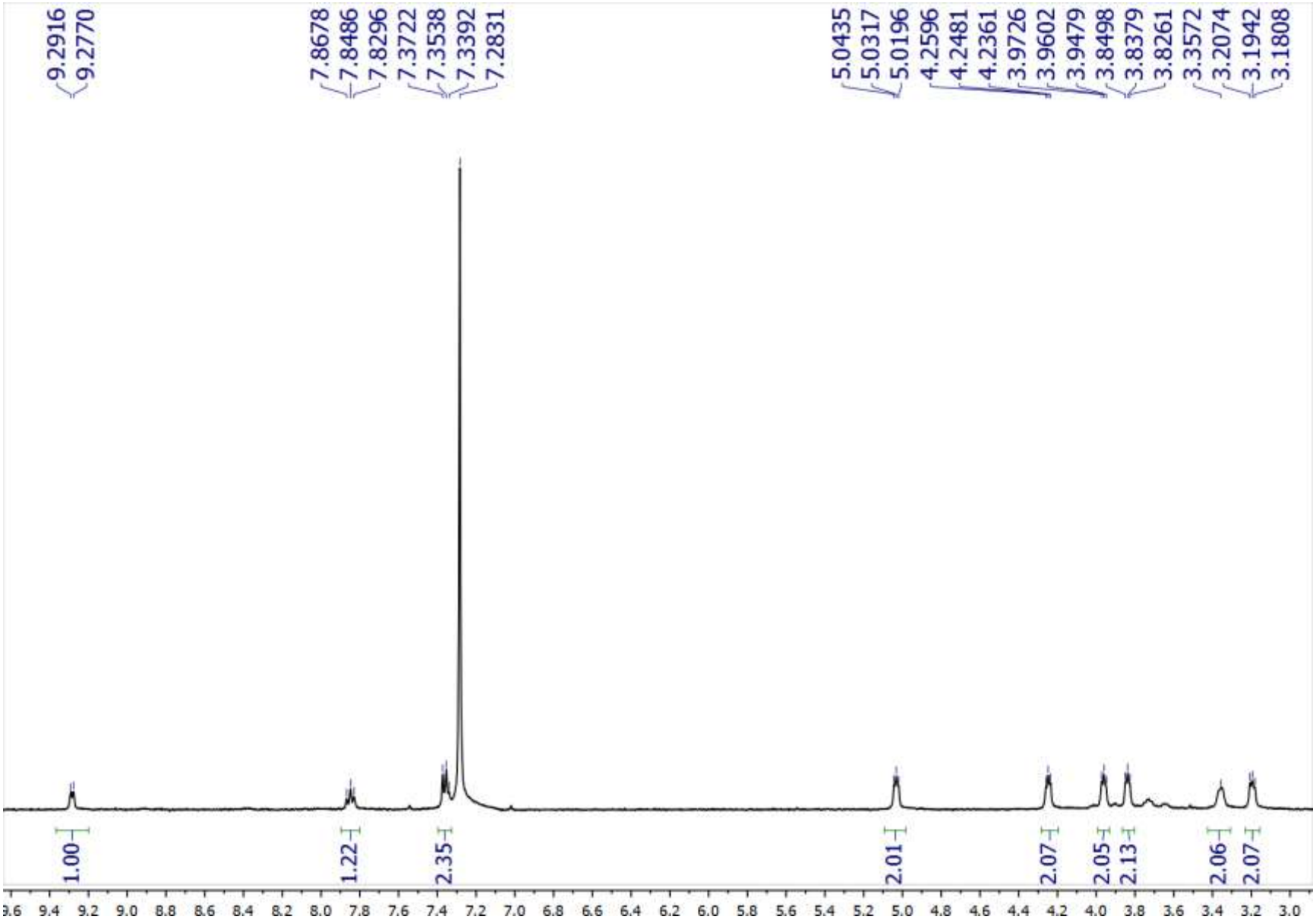

Fig. S65. ^{1}H NMR spectrum of complex **9** after grinding in a vibration ball mill for 7 min (400.13 MHz, $CDCl_3$)

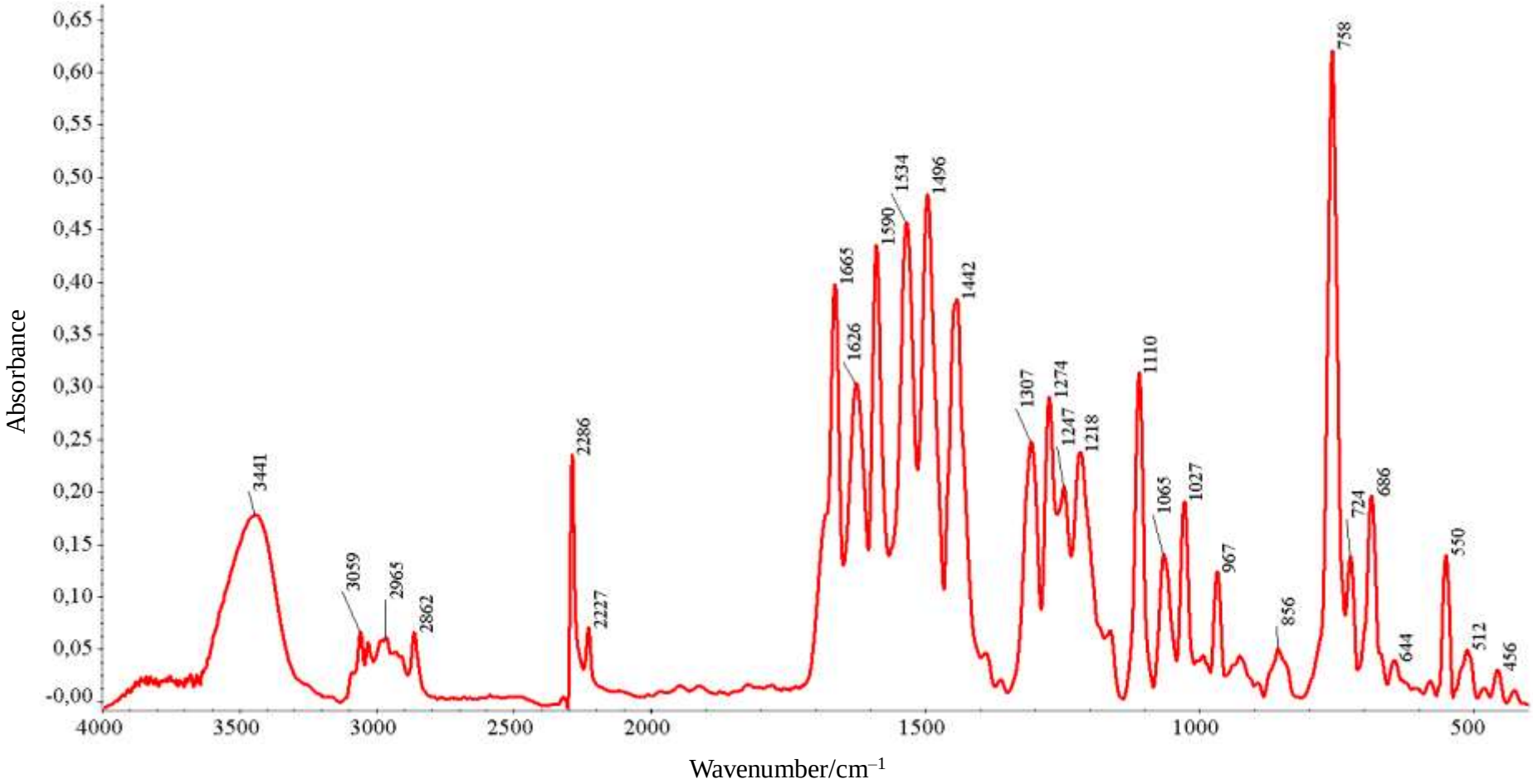

Fig. S66. IR spectrum of the residue obtained after a solid-phase reaction of ligand **4** with $PdCl_2(NCPh)_2$ in a vibration ball mill (registered in 35 min after the grinding cessation)

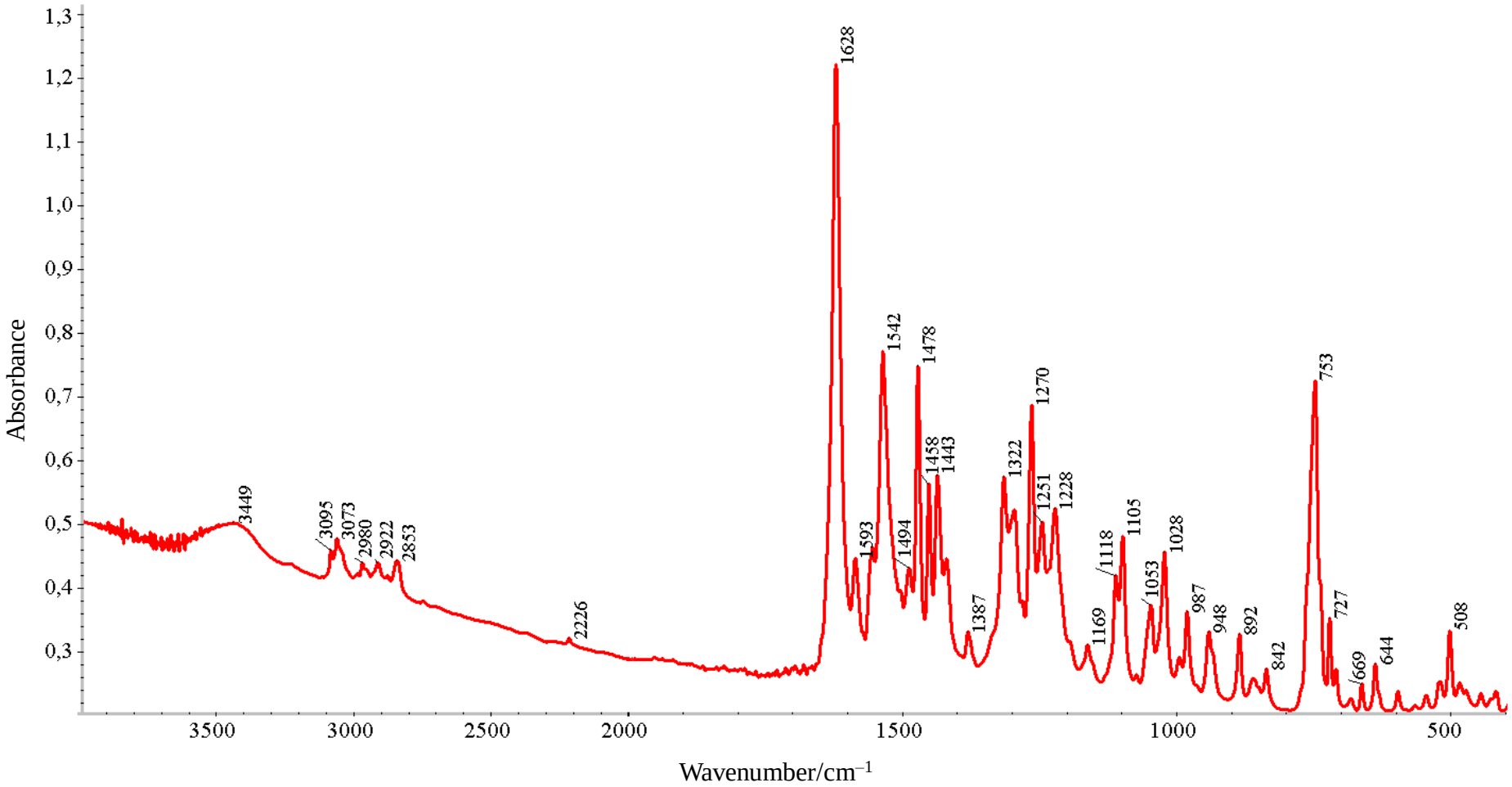

Fig. S67. IR spectrum of the residue obtained after a solid-phase reaction of ligand **4** with $PdCl_2(NCPh)_2$ in a vibration ball mill (registered in 3 days after the experiment)

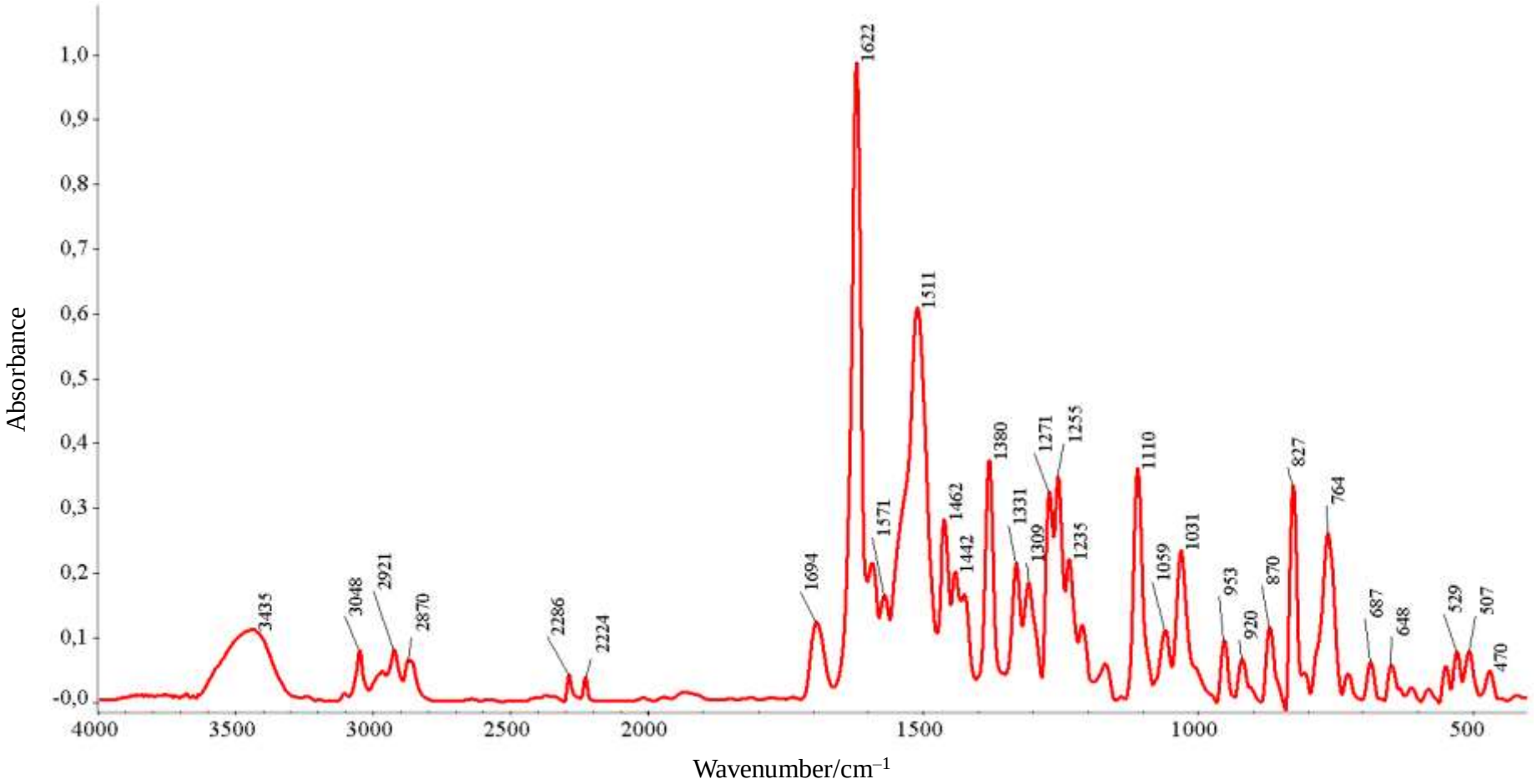

Fig. S68. IR spectrum of the residue obtained after a solid-phase reaction of ligand **3** with $PdCl_2(NCPh)_2$ in a vibration ball mill (registered in 30 min after the grinding cessation)

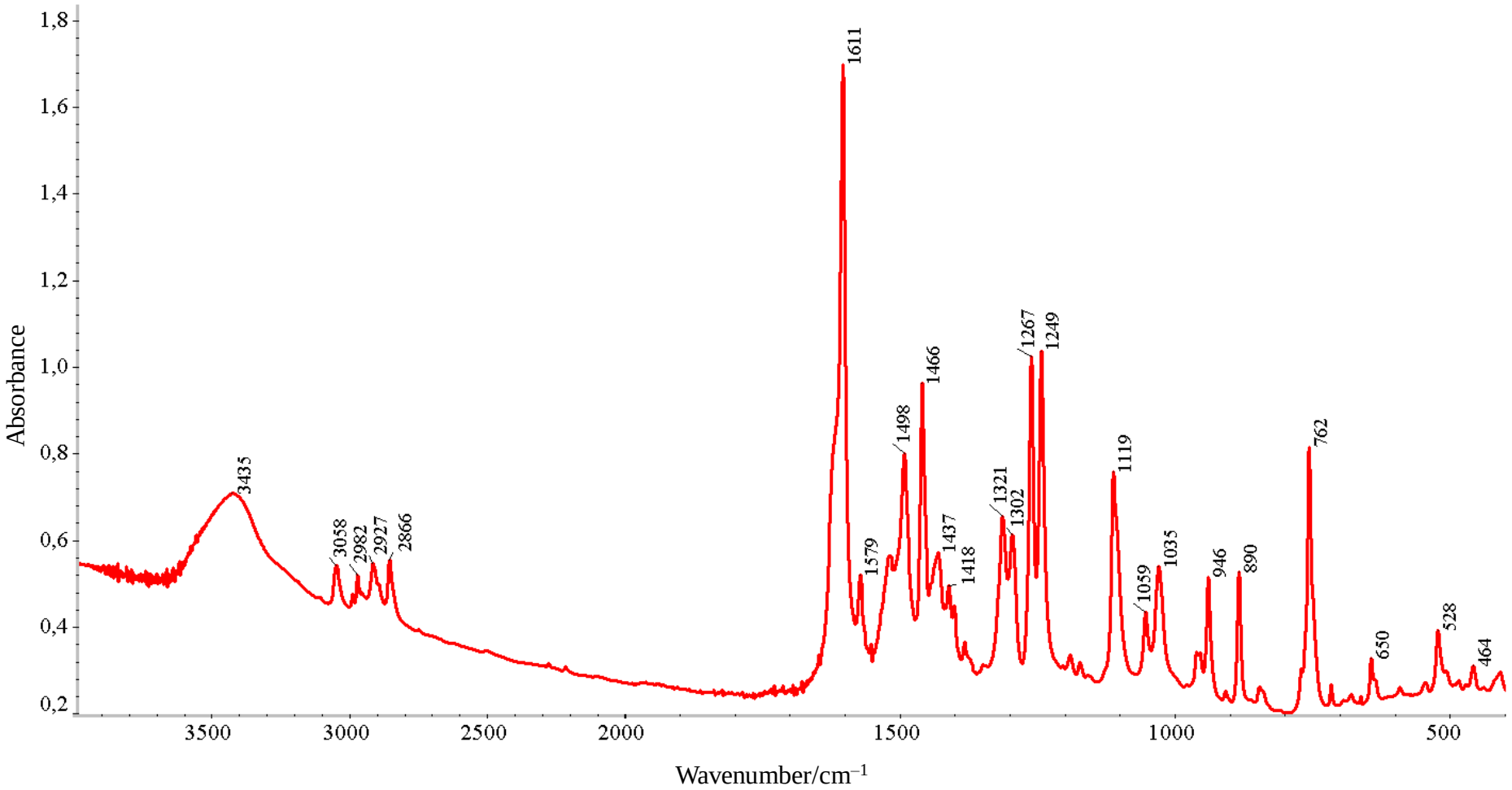

Fig. S69. IR spectrum of the orange paste obtained after grinding ligand **5** with $PdCl_2(NCPh)_2$ in a vibration ball mill for 60 s (registered in 20 min after the grinding cessation)

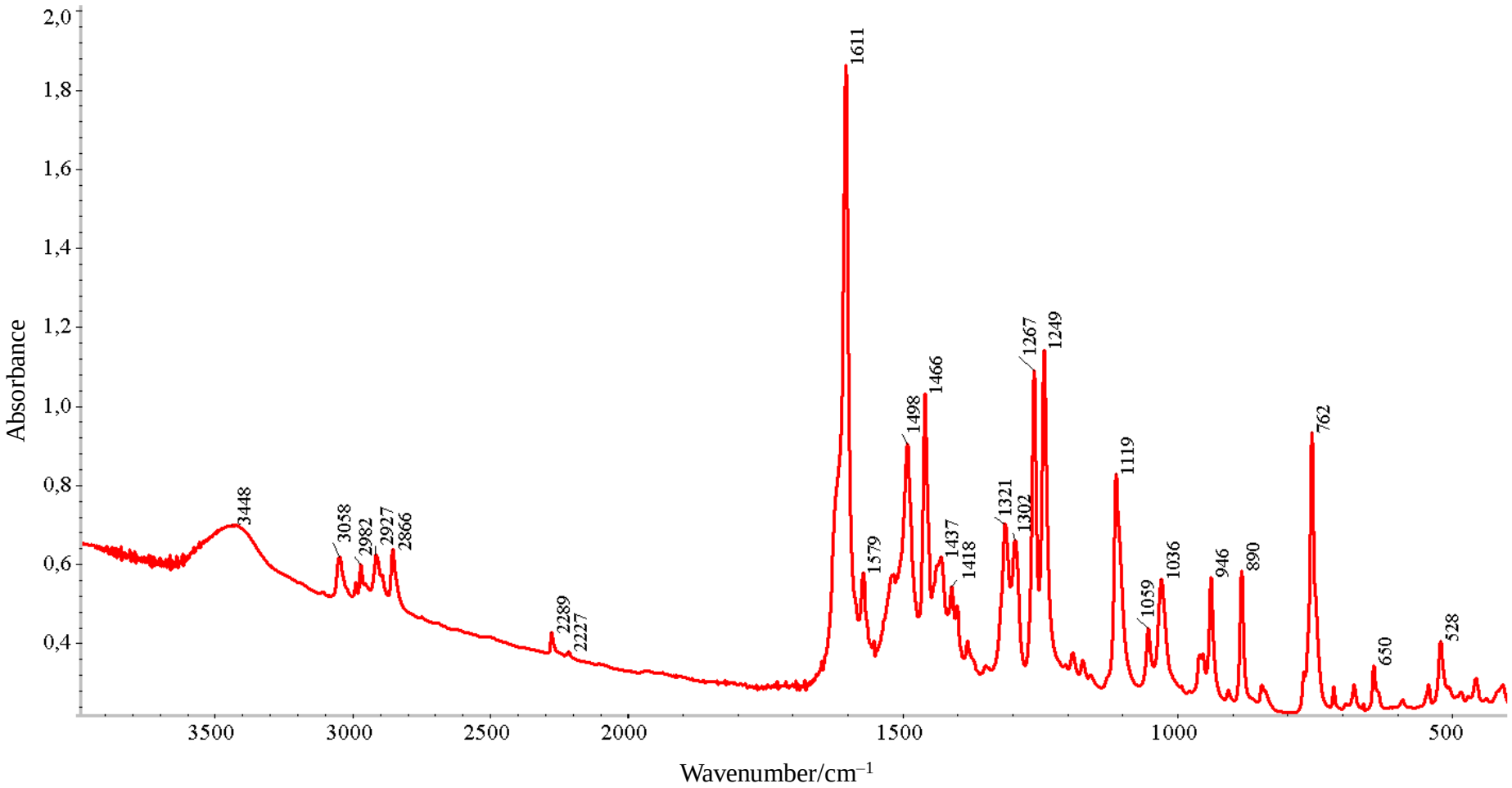

Fig. S70. IR spectrum of the orange paste (more fluidic) obtained after grinding ligand **5** with $PdCl_2(NCPh)_2$ in a vibration ball mill for 90 s (registered in 20 min after the grinding cessation)

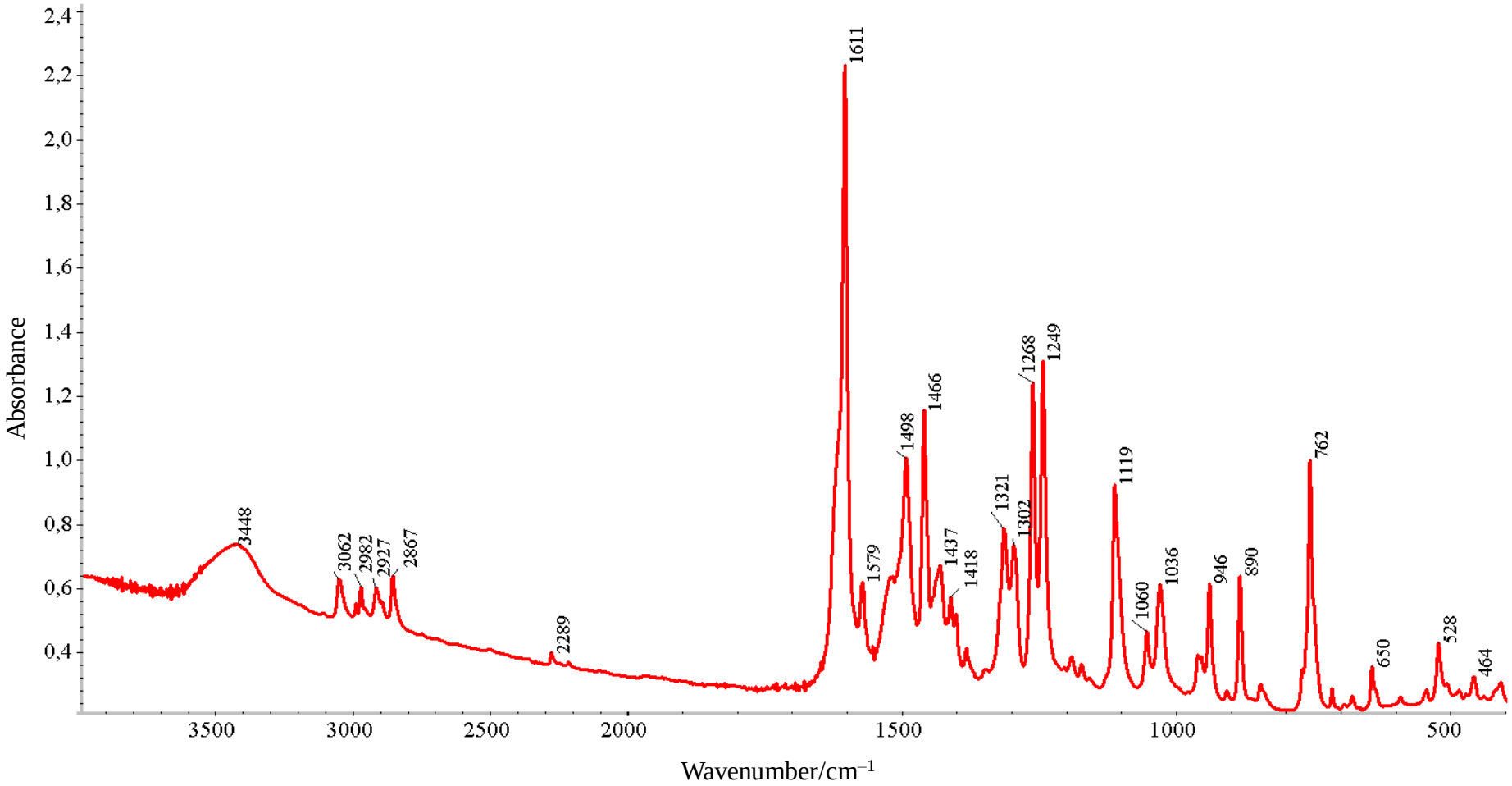

Fig. S71. IR spectrum of the residue obtained after a solid-phase reaction of ligand **5** with $PdCl_2(NCPh)_2$ in a vibration ball mill and rinsed with hexane

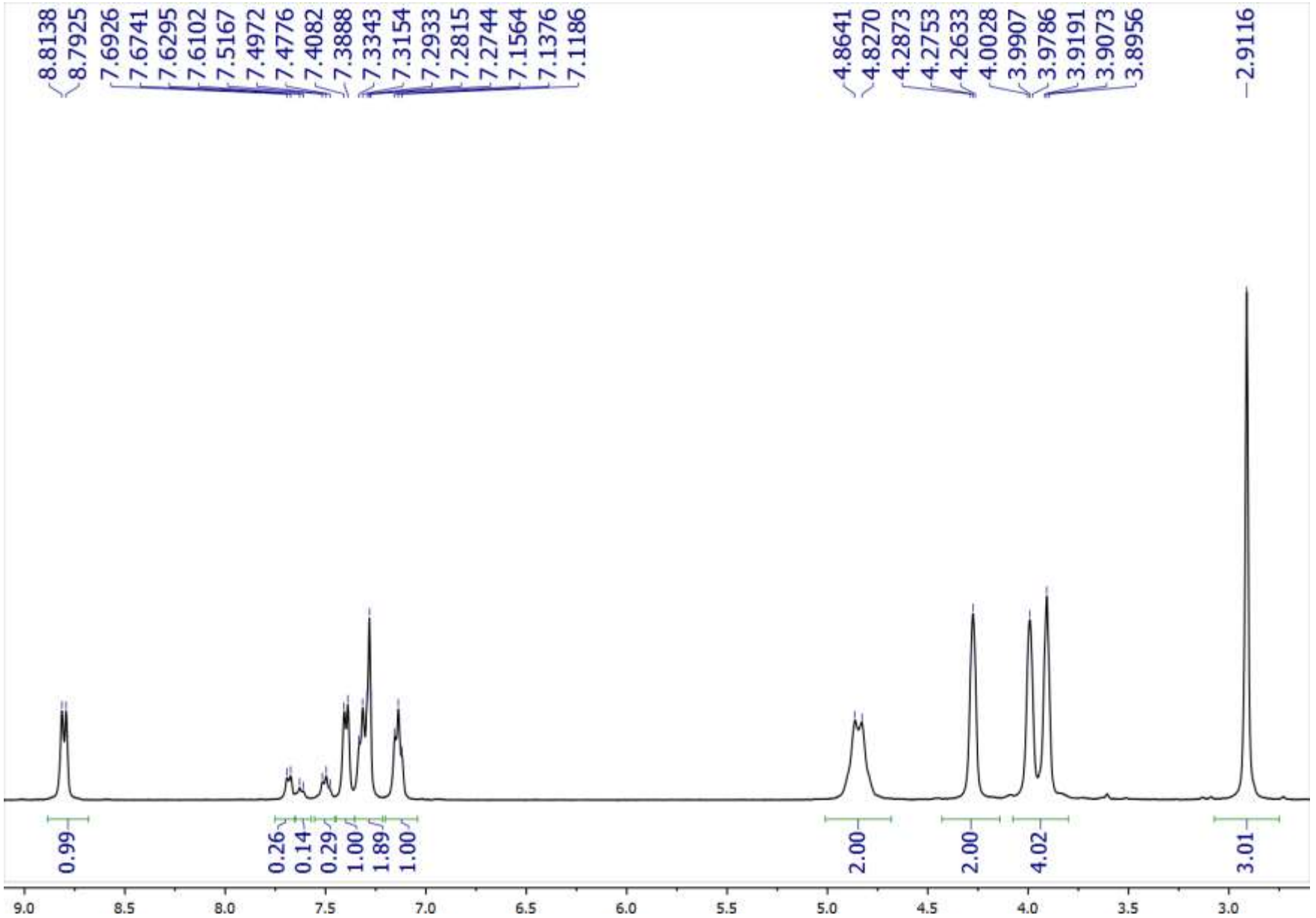

Fig. S72. ^{1}H NMR spectrum of the residue obtained after a solid-phase reaction of ligand **5** with $PdCl_2(NCPh)_2$ in a vibration ball mill and rinsed with hexane (400.13 MHz, $CDCl_3$)

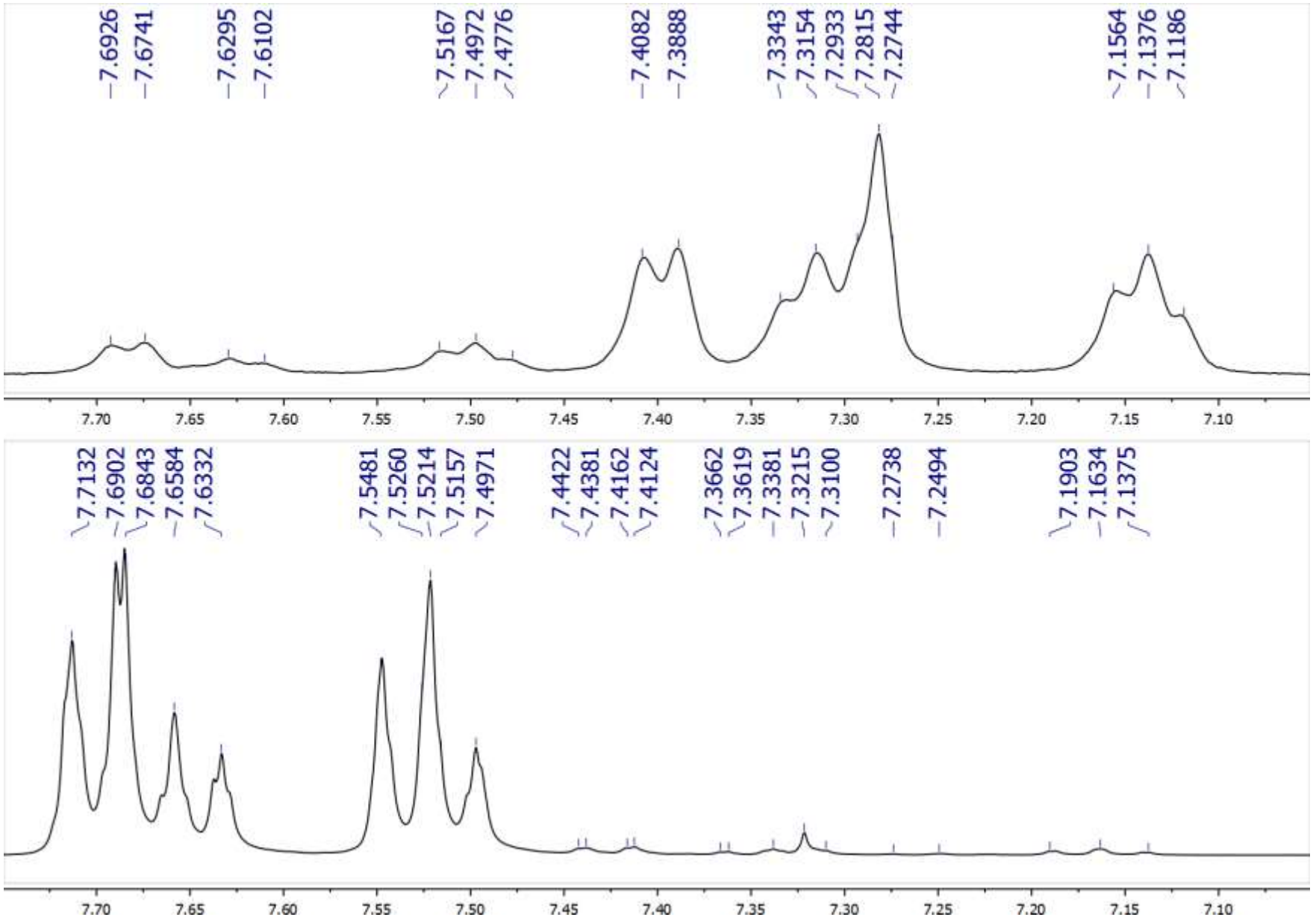

Fig. S73. Extended fragments of the ^{1}H NMR spectra of the neat residue obtained after a solid-phase reaction of ligand **5** with $PdCl_2(NCPh)_2$ in a vibration mill (top) and that with specially added PhCN (bottom) (400.13 MHz, $CDCl_3$)

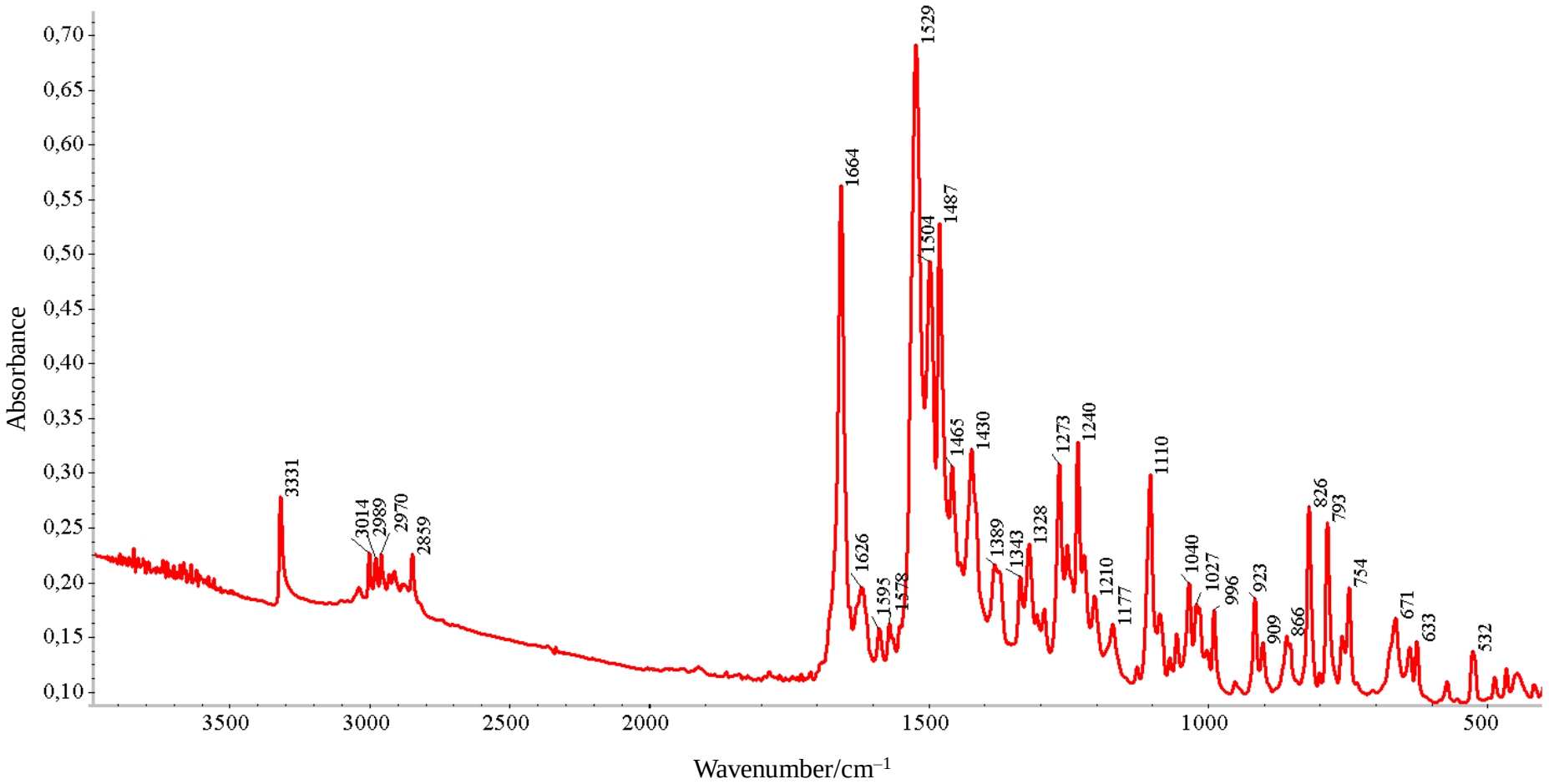

Fig. S74. IR spectrum of the mixture of ligand **3** with $PdCl_2$(COD) obtained by manual grinding in a mortar and left under ambient conditions for 6 days

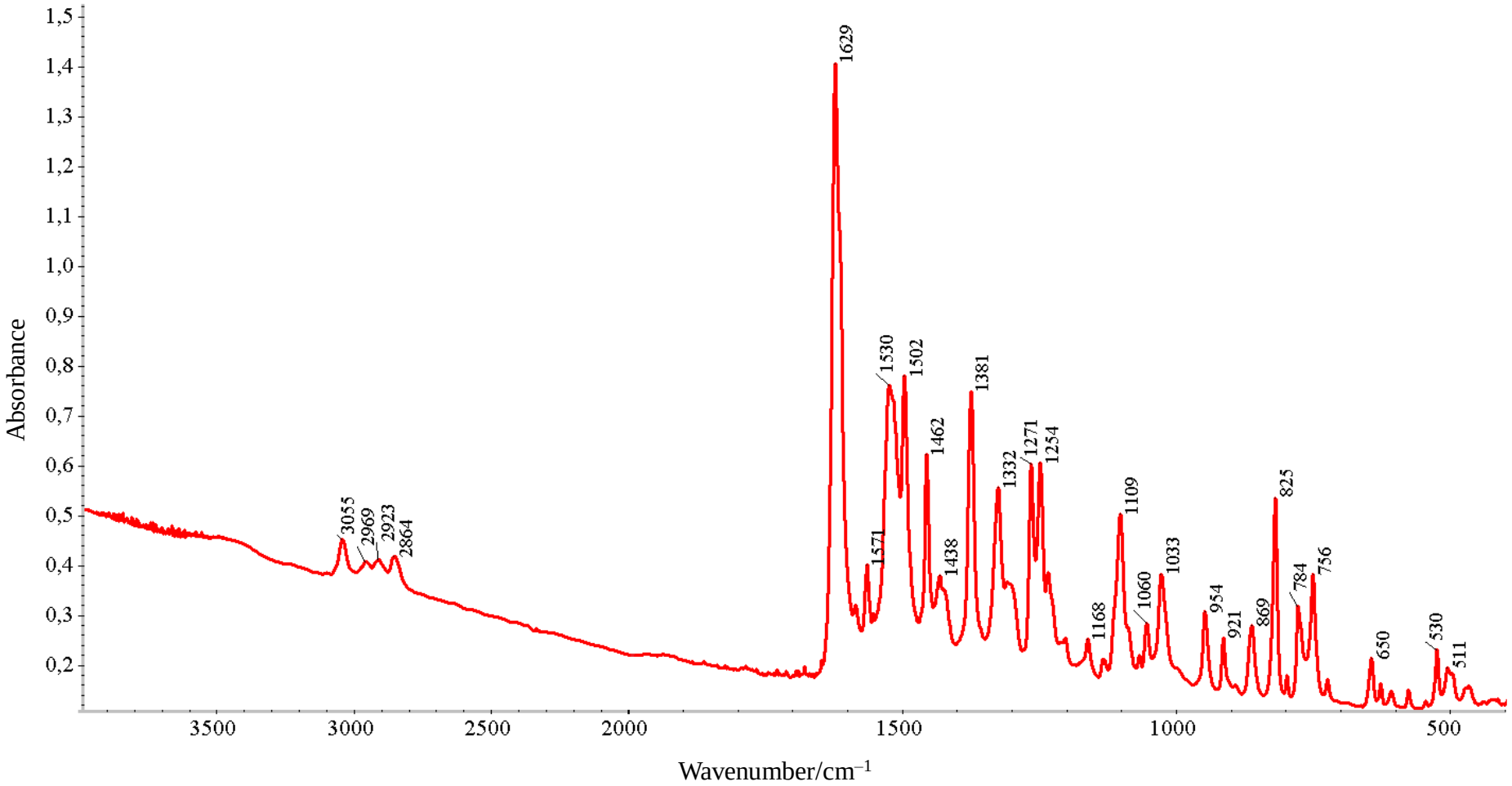

Fig. S75. IR spectrum of the mixture of ligand **3** with $PdCl_2$(COD) after heating at 80–175 °C for 20 min

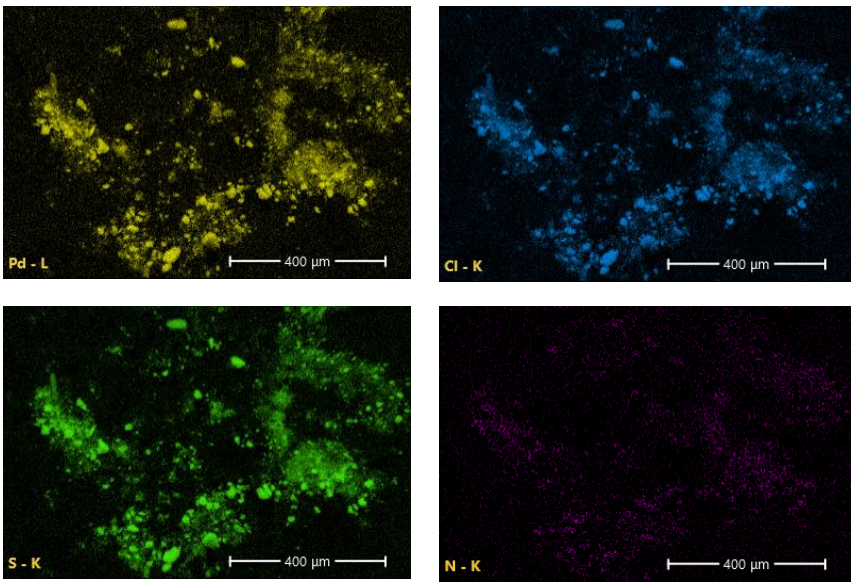

Fig. S76. EDS elemental distribution maps for complex **13** obtained by grinding in a mortar (100× magnification, 30kV)

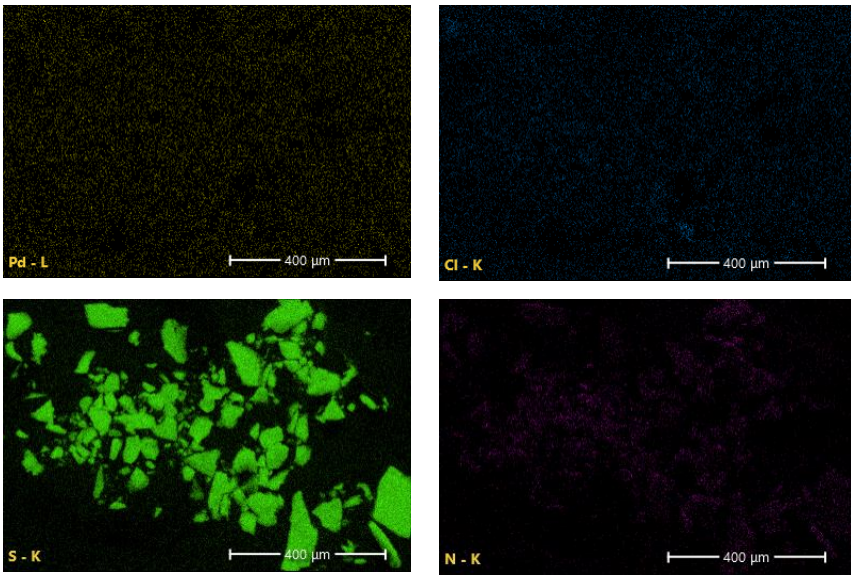

Fig. S77. EDS elemental distribution maps for ligand **5** (100× magnification, 30kV)

Table S1. Selected bond lengths (Å) and angles (°) for complexes **12** and **14**

12			
Pd1–N1	1.982(2)	C15–S1	1.722(3)
Pd1–Cl1	2.3205(7)	N3–C7	1.308(4)
Pd1–S1	2.2687(7)	Cl1–Pd1–N1	171.30(7)
Pd1–N3	2.056(2)	S1–Pd1–N3	166.15(6)
N1–C1	1.408(3)	Cl1–Pd1–S1	93.55(3)
N1–C14	1.356(3)	S1–Pd1–N1	85.26(7)
C14–O1	1.222(3)	N1–Pd1–N3	87.78(9)
C14–C15	1.537(4)	Cl1–Pd1–N3	95.09(7)
14			
Pd1–N1	2.0292(19)	C20–S1	1.716(2)
Pd1–Cl1	2.3123(6)	P1–S2	2.0160(8)
Pd1–S1	2.2922(6)	Cl1–Pd1–N1	170.35(6)
Pd1–S2	2.3526(6)	S1–Pd1–S2	164.98(2)
N1–C1	1.422(3)	Cl1–Pd1–S1	89.21(2)
N1–C19	1.346(3)	S1–Pd1–N1	85.36(6)
C19–O1	1.232(3)	N1–Pd1–S2	98.58(5)
C19–C20	1.523(3)	Cl1–Pd1–S2	88.70(2)

Table S2. Cytotoxic properties of the functionalized monothiooxamides and their palladium(II) pincer complexes (IC_{50} ± SD, μM)

Compound	Cell lines			
	HCT116	MCF7	PC3	HEK293
1	>200.0[a]	>200.0[a]	>200.0[a]	>200.0[a]
2	>200.0[a]	>200.0[a]	>200.0[a]	>200.0[a]
3	35.0 ± 5.0	38.0 ± 8.0	51.0 ± 14.0	24.5 ± 1.5
4	>40.0[b]	>40.0[b]	>40.0[b]	28.0 ± 3.0
5	>200.0[a]	>200.0[a]	>200.0[a]	>200.0[a]
8	25.5 ± 4.5	37.0 ± 9.0	19.5 ± 2.5	75.0 ± 12.0
9	74.0 ± 8.0	> 80.0[c]	28.5 ± 4.5	36.0 ± 6.0
11	72.0 ± 4.0	> 80.0[c]	67.0 ± 5.0	44.0 ± 4.0
12	65.0 ± 11	61.5 ± 3.5	32.0 ± 4.0	67.0 ± 5.0
13	52.5 ± 5.5	> 80.0[c]	40.0 ± 10.0	>100[d]
14	28.0 ± 8.0	58.0 ± 14.0	20.5 ± 4.5	14.0 ± 2.5
cisplatin	18.0 ± 2.0	25.0 ± 4.0	16.0 ± 3.0	12.5 ± 1.5

SD is the standard deviation of the value;

[a] the percentages of live cells at the compound concentration of 200.0 μM were above 90%;

[b] the percentages of live cells at the compound concentration of 40 μM were as follows: 71% (HCT116), 68% (MCF7), 82% (PC3).

[c] the percentages of live cells at the compound concentration of 80 μM were as follows: 100% (**9**), 70% (**11**), 66% (**13**);

[d] the percentage of live cells at the compound concentration of 100 μM was 70%.